Zwitterionic Ion Chromatography
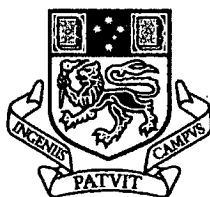
by

Helmy Alicia Cook B App Sc (Hons)

Submitted in fulfilment of the

requirements for the Degree of

Chemistry
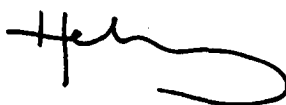
Doctor of Philosophy

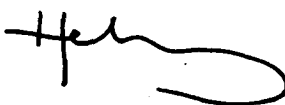
UNIVERSITY OF TASMANIA

May 2003

Declaration

To the best of my knowledge and belief, this thesis contains no material which has been

accepted for a degree or diploma by the University or any other institution, nor material

previously published or written by another person except where due reference is made

in the text of the thesis.

Helmy A. Cook

December 2002

This thesis may be available for loan and limited copying in

accordance with the Copyright Act 1968.

Helmy A. Cook

December 2002

Acknowledgments

List of Publications

Type of Publication	Number	Reference
Papers	4	1-4
Oral Presentations	2	5, 6
Posters	3	7-9

1 Cook H.A., Hu W., Fritz J.S. and Haddad P.R. A Mechanism of Separation in Electrostatic Ion Chromatography. *Anal. Chem.*, **2001**, 73 (13) 3022-3027. (Chapter 3)

2 Cook, H.A., Dicinoski, G.W. and Haddad P.R. Mechanistic Studies on the Separation of Cations in Zwitterionic Ion Chromatography. *J. Chromatogr. A.*, in press. (Chapter 4)

3 Hu W., Haddad P.R., Cook H., Yamamoto H., Hasebe K., Tanaka K. and Fritz J.S. Manipulation of Separation Selectivity of Inorganic Anions in Electrostatic Ion Chromatography by the use of Mixed Cationic-Zwitterionic Micelles as the Column Coating Solution. *J. Chromatogr. A.*, **2001**, 920, 95-100. (Chapter 5)

4 Hu W.Z., Haddad P.R., Hasebe K., Cook H. and Fritz J.S. Analysis of Inorganic Anions by Electrostatic Ion Chromatography using Zwitterionic/Cationic Mixed Micelles as the Stationary Phase. *Fres. J. Anal. Chem.*, **2000**, 367 (7) 641-644. (Chapter 5)

5   Cook H., Haddad P.R., Hu W., and Fritz J.S. A New Mechanism of Separation in Electrostatic Ion Chromatography. *Proc. International Ion Chromatography Symposium*, **2001**, Chicago, U.S.A., oral presentation No. 64.

6   Cook H.A., Haddad P.R., Hu W. and Fritz J.S. The Effect of the Eluent Anion and Cation Species on Retention in Electrostatic Ion Chromatography. *Proc. International Ion Chromatography Symposium*, **2000**, Nice, France, oral presentation No. 5.

7   Cook H.A., Okada T. and Haddad P.R. Modelling of Retention in Zwitterion Ion Chromatography. *Proc. Interact 2002*, **2002**, Sydney, Australia, poster presentation, p. 241.

8   Haddad P.R., Cook H.A., Hu W., Yamamoto H., Hasebe K., Tanaka K. and Fritz J.S. Electrostatic Ion Chromatography Using Mixed Micelles of Zwitterionic and Cationic Surfactants as the Stationary Phase. *Proc. International Ion Chromatography Symposium*, **2000**, Nice, France, poster presentation No. 75.

9   Cook H.A., Doble P.A. and Haddad P.R. Electrostatic Ion Chromatography. *Proc. Australian International Symposium of Analytical Science*, **1999**, Melbourne, Australia, poster presentation No. PS2.42.

Abstract

This work presents a comprehensive study on Zwitterionic Ion Chromatography (ZIC) for the separation of inorganic ions.

The elution characteristics of anions on a sulfobetaine-type stationary phase are examined and it is shown that the Hofmeister series could be used to predict the elution order, with retention increasing with increasing polarisability, as well as the effect of the mobile-phase anion on retention of anions. A mobile-phase anion with a greater polarisability than the analyte anion reduced retention, and vice versa. An increase in anion retention was also observed in changing the mobile-phase cation from Na^+ to Mg^{2+} to Ce^{3+}.

Electro-osmotic flow measurements in an analogous capillary electrophoresis system revealed a zeta potential on the stationary phase that could be modulated from positive (+40.2 mV for $CeCl_3$) to negative (-53.4 mV for $NaClO_4$) depending on the mobile-phase anion and cation. Thus the zwitterionic stationary phase is only neutral for mobile phases where the mobile-phase anion and cation equally shield the charges on the stationary phase.

A new retention mechanism for ZIC was developed, based the ability of an analyte to penetrate the repulsion effects of a Donnan membrane (established by the zeta potential) and to interact directly with the inner charge of the zwitterion. This mechanism was established on the basis of experimental data obtained for the anion

system, and an analogous mechanism was proposed for a cation system that utilised a phosphocholine-type stationary phase, where a systematic study of the elution effects of this system was found to mirror that of the anion system.

Manipulation of the separation selectivity of inorganic anions in ZIC was achieved by controlling the ratio of cationic and zwitterionic surfactants in the stationary phase coating solution. Even at a ratio of 2:8 cationic:zwitterionic surfactant, a large contribution of an ion-exchange mechanism from the cationic surfactant occurred, in particular for small, highly-charged analytes. This was evident in the slopes of log k' *versus* log [mobile phase] plots. For example, the slope for the analyte SO_4^{2-} changed from 0.23 to -1.22 when the ratio was changed from 1:10 to 2:8.

Hard and soft mathematical models were investigated to quantitatively describe the mechanism of ZIC. The non-stoichiometric hard model was successful in describing general experimental trends, but further work is required to achieve accurate predictions of retention factors. The experimental data obtained for the anion system were used successfully to train an artificial neural network capable of predicting retention factors for a wide range of mobile phases. Plots of calculated *versus* experimental retention factors for a test set of analytes gave an r^2 of 0.985.

Table of Contents

Introduction and Literature Review

1.1 Introduction

Inorganic ion analysis is important in a broad range of areas, as illustrated in a review by López-Ruiz [1]. Applications include the study of biogeochemical processes involving the elucidation of N, P and S cycles, requiring the speciation analysis of these elements. Drinking water quality treatment results in the by-production of BrO_3^-, which is said to be a carcinogen and must be monitored to keep concentrations less than the 10 $\mu g \ L^{-1}$ limit allowed by the US Environmental Protection Agency (US EPA). Cl^- and Br^- are important indicators of groundwater salinity, while I_2 is an important micronutrient for many organisms in seawater, monitored through the determination of I^- and IO_3^-. I^- also has clinical and epidemiological importance and must therefore be monitored in serum and urine. NO_2^- and NO_3^- are toxic, with NO_2^- forming carcinogenic nitrosamines in food products, and NO_3^- forming NO_2^- via microbial reduction. Trace metals, such as Cd(II), Cr(III) and Pb(II) at concentrations between 1 – 100 mg L^{-1}, can have a detrimental effect on the environment if concentrations increase above natural levels, hence they are continuously monitored to ensure toxic levels are not reached [2]. NH_4^+, Mg^{2+}, Ca^{2+}, Cl^-, PO_4^{3-}, SO_4^{2-}, oxalate and citrate levels provide a supersaturation index for the formation of kidney stones (calcium oxalates and phosphates) and can be measured in urine samples [3].

The applications listed above are just a few of many, but already it can be seen that the sample matrices vary widely. Although some samples may contain ions at similar concentrations, a great many involve the determination of a small concentration of ions of interest among a high concentration of matrix ions. This is still a major challenge to ion analysis.

Techniques such as neutron activation analysis, automated electrochemical procedures and cathodic stripping square wave voltammetry have been applied to such problems, but are time-consuming, hence there has been a turn towards ion chromatography [4], the focus of this thesis.

This review provides an overview of ion chromatographic theory and developments, introducing the technique of Electrostatic Ion Chromatography, or Zwitterionic Ion Chromatography (ZIC), and indicates its niche among other ion chromatographic techniques.

1.2 Ion Chromatography

The development of Ion Chromatography (IC) was driven by a need for automated systems to determine ionic species from a variety of samples quickly and effectively, which required liquid chromatography in conjunction with continuous detection. Conductivity was the detection method of choice, as it is a universal detector of a bulk property. However, its use was complicated by the large number of eluting ions accompanying analytes, resulting in high background conductivity. Small *et al.* [5]

introduced a new, extremely efficient, type of stationary phase and overcame the background conductance by introducing a stripper, later termed a suppressor, column. This laid the foundation for the great success and development of IC.

IC is now loosely defined as column liquid chromatographic techniques that are used for the determination of inorganic anions and cations (not including neutral metal chelates), low molecular weight carboxylic acids, organic bases and ionic organometallic compounds [6]. Types of ion chromatography include: ion-exchange chromatography; ion-interaction chromatography; ion-exclusion chromatography; reversed-phase liquid chromatography; the use of chelating stationary phases; and others.

1.2.1 Ion-Exchange Chromatography

The new and extremely efficient stationary phase developed by Small *et al.* [5] was a pellicular, agglomerated resin with an outer layer of positive charges, M^+, for the separation of anions, or negative charges for the separation of cations (see Section 1.3.2). Counter-ions, E^-, in the mobile phase maintain electroneutrality on the surface. Sample anions, A^-, may stoichiometrically displace, or exchange with, these ions, which is described as an ion-exchange mechanism, expressed by the following equilibrium equation:

$$M^+E^- + A^- \rightleftharpoons M^+A^- + E^- \tag{1.1}$$

The extent of retention of an analyte ion on an ion-exchange resin is determined by its ability to displace E^- and the strength of its attraction to M^+, which is described by the selectivity coefficient:

$$K_{A,E} = \frac{[A_r^{x-}]^y [E_m^{y-}]^x}{[A_m^{x-}]^y [E_r^{y-}]^x} \tag{1.2}$$

where subscripts r and m denote the species in the resin and mobile phases, and x and y are the charges on the analyte and eluent ion, respectively.

Retention models based on this theory are termed stoichiometric models, whereby a series of equilibrium equations are manipulated to reach a final retention equation. Although stoichiometric models may give good agreement with experiment, it has been argued that this does not imply the model is satisfactory from a physical point of view [7]. Non-stoichiometric models are not based on the formation of these complexes at equilibrium, but instead on the build up of an electrical double layer at the surface charge into which analytes may partition. The electrical surface potential is found by solving the Poisson-Boltzmann equation (see Chapter 6), and models of this type generally involve more complex mathematical equations compared with stoichiometric models [8].

Stationary phases in ion-exchange all contain a fixed site attached in some manner to a substrate. The fixed site is usually a sulfonic, carboxylic or phosphonic acid group for cation-exchangers, while anion-exchangers contain an amine group (quaternary,

tertiary, etc.). The substrate may be silica, polymer-coated silica, a synthetic polymeric resin or a hydrous oxide [6], with new packing technology still being explored [9,10]. The ion-exchange capacity, or number of functional groups per unit weight of the resin, is an important property in determining the retention of analytes (increased capacity leads to increased retention), as well as the strength of the eluting mobile-phase ion.

Selectivity in ion-exchange on a strong acid ($-SO_3^-$) cation-exchanger follows the order [6]:

$$Li^+ < H^+ < Na^+ < NH_4^+ < K^+ < Rb^+ < Ag^+ < Mg^{2+} < Ca^{2+} < Ba^{2+} << Al^{3+} << Pu^{4+} \quad (1.3)$$
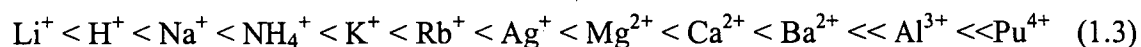
and on a strong base ($-R_3N^+$) anion-exchanger the order is [6]:

$$OH^- < F^- < IO_3^- < HCO_3^- < Cl^- < NO_2^- < Br^- < NO_3^- < HPO_4^{2-} < SO_4^{2-} < I^- < SCN^- <$$

$$ClO_4^- < citrate \quad (1.4)$$
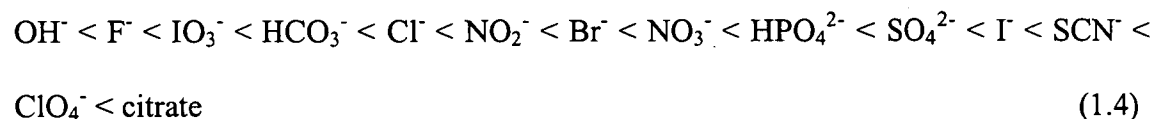
This retention order is determined by the charge on the analyte, the size of the hydrated ion, the degree of cross-linking of the resin, the polarisability of the analyte, the capacity and functional group of the ion-exchanger, and the hydrophobicity of the analyte. The stationary phase functional group structure has also been shown to be important [11,12].

1.2.2 Ion-Interaction Chromatography

Ion-interaction chromatography (also known as ion-pair chromatography, dynamic ion-exchange chromatography, hetaeric chromatography and soap chromatography [13]) is a simple means of separating inorganic ions by reversed-phase liquid chromatography, which otherwise shows little or no affinity for ions. This is achieved by adding a lipophilic species of opposite charge to the analytes of interest, called the ion-pair, or ion-interaction reagent (IIR) to the mobile phase [6]. IIRs may be inorganic [14-17] or organic ions (whereby hydrophobic and ion-exchange effects will determine retention) [18]. Much attention has been given to modelling retention in ion-interaction chromatography [13,19-23]. Theories include the formation of an ion-pair in solution between the IIR and the analyte, which is thus neutral and able to adsorb onto the hydrophobic stationary phase. Alternatively, the dynamic ion-exchange approach [24] assumes the IIR adsorbs onto the stationary phase with the charges exposed to the surface, creating an ion-exchange stationary phase. The ion-interaction model, supported by Bartha and Stahlberg [22], is a combination of both, with the IIR in equilibrium between the mobile and stationary phase, forming an electrical double layer at the surface that allows partition of analytes [6]. It is generally observed that retention of analytes of the same charge as the IIR decreases on addition of the IIR, while that for ions of opposite charge increases, and neutral molecules are relatively unaffected by the addition of the IIR [6]. Much attention, however, has been given to

understanding the behaviour of neutral solutes in ion-interaction chromatography [25-28].

If the IIR, such as tetrabutylammonium, is contained in the mobile phase during separation it is said to form a dynamic coating on the stationary phase. If an extremely hydrophobic IIR is passed through the column prior to separation and not included in the mobile phase during separation, the column is said to be 'permanently coated'. This effectively constitutes an ion-exchanger that has advantages over fixed site exchangers in that the ion-exchange capacity can be easily varied and the column can be stripped and recoated as either an anion- or cation-exchanger.

Parameters influencing retention include the nature (type and chain length) of the IIR [29,30], the co-anion species, the solvent, the added inert electrolyte, and pH [18].

1.3 Bi-Functional Stationary Phases in Ion Chromatography

Bi-functional stationary phases may contain opposite charges distributed evenly throughout the stationary phase, have one charge contained inside a core particle with a layer of opposite charge on the surface of the particle, or have positive and negative charges contained on an individual molecule, somehow bonded to the stationary phase. Nesterenko and Haddad recently reviewed zwitterionic ion-exchangers in liquid chromatography [31].

1.3.1 Ion-Exchangers with Continuous Distribution of Opposite Charges Throughout the Stationary Phase

There are two types of stationary phases containing opposite charges distributed throughout the packing particles. Firstly, polyampholyte resins, with alternating sequences of anion and cation-exchange groups, such as polysulfobetaines and polycaboxybetaines, have gained renewed interest since their earlier use [32,33]. Secondly, the so-called retardion, or snake cage type, resins are formed by polymerising a cation-exchange monomer (the snake) inside a commercial anion-exchange material (the cage) [34]. The Retardion 11A8 columns, commercially available since 1957 [35], can be used with a water mobile phase as ions are held rather weakly due to the near neutral stationary phase. This column has a low affinity for SO_4^{2-}, compared to that of CH_3COO^-, which is opposite to that seen for ion-exchange, but the elution order for cations is similar with divalent anions being more highly retained than monovalent ions [31]. This type of stationary phase has been used for the desalting of proteins [34] and the analysis of ionic and non-ionic analytes [36], including metals [37-39].

1.3.2 Pellicular Ion-Exchange Bi-Functional Stationary Phases

Pellicular stationary phase material contains a solid inner core with functional groups restricted to the outer surface [6]. So-called agglomerated ion-exchange resins that are synthesised by electrostatically bonding a functionalised latex of opposite charge to the

functionalised core [5,6,40] are effectively bi-functional. However, those that are bound with an outer layer of aminated latex are generally suitable only for the ion-exchange separation of anions, and those bound with sulfonated latex particles are generally suitable only for the separation of cations. These types of resins are stable and very efficient with excellent mass-transfer characteristics due to the repulsion an analyte feels from the like-charged inner core, disallowing its partition into the particle, and have gained widespread use [41-45] with many resins available commercially [6]. This type of stationary phase has also been exploited for its ability to separate anions and cations simultaneously due to its bi-functionality, despite the outer functional groups clearly having a much stronger interaction with mobile phase ions than the inner functional groups. "Anion-exchange" columns have been applied to the separation of inorganic cations [46] as well as Cr(III) and chromate [46], while "cation-exchange" columns have been shown to successfully separate inorganic anions, NO_3^-, NO_2^- from NH_4^+ [41] and $HGeO_3^-$ from Sn^{2+} [48].

Bi-functional stationary phases of the pellicular type have also been produced by adsorbing a positive and negative polymer onto an uncharged solid inner core particle [49]. Three layers result – the inner core particle (e.g. ODS bonded to silica), adsorbed negatively-charged molecules and electrostatically bonded positively-charged molecules, thus this type of stationary phase is referred to as being multilayered [31].

Yet another approach has been to treat an anion-exchange resin with sulfuric acid, optimising conditions such that the degree of sulfonation, and concentration and depth

of the surface layer could be controlled [50,51]. The stationary phase may be left

predominantly as an anion-exchanger, cation-exchanger or zwitterionic phase

depending on sulfonation conditions.

Mixed-bed ion-exchangers produced by mixing anion- and cation-exchange resins

before packing into a column have been shown to be successful in the simultaneous

separation of anions and cations [52].

1.3.3 Polyampholyte Polymer Ion-Exchange Stationary Phases

Proteins, such as bovine serum albumin, adsorbed onto a silica substrate provide a

stationary phase that can be modulated between a cation, anion and zwitterionic

exchanger, by careful control of the pH. Such columns are commercially available

with a variety of proteins used as the stationary phase [53]. They have found

application to the separation of inorganic anions [53-55], inorganic cations [56,57] and

enantiomers [58,59]. Other polymers have been used, such as chondroitin sulfate-C

[60], with one approach crosslinking the polymer after adsorption [61].

1.3.4 Bi-Functional Ion-Exchange Stationary Phases with Separately Distributed
Charges

These types of stationary phases include alumina as the packing material, which being

an amphoteric material allows the simultaneous separation of inorganic anions and

cations on a single column. As the pH increases the retention of cations increases and the retention of anions decreases [62]. At low pH, the stationary phase acts as an anion-exchanger, although the retention order observed is the opposite of that seen with a quaternary ammonium stationary phase [63]. This was thought to be a result of complexation of halide ions with aluminium atoms [31]. Other amphoteric oxides have been examined for their application to chromatography, including silica, titania, zirconia and an aluminosilicate (MCM-41 [64]) [65]. Brown and Pietrzyk [66] mixed alumina and silica to create a mixed-bed ion-exchange column for the separation of anions and cations at pH 5.

Similarly, amino acids immobilised onto a silica surface have been used for the simultaneous separation of inorganic anions and cations [67,68]. Separation characteristics were dependent on the structure of the amino acid, with for example, glutamic acid exhibiting ion-exchange and complex forming characteristics [69], and of course, pH.

A synthesised zwitterionic stationary phase was achieved by adding an s-triazine derivative, introducing sulfonate and amino groups to the already aminated silica gel [70]. The resultant stationary phase (shown in Figure 1.1) was used for the separation of organic acids and bases as well as amino acids. A similar technique was used by Yang *et al.* [71].
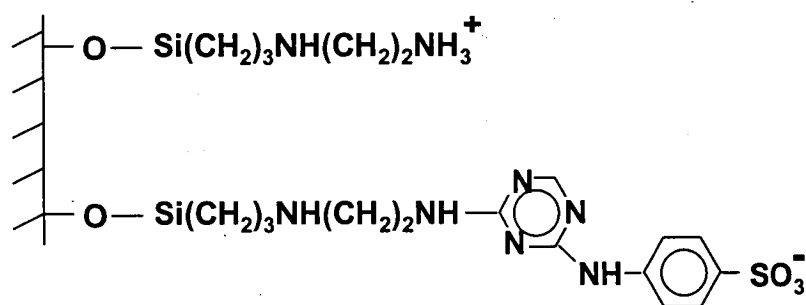
Figure 1.1 Zwitterion-exchange stationary phase with charges separately distributed on the surface [70].

Dynamic bi-functional coatings have been produced by hydrophobically adsorbing a mixture of anionic and cationic surfactants onto a reversed-phase column [72]. Due to the different adsorbing properties of the anionic and cationic surfactants, the ratios of each in the coating mixture must be varied until a stationary phase is obtained that contains equal amounts of both types of surfactant, such that the surface is effectively neutral. Such stationary phases have been shown to be effective in the separation of neutral, positively and negatively-charged platinum(II) complexes, allowing the determination of cisplatin purity and understanding the reactions of platinum(II) complexes in solution [72].

1.3.5 Zwitterionic Surfactants in the Mobile Phase

Zwitterion-Pair Chromatography is the name given to reversed-phase liquid chromatography where a zwitterionic pairing agent is added to the mobile phase [73]. It has been applied to the separation of zwitterionic analytes, including nucleotides, tryptophan and lysergic acid, via the formation of quadrupolar ion pairs [74]. Zwitterionic pairing agents used include 11-aminoundecanoic acid and L-leucyl-L-leucyl-L-leucine [75].

Zwitterions, such as (N-morpholino)ethanesulfonic acid (MES), have also been used in the mobile phase for suppressed ion chromatography as a means of buffering the mobile phase without interfering with the conductivity. This allows the use of the

suppressible NaOH eluent without detrimental effect to the efficient silica bonded columns [76].

Sulfobetaine-type zwitterionic surfactants in the mobile phase have been used with reversed-phase [77,78] and ion-exchange columns [79,80], which has been termed zwitterionic micellar chromatography. The former took advantage of an extra partitioning contribution to the retention of benzene derivatives, while the latter allowed the direct injection of biological fluids for the analysis of inorganic ions, as the zwitterionic micelles solubilised proteins in the sample.

These types of zwitterionic surfactants have also found application as additives in the buffers and dynamic coatings of capillaries in capillary electrophoresis [81-88].

1.4 Zwitterionic Ion Chromatography

The term Electrostatic Ion Chromatography (EIC), was introduced by Hu *et al.* [89], to describe the form of ion chromatography that utilises a bi-functional stationary phase where the opposite charges on the same molecule are in close proximity. The opposite charges may have just 3 carbon atoms separating them, so that they exert a significant influence on each other and this characteristic distinguishes them from other bi-functional stationary phases. Hu *et al.* [89] named the technique to reflect their proposed mechanism of separation, which was largely based on electrostatic effects. Findings in this present research dispute this suggestion, thus the broad term

Zwitterionic Ion Chromatography (ZIC) will be used in place of EIC throughout this thesis.

1.4.1 Stationary Phase

1.4.1.1 Nature of the Zwitterionic Molecule

Ionic surfactants are true salts in that they consist of an electrically neutral set of two or more formally-charged ions, whereas zwitterionic surfactants are non-ionic, consist of a single neutral molecule and do not form salts with other ions. They do not conduct electricity, contribute to electrophoretic mobility or contribute to ionic strength [90]. However, due to their formal charges, their properties are markedly different from other neutral molecules [91]. They should also be distinguished from amphoteric compounds, such as alumina, which are referred to as semipolar [91] and are only zwitterionic depending on the pH [6]. Hu and Haraguchi [92] first used the taurine-conjugated bile salts sodium taurodeoxycholate (NaTDC) and sodium taurocholate (NaTC), whose properties are summarised in Table 1.1 and structures are given in Figure 1.2. At pH 4.5 they consisted of a weak positive amino group and a strong negative sulfonate group.

Subsequently, zwitterionic surfactants used in ZIC consisted of a long hydrophobic chain and a hydrophilic head group with strong charges in close proximity, usually

Table 1.1 Physical properties of zwitterionic surfactants used in ZIC.

Zwitterionic Surfactant	FW	cmc (mM)	Aggregation Number	Reference
C12SB	335.5	3.0	-	[93]
C14SB	363.6	0.32	-	[93]
CHAPS	614.9	8	10	[90]
CHAPSO	630.9	8	11	[90]
C14PC	379.5	~0.12	-	[94]
C12PC	315.5	~1.5	50-60	[94]
NaTDC	498.68	4.0	3.5	[95]
NaTC	514.68	~7	9-10	[96]

NaTC

(Sodium Taurocholate)

NaTDC

(Sodium Taurodeoxycholate)

CHAPS

(3-[(3-cholamidopropyl)
dimethylammonio]-1-propanesulfonate)
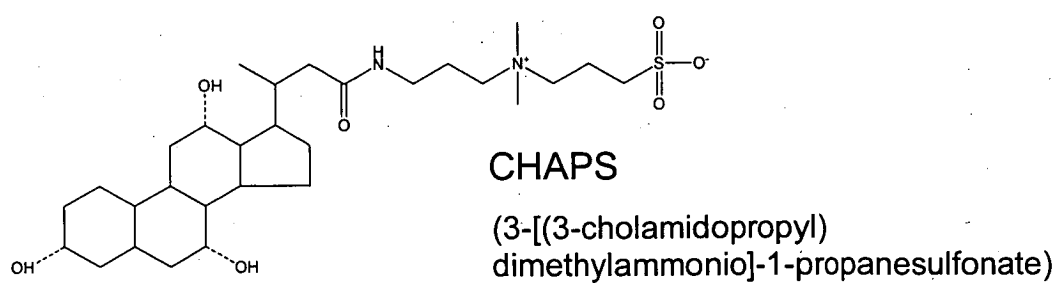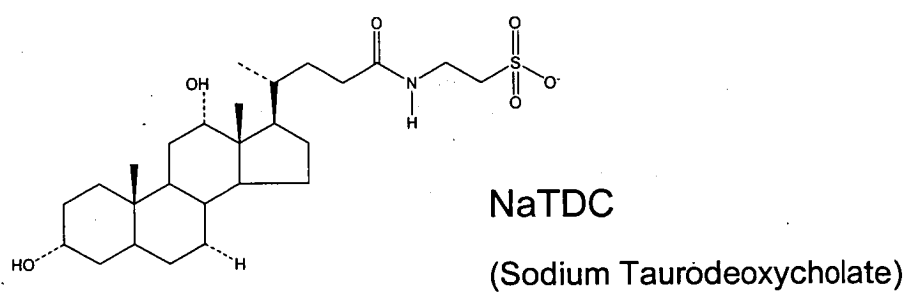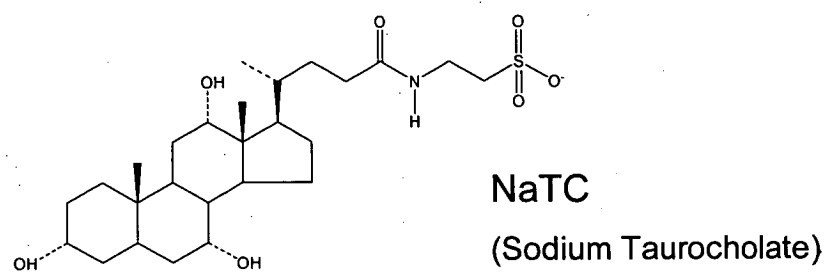
Figure 1.2 Structure of zwitterions used in ZIC.
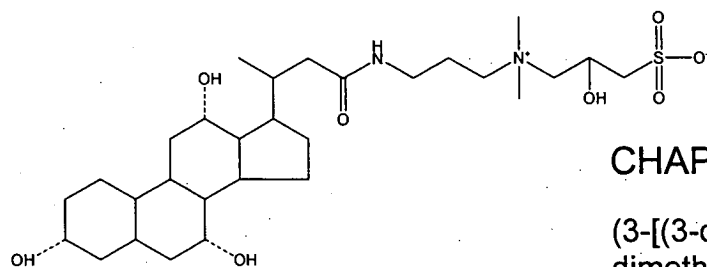
CHAPSO

(3-[(3-cholamidopropyl)
dimethylammonio]-2-hydroxy-1-
propanesulphonate)
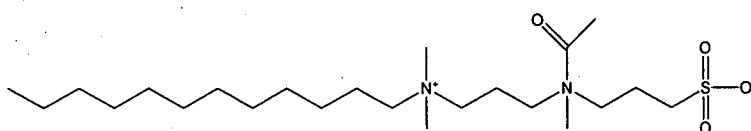
Ammonium sulfobetaine-3

(N-[3-acetyl-3-(sulfopropyl)aminopropyl]-
N,N-dimethyldodecanaminium hydroxide)
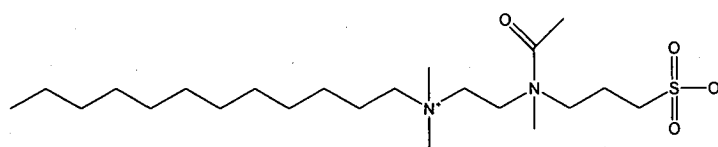
Ammonium sulfobetaine-1

(N-[2-acetyl(3-sulfopropyl)amino]ethyl]-
N,N-dimethyldodecanaminium hydroxide)

Figure 1.2 Structure of zwitterions used in ZIC.
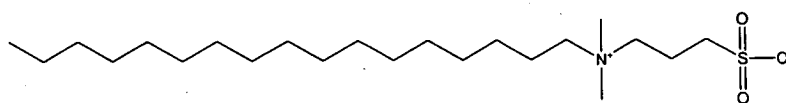
C14SB

3-(N-tetradecyl-N,N-dimethylammonio)propanesulfonate
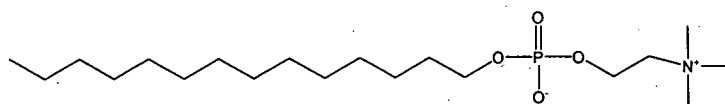
C14PC

N-tetradecylphosphocholine

Figure 1.2 Structure of zwitterions used in ZIC.

separated by a three methylene group bridge. The structures of the commonly used

zwitterionic surfactants: 3-(N-tetradecyl-N,N-dimethylammonio)propanesulfonate

(C14SB); N-[3-acetyl-3-(sulfopropyl)aminopropyl]-N,N-dimethyldodecanaminium

hydroxide (ammonium sulfobetaine-3); N-[2-acetyl(3-sulfopropyl)amino]ethyl]-N,N-

dimethyldodecanaminium hydroxide (ammonium sulfobetaine-1); 3-[(3-

cholamidopropyl)dimethylammonio]-1-propanesulfonate (CHAPS); 3-[(3-

cholamidopropyl)dimethylammonio]-2-hydroxy-1-propanesulphonate (CHAPSO); and

N-tetradecylphosphocholine (C14PC), are given in Figure 1.2, with their

physicochemical properties listed in Table 1.1. It can be seen that the length of the

chain affects the critical micelle concentration (cmc), whereby longer-chained

surfactants generally have a lower cmc and the bulkier CHAPS and CHAPSO have a

higher cmc. Weers *et al.* [97] stated that the cmc for sulfobetaines decreases by

approximately one order of magnitude for each addition of two carbons to the

surfactant tail group. The aggregation number is dependent on the surfactant

concentration and ionic strength, except where the system contains only spherically-

shaped micelles [98].

C12SB and C14SB are linear surfactants while CHAPS and CHAPSO are steroidal,

forming linear and reversed helices similar to bile salt micelles, respectively [89,90].

Hu *et al.* [89] observed no reversed-phase activity with a CHAPS-micelle coated

column in the separation of amino acids and assumed this was due to the hydrophilic

part of the micelle being inner.

1.4.1.2   General Ion Uptake Properties of Zwitterions

Despite the neutral nature of the zwitterionic surfactants described, and their relative indifference to ionic strength [90], they do have the ability to bind electrolyte ions, shown unambiguously by the results of several studies using methods including radioactive tracer self-diffusion and fluorescence-quenching [99-104]. Kamenka *et al.* [100] found that anions bind more strongly than cations to zwitterionic surfactants with an inner positive and outer negative charge, with cation binding being relatively weak and non-specific [105]. Chevalier *et al.* [106] observed that although the zwitterionic micelles became charged in the presence of NaCl due to the different binding constants for Na^+ compared with Cl^-, interactions between micelles were negligible. For a C12SB surfactant, binding constants for Na^+ and Cl^- were found to be 0.43 and 0.56 M^{-1}, respectively [100]. Zwitterionic surfactants where the head group was $-COO^-$ instead of $-SO_3^-$ were found to bind anions more strongly [100], possibly due to the $-COO^-$ being weakly charged and therefore less repellent of anions.

Ion binding to zwitterionic micelles has been thought to be purely electrostatic, but these electrostatic effects are extremely short range [100]. The strength of binding of anions to long chain zwitterionic micelles was found to increase across the sequence $SO_4^{2-} < Cl^- < Br^- < I^-$ [107]. These data were supported by published binding constants (with C14SB) of 1.5, 4.3, 21 and 40 M^{-1} for Na^+, Br^-, I^- and ClO_4^-, respectively [108].

CHAPS-coated stationary phases have been shown to have a much lower affinity for highly polarisable ions, such as I^- and SCN^-, compared to that of C14SB, and

combining the two surfactants on the stationary phase has been explored [109]. The greater distance between opposite charges on ammonium sulfobetaine-1 also resulted in a lower affinity for highly polarisable ions compared with C14SB [110]. This is contrary to that found by Kamenka *et al.* [100], who found that ion binding increased with an increasing number of carbons between the opposite charges. However, they studied surfactants with a COO⁻ end group, with charges spaced by up to 10 carbons. Thus eventually, particularly with a weak negative charge, the surfactant would behave more like cationic surfactants, which are known to give long retention times for anions [12].

As stated above, the zwitterionic surfactants with an outer negative and an inner positive charge showed a greater affinity for anions over cations, with cations only being able to be separated into charge groups [105,111]. Alternatively, a phosphocholine-type surfactant (N-tetradecylphosphocholine (C14PC)) was investigated to create the stationary phase [112-114]. This surfactant is analogous to C14SB used for the analysis of anions, but the charge positions are reversed to give the surfactant a negative inner charge (phosphonate group) and a positive outer charge (quaternary ammonium). It was found that while the C14SB showed a higher selectivity for anions, the C14PC displayed a high selectivity for cations. Also, addition of electrolyte to the mobile phase diminished the selectivity of the C14PC for anions, analogous to the effect observed on selectivity of cations for the C14SB [115].

The difference between anion and cation uptake by the zwitterionic surfactants has been investigated by measuring the zeta potential. The use of zwitterionic surfactants as electro-osmotic flow (EOF) modifiers in capillary electrophoresis (CE) has revealed that the zeta potential arising on a zwitterionic-coated capillary could be modulated by the addition of different anions in the electrolyte [81]. It was suggested that different electrolyte anions became incorporated to different extents into the zwitterionic layer and this in turn altered the zeta potential and hence the EOF. The existence of such a zeta potential has also been suggested by the calculations of Patil and Okada [116] and experimental data of Iso and Okada [117-119]. Such processes of anion incorporation into the zwitterion in CE are similar to those governing retention in ZIC, thus measurements of the zeta potential can give further information about the ZIC retention mechanism. Jiang and Irgum [120] measured the zeta potential of a covalently-bound zwitterionic stationary phases by photon correlation spectroscopy where similar trends were seen. However, these results were not clear due to the imbalance in the number of positive and negative charges on the stationary phase.

1.4.1.3   Dynamic Stationary Phases in ZIC

The most common preparation of the stationary phase in ZIC is the hydrophobic adsorption of a zwitterionic surfactant to a hydrophobic column, such as a C18 octadecylsilica (ODS) column, by pumping a solution of the surfactant through the column until breakthrough is observed, which is generally monitored using UV detection [89,111,121].

The adsorption process of various zwitterionic surfactants used in ZIC has been studied, with similar characteristics observed for all [121]. It has been proposed that the breakthrough of micelles did not occur until the stationary phase had become saturated with monomers, and although a micellar coating solution may have been used, only monomers were adsorbed [121]. It was proposed that as monomers are adsorbed the micelles break up (keeping the monomer concentration constant), forming more monomers that will adsorb until the stationary phase is saturated. The properties of the stationary phase were dependent on the total amount of surfactant adsorbed, not the concentration of the coating solution, nor whether it was micellar or not. However, those surfactants with a low cmc were found to be more readily adsorbed onto the column, and the bulkiness of CHAPS and CHAPSO compared with that of C12SB and C14SB contributed to lower adsorption ability [121].

Adsorption was observed to be less for the linear alkyl betaines than for CHAPS and CHAPSO and the amount of surfactant adsorbed varied considerably, with 461, 480, 777 and 1045 μmol·column^{-1} adsorbed for CHAPS, CHAPSO, C12SB and C14SB, respectively. The best separations of inorganic anions were achieved on the C14SB stationary phase [121]. Ammonium sulfobetaine-1 was found to have a similar adsorption rate to C12SB, adsorbing 768 and 771 μmol·column^{-1}, respectively [110].

Following coating of the stationary phase, the column must be rinsed to remove excess surfactant. A certain amount of surfactant is initially desorbed [111], thus a small

amount (~0.1%) is added to all rinses and mobile phases to maintain a saturated stationary phase [122].

The surface charge density resulting from the adsorption of zwitterionic surfactants is much higher than that found with singly-charged surfactants in ion-interaction chromatography, due to the lower repulsion between surfactant molecules [111]. However, as interactions of analytes with a zwitterionic stationary phase are weak, it is necessary to have a high capacity for efficient separations to be achieved.

A similar stability and reproducibility to the sulfobetaine-coated stationary phases was found for phosphocholine-coated column [112], while double-chained surfactants have been shown to form a coating with a stability similar to permanent coatings. However when compared with single-chained surfactants, double-chained surfactants are more likely to form bilayers rather than spherical micelles [86]. This may be a useful alternative to the single-chained surfactants used in the dynamic coating method in ZIC to date.

1.4.1.4   Permanent Stationary Phases in ZIC

There have been relatively few attempts at producing chemically-bonded stationary phases for ZIC [120,123-126], with problems occurring in the ability to achieve a stationary phase with an even charge balance. Yu *et al.* [123] synthesised a stationary phase containing amine and carboxylate groups with 3 carbons between them. This

stationary phase was pH dependent, behaving as a cation-exchanger at pH values less than 4.5, and as an anion-exchanger above pH 7, while in between these values the stationary phase was zwitterionic. Jiang and Irgum [120,125] utilised various reaction schemes to obtain covalently-bound zwitterionic stationary phases, all based on the attachment of zwitterionic (sulfobetaine) monomers to a 2-hydroxyethyl methacrylate (HEMA) base. The first attempt [125] was hindered by a side reaction resulting in a percentage of weak anion-exchange groups. Although later attempts [120] resulted in the ability to separate anions with ZIC selectivity, and also cations, there were still difficulties in characterising the material and obtaining an exact charge balance ratio between positive and negative charges. Nevertheless, these stationary phases still offer unique selectivities and retention patterns that differ from ion-exchange.

A commercial covalently-bonded ZIC sulfobetaine stationary phase has recently become available [127] that is marketed for the separation and purification of proteins and peptides, taking advantage of the relatively weak electrostatic effects of the stationary phase and pH independence. This stationary phase has a polymethacrylate backbone with covalently bonded functional groups, allowing the use of a solvent mobile phase, unlike the dynamic, hydrophobically-bonded stationary phases used in ZIC, which have been shown to desorb with mobile phases containing >13% acetonitrile [128].

1.4.2 Effect of the Mobile Phase

1.4.2.1   Water Mobile Phase

The opposite charges on the stationary phase exert an effect on both anions and cations in a sample, although interaction is stronger for anions with sulfobetaine-type surfactants [111]. There is no need for an eluting ion in the mobile phase with this technique because the electrostatic effect of this type of stationary phase is low compared to a singly-charged stationary phase. Also, the analyte anion is attracted to the positive charge, but feels simultaneous repulsion from the negative charge [89]. Hence it is possible to use a pure water mobile phase, which has the major advantage of decreased baseline noise and lower detection limits [129]. However, as with the crown ether stationary phases [130], to maintain electroneutrality each analyte anion must be accompanied by a counterion and with no cations in the mobile phase, these counterions must come from the sample. Thus, if there are two anion and two cation species present in the sample, there is the possibility of four peaks in the chromatogram, one for each possible combination of "ion-pairing-like" forms [89]. However, it was found that not all combinations were observed, and that the formation of eluted "ion-pairs" could be predicted by referring to the molal energies (ΔG) of the cations and anions [109]. The most stable "ion-pairing-like" forms are those with the lowest molal energies (ΔG_{min}) for the anion and cation. However, if these pairs form preferentially, then what remains are the pairs with the greatest molal energies (ΔG_{max}),

i.e. the most unstable pairs. Hence, the most prolific are the medium-stable "ion-pairs". The medium stable "ion-pairs" are combinations of the ΔG_{min} for the cation and ΔG_{max} for the anion and vice versa, and these are the peaks observed with the greatest area in the chromatogram.

The retention of an anion with a water mobile phase is therefore dependent not only on its own interaction with the stationary phase, but also how much interaction its counter-cation has with the stationary phase. Thus, a Cl^- ion paired with a Na^+ ion has a shorter retention than one paired with a Mg^{2+} ion. As sulfobetaine-type stationary phases only separate cations into charge groups, "ion-pairs" of Na^+-Br^- and K^+-Br^- are eluted together [131].

In a sample containing many anions and cations, there are many possible "ion-pair" combinations, and even if some are not seen, the chromatogram may still be quite complex and elucidation has required a combination of conductivity and photodiode array UV detection [109], or ICP-AES [131-134].

The pairing of ions can be controlled by the addition of a specific salt to the sample, i.e. $NaNO_3$ or $MgSO_4$, that is in excess compared with other ions in the solution [134,135]. In the case of $NaNO_3$, all analyte anions and cations would be preferentially eluted as "ion-pairs" with Na^+ and NO_3^-, respectively, thus one peak would be observed for each analyte. $MgSO_4$ may be used instead of $NaNO_3$ to achieve a better separation between anions (as they are retained longer with Mg^{2+} compared with Na^+). A disadvantage of

this technique is that a large peak is seen for the added ion, which is in excess, and this could be detrimental to the chromatographic analysis [136]. An alternative approach to the problem is the use of a small pre-column to convert the counter-cation of the sample anions to a single common species [133,137].

The partitioning effect seen for anions on the betaine-type coated columns was also observed for cations on a phosphocholine-type stationary phase [112], with each cation eluted in more than one peak, depending on the number of anions in the solution. Again, this could be overcome by adding an excess of a particular anion to the sample, for example, SCN⁻ [112].

Utilisation of the greater sensitivity provided by a water mobile phase also had the disadvantage of peak splitting at trace analysis level [129,138,139]. This was proposed to be due to analyte ions having a shorter retention time in the diffuse layer compared with the Stern layer, which is not seen in conventional ion-exchange due to the large number of eluting ions in the mobile phase.

1.4.2.2   Electrolyte in the Mobile Phase

Hu and Haraguchi [140] found the use of a phosphate buffer in the mobile phase improved the separation coefficient of both inorganic ions and organic zwitterions (proteins). The pH of this mobile phase had little effect on the retention of strong anions as expected, due to the charges on the stationary phase being strong. Increasing the concentration of the mobile phase was found to increase retention and it was

assumed that interaction with the charges occurred more easily in an ionic environment compared with pure water. Above a certain concentration, there was little further effect on retention [136].

Mobile phases containing electrolytes suitable for suppressed conductivity detection (e.g. $NaHCO_3$ and NaB_4O_7) were found to maintain a sensitivity similar to a water mobile phase, without the formation of a complex set of peaks. Each anionic analyte was eluted with the mobile-phase cation, as seen in conventional ion-exchange [136,141]. Na_2SO_4 and Na_3PO_4 were also investigated as mobile phases and showed selectivities and retention times which were similar to that of $NaHCO_3$ [136]. Hydroxide was utilised as a suppressible mobile phase for this system [142], although like $NaHCO_3$, it should be used with a polystyrene/divinylbenzene substrate column since silica-based columns should not be operated above pH 8. Na^+, Li^+, Ba^{2+} and Ca^{2+} hydroxide mobile phases were utilised and it was found that the divalent mobile-phase cations resulted in a better separation and longer retention than the monovalent variants.

Acidic mobile phases selectively retained NO_2^- over other ions, which was thought to be due to the formation of HNO_2 [143,144]. The slopes of log k' *versus* log [mobile phase] plots in this case were much more negative in comparison to other mobile phases, and it was proposed that this was due to protonation of the sulfonate group, resulting in ion-exchange effects.

An ampholytic mobile phase (histidine at pH = pI) was able to buffer the system as well as provide counterions to the anions and cations in the sample [145].

Matrix elimination, a technique common in ion chromatography whereby the mobile-phase ions are matched to the matrix ions such that they are unretained on the stationary phase, was applied to ZIC and was found to be suitable for the analysis of seawater. Increasing the concentration of the mobile phase used (containing Na^+, K^+, Mg^{2+}, Ca^{2+}, Cl^- and SO_4^{2-}) resulted in a decrease in retention of analytes [146]. This is similar to that seen for the increase in ClO_4^- concentration [125]. Patil and Okada [116] stated that the stationary phase can be modulated between one that acts as a cation-exchanger by adding a large and poorly-hydrated anion to the mobile phase (such as ClO_4^-) or as an anion-exchanger by adding small and well-hydrated anions to the mobile phase (such as Cl^-).

The addition of electrolyte to the mobile phase resulted in a diminished retention of cations on the sulfobetaine-type stationary phase [107,135,147] and a similar reduction of anion retention on a phosphocholine-type stationary phase [112].

1.4.3 Applications

The stationary phase synthesised by Yu *et al.* [123] containing amine and carboxylate groups with a 3 carbon spacer was used successfully for the separation of nucleotides, but was not applied to inorganic ions.

The taurine-conjugated bile salts, sodium taurodeoxycholate (NaTDC) and sodium taurocholate (NaTC), were found to be suitable for the simultaneous separation of inorganic anions and cations [92]. With an aqueous $CuSO_4$ mobile phase the highly polarisable ions I^- and SCN^- were eluted in less than 10 minutes. A mixed coating of CHAPS and NaTDC eliminated the need to control the pH for the simultaneous separation of anions and cations, with the CHAPS moiety effectively separating the anions, and cations were separated via an ion-exchange mechanism with the anionic NaTDC [148].

CHAPS-coated stationary phases have been shown to be suitable for relatively rapid elution of the highly polarisable I^- and SCN^- ions [109]. The C14SB stationary phase displayed a high affinity for these ions resulting in impracticably long retention times with a water mobile phase, and had the advantage over CHAPS in that baseline separation of NO_2^-, Br^- and NO_3^- could be achieved in a reasonable time (~5 minutes). A stationary phase consisting of both CHAPS and C14SB was utilised to combine the advantages of each and produced a better separation of NO_2^-, Br^- and NO_3^- with a water mobile phase than CHAPS alone, and could simultaneously separate a standard solution of all analytes, from SO_4^{2-} to SCN^-, in a reasonable run time (<15 minutes). This stationary phase was applied to the determination of inorganic ions at sub-ppb levels [138], as well as to study the retention mechanism [129].

Ammonium sulfobetaine-1, which has a greater distance between opposite charges, also resulted in a decreased retention for the more polarisable anions, such as I^- and

32

SCN⁻, compared with C14SB [110]. Interestingly, a SO_4^{2-} mobile phase resulted in a lower k' than a Cl⁻ mobile-phase, with the k' for I⁻ being approximately 16 and 12, respectively. Additionally, slopes of log k' *versus* log [eluent] plots were slightly positive for C12SB, but were negative for ammonium sulfobetaine-1. This suggested that the charges became increasingly independent of each other as the distance between them increased, resulting in a shift from a ZIC mechanism to that of ion-exchange.

ZIC has been shown to be useful for the analysis of high ionic strength samples, due to the lack of effect of higher mobile phase concentrations on retention, allowing the analysis of Br⁻, NO_3^- and I⁻ in saline matrices [136,144,146,149].

Biological samples have also received attention, including human blood serum for theophylline and caffeine [150] and human saliva for inorganic ions and amino acids [140]. Direct injection was possible due to the hydrophilic outer layer of the zwitterionic stationary phase preventing proteins from entering the internal hydrophobic region. These stationary phases eliminated the need for solvent in the mobile phase in reversed-phase liquid chromatography of organic analytes, due to the decreased hydrophobicity of the surface. The presence of the zwitterionic functional groups resulted in a decrease in the retention of nucleosides and their bases, and an increase in the retention of inorganic ions [151].

As the sulfobetaine-type surfactant used for the analysis of anions was effective only in separating cations into charge groups [129,131], other methods for cation separations

were investigated. Transition metal ions were separated as anionic complexes on this stationary phase with a mobile phase containing 0.1 M $NaClO_4$ and 20mM tartaric acid [116], but for direct separation of cations, stationary phases were investigated with various positions, spacing or acid-base strength of the charged functional groups on the zwitterion [129]. Altering the acid-base strength of the functional groups [92] or utilising a mixture of anionic and zwitterionic surfactants on the stationary phase [152] allowed the separation of cations, but this was attributed to additional ion-exchange interactions introduced into the separation. In an alternative approach, phosphocholine-type surfactants with an inner negative phosphonate group and an outer quaternary ammonium group exhibited a greater affinity for cations over anions [112]. Separation of inorganic divalent cations was achievable with this surfactant and a water mobile phase. The elution order was found to be $Ba^{2+} < Mg^{2+} < Ca^{2+}$, which differs to the selectivity observed in ion-exchange ($Mg^{2+} < Ca^{2+} < Ba^{2+}$ [6]). Poor peaks and reproducibility were found for Mn^{2+} and Zn^{2+}, which were separated from Cu^{2+} in the order $Cu^{2+} < Mn^{2+} < Zn^{2+}$. This type of stationary phase was also used for the analysis of inorganic acids with a water mobile phase [153].

A summary of the applications for ZIC are detailed in Table 1.2.

Table 1.2 Summary of applications of ZIC to real samples.

Solutes (min)	Sample Matrix	Column	Coating	Eluent	Detection	Ref.
I^- (~27)	Artificial seawater (0.6M NaCl)	CERI ODS L-column 250 × 4.6 mm ID	CHAPS and C14SB two-step coating	Dilute electrolyte	Direct UV at 210 nm	[136]
SO_4^{2-} (~2), Cl^- (~3), NO_2^-(~5), Br^- (~11), NO_3^- (~17)	Snow and rainwater	As above	C14SB	10 mM $Na_2B_4O_7$	Suppressed conductivity	[141]
Br^- (~4), NO_3^- (~6), I^-(~30)	Seawater	As above	C14SB	20-fold-diluted artificial seawater	UV at 210nm	[146]
Br^- (4.3)	Seawater	As above	C14SB	water	conductivity	[149]
Cu^{2+}, Pb^{2+}, Zn^{2+}, Ni^{2+}, Co^{2+}, Cd^{2+}, Mn^{2+}	-	Wakosil 5C8 150 × 4.6 mm ID	C12SB	2mM C12SB, 20mM tartaric acid, 0.1 M $NaClO_4$ (pH = 4)	PAR post-column reaction at 540 nm	[116]
Cl^- (~5), Br^- (~6), NO_3^- (~7)	Radish	CERI ODS L-column 250 × 4.6 mm ID	C14SB	water	conductivity	[134]

cytosine (~2.5), guanine (~3.5), adenine (~4.5), deoxyadenosine (8.5)	DRNA from salmon spermary	As Above	C14SB	water	UV at 210 nm	[128]
Theophylline (~9), caffeine (~16)	Human blood serum	As above	CHAPS	0.2 mM Na$_2$HPO$_4$, pH 7.4	UV at 273 nm	[150]
Na$^+$ (~5), Ca^{2+} (~6), Cl$^-$ (~5), NO$_3^-$ (~6.8), SO$_4^{2-}$ (~4.5)	Tap water	As above	CHAPS	water	conductivity	[109]
cytosine (~2.5), guanine (~3.5), adenine (~4.5), deoxyadenosine (8.5)	DRNA from salmon spermary	As Above	C14SB	water	UV at 210 nm	[128]
Speciation of boron	50 mM boric acid solution	As Above	CHAPSO	water	refractometry	[154]

Tryptophan (~11), NO$_2^-$ (~4), NO$_3^-$ (~5), I$^-$ (~8), SCN$^-$ (~13)	Human saliva	CERI ODS L-column 250 × 4.6 mm ID	CHAPS micelles	Phosphate buffer	UV at 230 nm	[140]
NO$_2^-$ (~11), Br$^-$ (~5), NO$_3^-$ (~6.5)	Seawater	As Above	C18SB	20 mM HCl	UV at 210nm	[144]
I$^-$ (~4), SCN$^-$ (~6)	Human saliva	Nomura Chemical Develosil ODS-5 150 × 0.35 mm ID	CHAPS	water	UV at 230 nm	[89]
Inorganic acids (NO$_X$, SO$_X$, HCl)	Aerosols	CERI ODS L-column 250 × 4.6 mm ID	C14PC	water	conductivity	[153]
H$^+$, Ba^{2+}, Ca^{2+}, Mg^{2+}	Hot-spring water	As Above	C16PC	water	conductivity	[114]

1.4.4 Proposed Mechanisms

There have been several explanations offered for the ZIC retention mechanism. These have involved a number of concepts, including: simultaneous electrostatic attraction and repulsion of analyte ions from the two oppositely-charged functional groups of the zwitterion [89]; the formation of "ion-pairs" between oppositely-charged ions in solution [131] (see Figure 1.3); and the establishment of a binary electrical double layer comprising the accumulation of oppositely charged ions (from the mobile-phase electrolyte) around the charge centres of the zwitterion [129]. Other possible contributors to the mechanism are ion-exclusion effects, induced ion-exchange, and complex formation.

The binary electrical double layer (binary-EDL) mechanism was based on the Gouy-Chapman double layer model and is illustrated in Figure 1.4a for anion and cation-exchange systems [113,146,155]. A depiction of the potential proposed for the zwitterionic stationary phase is shown in Figure 1.4b. According to this model, ZIC differs from ion-exchange in that the stationary phase is neutral and mobile-phase counterions are not required to maintain electroneutrality. Thus, the mobile-phase anions and cations are counterions to each other whereby the number of cations in the cation-EDL must equal the number of anions in the anion-EDL (illustrated in Figure 1.5).
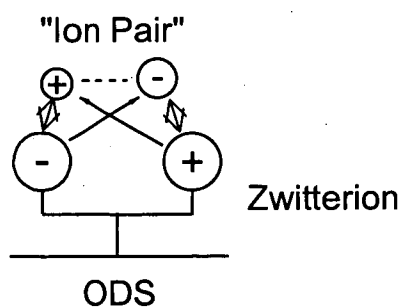
Figure 1.3 The interaction of analytes with the zwitterionic stationary phase. The simultaneous electrostatic repulsion/attraction and formation of the "ion-pair" is illustrated, where double- and single-headed arrows indicate attraction and repulsion to/from the stationary phase, respectively.

(a)
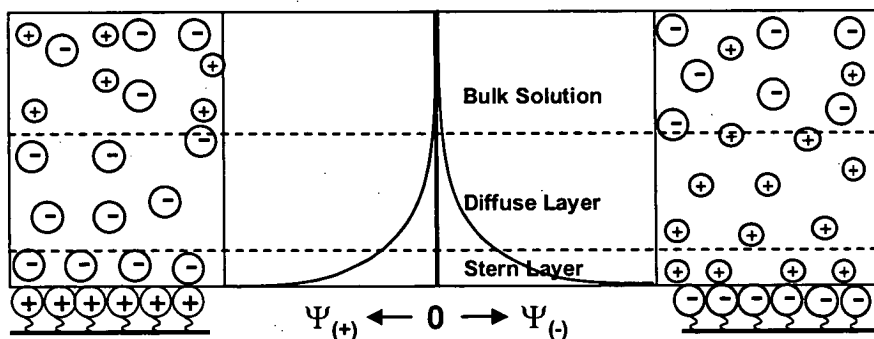
(b)
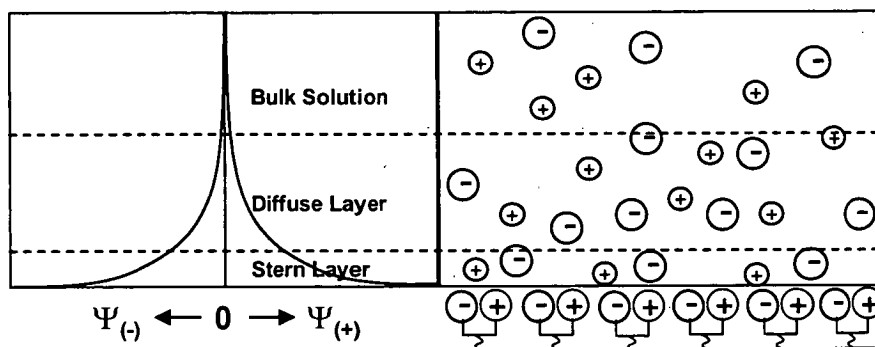
Figure 1.4 Electrical double layer created by (a) a mono-functional stationary phase and (b) a bi-functional stationary phase. The electrostatic potential, Ψ, is given as a function of distance from the stationary phase.
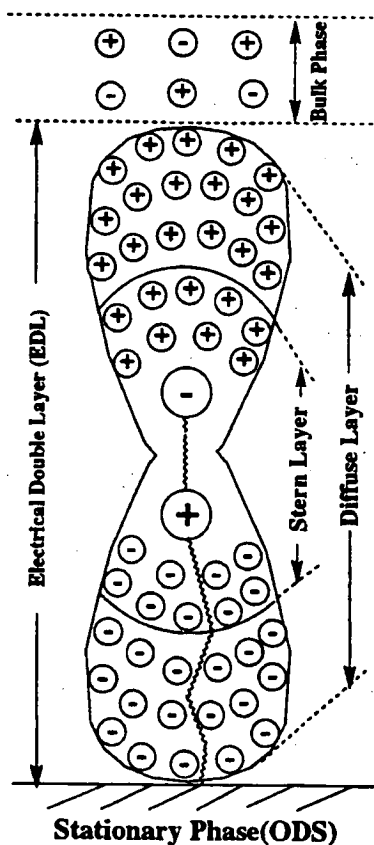
Figure 1.5 Diagram shows the electrical double layer established by the eluent cations and eluent anions retained by the negative and positive charge on the zwitterion respectively. Reproduced from [146].

The large number of ions in each EDL was explained by the extremely strong and long-ranging nature of the electrostatic force.

In the case of a zwitterionic stationary phase in which the negative functional group is outermost (such as the sulfobetaine-type, C14SB), the EDL surrounding the negative functional group and comprising cations repels analyte cations, hence their lack of retention with this stationary phase. It allows the partition of analyte anions, as they form "temporary ion-pairs" with cations in the cation-EDL [89]. As the formation of these "ion-pairs" is in equilibrium, ions feel repulsion from the anion-EDL (surrounding the cationic functional group of the zwitterion) as they dissociate. Those analyte anions with a high propensity for forming neutral ion-pairs show strong retention, while those with a low propensity are expelled due to repulsion from the anion-EDL. Hence the following retention order for ZIC is explained in terms of increasing propensity for ion-pair formation [89], and for anions is [111]:

$$F^- \sim IO_3^- \sim SO_3^{2-} \sim SO_4^{2-} \sim CH_3COO^- < S_2O_3^{2-} < Cl^- < NO_2^- < Br^- < NO_3^- < ClO_3^- < I^- <$$
$$SCN^- < ClO_4^- \qquad\qquad\qquad (1.5)$$

and for cations is:

$$K^+ \cong Na^+ < NH_4^+ < Li^+ < Tl^+ < Ag^+ < Ba^{2+} \cong Sr^{2+} < Co^{2+} < Ca^{2+} < Cu^{2+} < Cd^{2+} < Zn^{2+} <$$
$$Ce^{3+} \qquad\qquad\qquad (1.6)$$
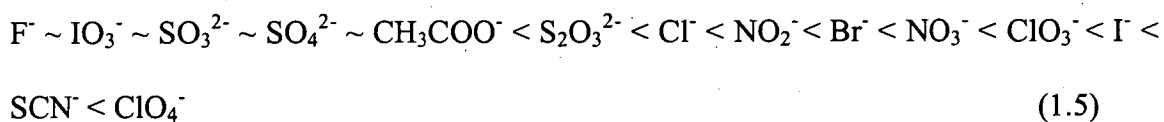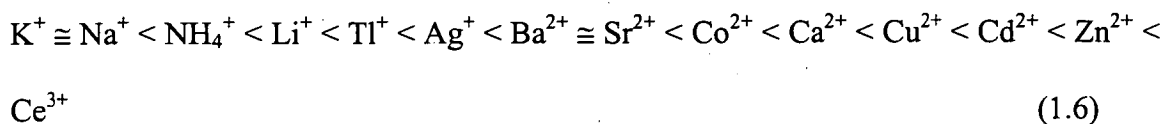
This selectivity follows the Hofmeister (chaotropic or lyotropic) series [156,157], which arranges ions in order of their effects (eg. salting-out effects) on the solubility of proteins. The term "chaotropic" refers to an increase in entropy resulting from disruption of the water structure surrounding these ions in solution. Chaotropic anions have a large number of electrons spread over an appreciable volume such that the electrons are not tightly held by the nucleus and can induce dipoles in water molecules, disrupting their structure. Hence, highly chaotropic ions have a great ability to interact and form ion-pairs.

The increase in retention with increasing mobile phase concentration was proposed to be due to an increase in the thickness of the double layers [142], and above a certain threshold concentration of electrolyte the binary-EDL becomes saturated resulting in no further change in retention [136,146]. This model suggests that analyte ions interact with ions in a double layer, meaning that another double-layer should form at the first double layer. The possibility of ions forming strong interactions with other free ions in solution is questionable.

Okada *et al.* [116,158,159] proposed a mechanism based on an ion-pair model describing the retention of small, largely-hydrated ions and a partition model describing retention of large and poorly-hydrated ions and attempted to apply a mathematical model to the mechanism. This will be discussed further in Chapter 6.

1.5 Aim of the Project

Despite the previous studies discussed above, the lack of a systematic and comprehensive set of analyte retention data covering a wide range of mobile phase compositions and analytes has made it difficult to fully characterise ZIC and to develop a mechanism which applies under all conditions. The detailed effects of the mobile-phase cation and anion on the retention of analyte anions are not well known and the nature of the stationary phase has not yet been examined fully. The aim of this research was to address the deficiencies in the existing retention data and knowledge of the system, and to develop a physically acceptable mechanistic model that explains all experimental data and is applicable to all types of analyte.

1.6 References

(1) B. Lopez-Ruiz, J. Chromatogr. 881 (2000) 607-627.

(2) M.J. Shaw. University of Plymouth, PhD Thesis, 2000.

(3) R.P. Singh, S.A. Smesko, N.M. Abbas, J. Chromatogr. A 774 (1997) 21-35.

(4) K. Ito, Anal. Chem. 69 (1997) 3628-3632.

(5) H. Small, T.S. Stevens, W.C. Bauman, Anal. Chem. 47 (1975) 1801-1809.

(6) P.R. Haddad, P.E. Jackson. *Ion Chromatography: Principals and Applications.*, Elsevier, Amsterdam: 1990.

(7) J. Stahlberg, Anal. Chem. 66 (1994) 440-449.

(8) J. Stahlberg, J. Chromatogr. A. 855 (1999) 3-55.

(9) L.M. Nair, R. Saari-Nordhaus, R.M. Montgomery, J. Chromatogr. A 789 (1997) 127-134.

(10) A. Klingenberg, A. Seubert, J. Chromatogr. A 946 (2002) 91-97.

(11) R.E. Barron, J.S. Fritz, J. Chromatogr. 316 (1984) 201-210.

(12) R.E. Barron, J.S. Fritz, J. Chromatogr. 284 (1984) 13-25.

(13) T. Cecchi, F. Pucciarelli, P. Passamonti, Anal. Chem. 73 (2001) 2632-2639.

(14) Z. Iskandarani, D.J. Pietrzyk, Anal. Chem. 54 (1982) 2427-2431.

(15) T. Takeuchi, E.S. Yeung, J. Chromatogr. 370 (1986) 83-92.

(16) D. Connolly, B. Paull, J. Chromatogr. , A 917 (2001) 353-359.

(17) L. Guo, M.Y. Ding, J. Chromatogr. A 946 (2001) 169-175.

(18) Z. Iskandarani, D. Pietrzyk, Anal. Chem. 54 (1982) 1065-1071.

(19) J. Stahlberg, A. Bartha, J. Chromatogr. A 456 (1988) 253-265.

(20) A. Bartha, J. Stahlberg, J. Chromatogr. 535 (1990) 181-187.

(21) J. Narkiewicz-Michalek, Chromatographia 35 (1993) 527-538.

(22) A. Bartha, J. Stahlberg, J. Chromatogr. 668 (1994) 255-284.

(23) J.G. Chen, S.G. Weber, L.L. Glavina, F.F. Cantwell, J.Chromatogr. A. 656 (1993) 579-576.

(24) C.P. Terweij-groen, S. Heemstra, J.C. Kraak, J. Chromatogr. 161 (1978) 69-82.

(25) T. Cecchi, F. Pucciarelli, P. Passamonti, Chromatographia 53 (2001) 27-34.

(26) T. Cecchi, F. Pucciarelli, P. Passamonti, J. Liq. Chromatogr. & Rel. Tech. 22 (1999) 969-979.

(27) T. Cecchi, F. Pucciarelli, P. Passamonti, J. Liq. Chromatogr. & Rel. Tech. 21 (1998) 2423-2433.

(28) T. Cecchi, F. Pucciarelli, P. Passamonti, J. Liq. Chrom. Rel. Technol. 24 (2001) 291-302.

(29) A. Bartha, G. Vigh, H.A.H. Billiet, L. De Galan, J. Chromatogr. 303 (1984) 29-38.

(30) Y. Michigami, K. Fujii, K. Ueda, J. Chromatogr. A 664 (1994) 117-122.

(31) P.N. Nesterenko, Haddad P.R., Anal. Sci. 16 (2000) 565-574.

(32) A.B. Davankov, N.E. Ogneva, V.M. Laufer, Khimicheskaya Promyshlennost (Chemical Industry) N11 (1951) 16.

(33) E.E. Kathmann, C.L. McCormick, J. Polym. Sci. 35 (1996) 243-253.

(34) C. Rollins, L. Jensen, A.N. Schwartz, Anal. Chem. 34 (1962) 711-712.

(35) M.J. Hatch, J.A. Dillon, H.B. Smith, Indust. Eng. Chem. 49 (1957) 1812-1819.

(36) M. Goto, N. Hayashi, S. Goto, Sep. Sci. Tech. 18 (1983) 475-484.

(37) S.S. Aldabbagh, R. Dybczynski, J. Radioanal. Nucl. Chem. 92 (1985) 37-50.

(38) R. Dybczynski, S.S. Aldabbagh, Analyst 112 (1987) 449-753.

(39) A. Samczynski, R. Dybczynski, J. Chromatogr. A 789 (1997) 157-167.

(40) H. Small, US Patent 4 (1978) 460.

(41) S. Mou, W. Huitong, Q. Sun, J. Chromatogr. A 640 (1993) 161-165.

(42) G. Revesz, P. Hajos, H. Csiszar, J. Chromatogr. A 753 (1996) 253-260.

(43) M.C. Bruzzoniti, E. Mentasti, C. Sarzanini, S. Cavalli, Chromatographia 46 (1997) 49-56.

(44) G.E. Taylor, J. Chromatogr. A 770 (1997) 261-271.

(45) E.F. Hilder, C.W. Klampfl, P.R. Haddad, J. Chromatogr. A 890 (2000) 337-345.

(46) D. Pietrzyk, S.M. Senne, D.M. Brown, J. Chromatogr. A 546 (1991) 101-110.

(47) H.G. Beere, P. Jones, Anal. Chim. Acta 293 (1994) 237-243.

(48) Q. Sun, H. Wang, S. Mou, J. Chromatogr. A 708 (1995) 99-104.

(49) O.V. Krokhin, A.D. Smolenkov, N.V. Svintosa, O.N. Obrezkov, O.A. Shpigun, J. Chromatogr. A 706 (1995) 93-98.

(50) A.M. Dolgonosov, J. Chromatogr. A 671 (1994) 33-41.

(51) A.M. Dolgonosov, A.N. Krachak, J. Chromatogr. A 640 (1993) 351-353.

(52) D.J. Pietrzyk and D.M. Brown, Anal. Chem. 58 (1986) 2554-2557.

(53) R. Zein, E. Munaf, T. Takeuchi, T. Miwa, Anal. Chim. Acta 335 (1996) 261-266.

(54) T. Takeuchi, R. Zein, E. Munaf, T. Miwa, J. Chromatogr. A 755 (1996) 37-42.

(55) E. Munaf, R. Zein, T. Takeuchi, T. Miwa, Chromatographia 43 (1996) 304-308.

(56) W. Hu, H. Haraguchi, Anal. Chim. Acta 289 (1994) 231-236.

(57) W. Hu, T. Takeuchi, H. Haraguchi, Anal. Chim Acta. 267 (1992) 141-146.

(58) W. Hu, T. Takeuchi, H. Haraguchi, Chromatographia 33 (1992) 63-66.

(59) W. Hu, H. Haraguchi, Bull. Chem. Soc. Jpn. 66 (1993) 1967-1970.

(60) T. Takeuchi, Safni, T. Miwa, J. Chromatogr. A 789 (1997) 201-206.

(61) W. Kopaciewicz, F.E. Regnier, J. Chromatogr. A 358 (1986) 107-117.

(62) T. Takeuchi, E. Suzuki, D. Ishii, Chromatographia 25 (1988) 480-482.

(63) G.L. Schmitt and D.J. Pietrzyk, Anal. Chem. 57 (1985) 2247-2253.

(64) C.T. Kresge, M.E. Leonowicz, W.J. Roth, J.C. Vartuli, J.S. Beck, Nature 359 (1992) 710-712.

(65) M. Gruen, A.A. Kurganov, S. Schacht, F. Schueth, K.K. Unger, J. Chromatogr. A 740 (1996) 1-9.

(66) D.M. Brown and D.J. Pietrzyk, J. Chromatogr. 466 (1989) 291-300.

(67) P.N. Nesterenko, A.I. Elefterov, D.A. Tarasenko, O.A. Shpigun, J. Chromatogr. A. 706 (1995) 59-68.

(68) M.G. Kiseleva, P.A. Kebets, P.N. Nesterenko, Analyst 126 (2001) 2119-2123.

(69) A.I. Elefterov, M.G. Kolpachnikova, P.N. Nesterenko, O.A. Schpigun, J. Chromatogr. A 769 (1997) 179-188.

(70) T.Y. Chou, M.H. Yang, J. Liq. Chrom. Rel. Technol. 19 (1996) 2985-2996.

(71) M.H. Yang, K.C. Chang, J.Y. Lin, J. Chromatogr. A 722 (1996) 87-96.

(72) M. Macka and J. Borak, J. Chromatogr. A 641 (1993) 101-113.

(73) J.H. Knox, J. Jurand, J. Chromatogr. 203 (1981) 85-92.

(74)   J.H. Knox, J. Jurand, J. Chromatogr. 218 (1981) 355-363.

(75)   J.H. Knox, J. Jurand, J. Chromatogr. 218 (1981) 341-354.

(76)   J.P. Ivey, J. Chromatogr. 287 (1984) 128-132.

(77)   M.H. Guermouche, D. Habel, S. Guermouche, Fluid Phase Equilib. 147 (1998) 301-307.

(78)   S.A. Zibas, L.J.C. Love, Anal. Chim. Acta. 299 (1994) 17-27.

(79)   W. Hu, H. Matsukami, A. Iles, K. Hasebe, S. Cao, K. Tanaka, Fres. J. Anal. Chem. 370 (2001) 426-428.

(80)   W. Hu, K. Hasebe, K. Tanaka, Fres. J. Anal. Chem. 367 (2000) 56-59.

(81)   N.E. Baryla, C.A. Lucy, Anal. Chem. 72 (2000) 2280-2284.

(82)   M. Mori, K. Kodama, W. Hu, S. Tanaka, J. Liq. Chromatogr. & Rel. Tech. 22 (1999) 3139-3150.

(83)   K.K.C. Yeung, C.A. Lucy, Anal. Chem. 69 (1997) 3435-3441.

(84)   M. Mori, W. Hu, J.S. Fritz, T. Hirohito, T. Kaneta, S. Tanaka, Fres. J. Anal. Chem. 370 (2001) 429-433.

(85)   M.A. Woodland, C.A. Lucy, Analyst 126 (2001) 28-32.

(86)   J.E. Melanson, N.E. Baryla, C.A. Lucy, Anal. Chem. 72 (2000) 4110-4114.

(87)   M. Mori, W. Hu, P.R. Haddad, J.S. Fritz, K. Tanaka, H. Tsue, S. Tanaka, Anal. Bioanal. Chem. 372 (2002) 181-186.

(88)   E.S. Ahuja, B.P. Preston, J.P. Foley, J. Chromatogr. B: Biomed. Appl. 657 (1994) 271-284.

(89)   W. Hu, T. Takeuchi, H. Haraguchi, Anal. Chem. 65 (1993) 2204-2208.

(90) L.M. Hjelmeland, Anal. Biochem. 130 (1983) 72.

(91) R.G. Laughlin, Langmuir 7 (1991) 842-847.

(92) W. Hu, H. Haraguchi, Anal. Chem. 66 (1994) 765-767.

(93) J. Zajac, C. Chorro, M. Lindheimer, S. Partyka, Langmuir 13 (1997) 1486-1495.

(94) Anatrace Inc. Catalogue, 3rd ed. 2002/2003.

(95) J.P. Kratohvil, W.P. Hsu, D.I. Kwok, Langmuir 2 (1986) 256-258.

(96) H. Naganuma, C.-L. Liu, U.K. Jain, Y. Adachi, W.I. Higuchi, J. Colloid & Interface Sci. 189 (1997) 17-22.

(97) J.G. Weers, J.F. Rathman, F.U. Axe, C.A. Crichlow, L.D. Foland, D.R. Scheuing, R.J. Wiersema, A.G. Zielske, Langmuir 7 (1991) 854-867.

(98) K.J. Mysels and L.H. Princen, J. Phys. Chem. 63 (1959) 1696.

(99) N. Kamenka, Y. Chevalier, R. Zana, Langmuir 11 (1995) 3351-3355.

(100) N. Kamenka, Y. Chevalier, R. Zana, Langmuir 11 (1995) 4234-4240.

(101) C.A. Bunton, M.M. Mhala, J.R. Mottatt, J. Phys. Chem. 93 (1989) 854-858.

(102) M.S. Baptista, M.J. Politi, J. Phys. Chem. 95 (1991) 5936-5942.

(103) S. Brochsztein, P.B. Filho, V.G. Toscano, H. Chaimovich, M.J. Politi, J. Phys. Chem. 94 (1990) 6781-6785.

(104) D.J. Hodge, R.G. Laughlin, R.H. Ottewill, A.R. Rennie, Langmuir 7 (1991) 878-884.

(105) C.A. Bunton, M.M. Mhala, J.R. Moffatt, J. Org. Chem. 52 (1987) 3832.

(106) Y. Chevalier, N. Kamenka, M. Chorro, R. Zana, Langmuir 12 (1996) 3225-3232.

(107) R. Bongiovanni, R.H. Ottewill, A.R. Rennie, R.G. Laughlin, Langmuir 12 (1996) 4681-4690.

(108) P. Di Profio, R. Germani, G. Savelli, G. Cerichelli, M. Chiarini, G. Mancini, C.A. Bunton, N.D. Gillitt, Langmuir 14 (1998) 2662-2669.

(109) W. Hu, H. Tao, M. Tominaga, A. Mayazaki, H. Haraguchi, Anal. Chim. Acta 299 (1994) 249-256.

(110) W. Hu, K. Hasebe, K. Tanaka, P.R. Haddad, J. Chromatogr. 850 (1999) 161-166.

(111) T. Umemura, S. Kamiya, A. Itoh, K. Chiba, H. Haraguchi, Anal. Chim. Acta. 349 (1997) 231-238.

(112) W. Hu, P.R. Haddad, K. Hasebe, K. Tanaka, Anal. Commun. 36 (1999) 97-100.

(113) W. Hu, Langmuir 15 (1999) 7168-7171.

(114) W. Hu, K. Hasebe, K. Tanaka, J.S. Fritz, J. Chromatogr. A 956 (2002) 139-145.

(115) W. Hu. *International Ion Chromatography Symposium '98*, September 1998, Osaka, Japan, presentation 57.

(116) J.M. Patil, T. Okada, Anal. Commun. 36 (1999) 9-11.

(117) K. Iso, T. Okada, Langmuir 16 (2000) 9199-9204.

(118) K. Iso, T. Okada, J. Chromatogr. A 920 (2001) 317-323.

(119) K. Iso, T. Okada, Stud. Surf. Sci. Catal. 132 (2001) 117-120.

(120) W. Jiang, K. Irgum, Anal. Chem. 73 (2001) 1993-2003.

(121) W. Hu, P.R. Haddad, Chromatographia 52 (2000) 543-551.

(122) W. Hu, University of Hokkaido, Sapporo, Japan, personal communication, May 1999.

(123) L.W. Yu, T.R. Floyd, R.A. Hartwick, J. Chromatogr. Sci. 24 (1986) 177-182.

(124) L.W. Yu, R.A. Hartwick, J. Chromatogr. Sci. 27 (1989) 176-185.

(125) W. Jiang, K. Irgum, Anal. Chem. 71 (1999) 333-344.

(126) C. Viklund, K. Irgum, Macromolecules 33 (2000) 2539-2544.

(127) SeQuant, www.sequant.com, 2002, internet communication.

(128) W. Hu, K. Hasebe, D.M. Reynolds, H. Haraguchi, Anal. Chim. Acta. 353 (1997) 143-149.

(129) W. Hu, P.R. Haddad, Trends in Anal. Chem. 17 (1998) 73-79.

(130) J.D. Lamb and R.G. Smith, J. Chromatogr. 546 (1991) 73-88.

(131) W. Hu, H. Tao, H. Haraguchi, Anal. Chem. 66 (1994) 2514-2520.

(132) T. Umemura, S. Kamiya, R. Kitaguchi, H. Haraguchi, Chem. Letters (8) (1997) 755-756.

(133) T. Umemura, R. Kitaguchi, H. Haraguchi, Anal. Chem. 70 (1998) 936-942.

(134) T. Umemura, S. Kamiya, H. Haraguchi, Anal. Chim. Acta. 379 (1999) 23-32.

(135) W. Hu, H. Haraguchi, J. Chromatogr. 723 (1996) 251-258.

(136) W. Hu, P.R. Haddad, Anal. Commun. 35 (1998) 317-320.

(137) K. Hasebe, T. Sakuraba, W. Hu, J. Liq. Chrom. Rel. Technol. 22 (1999) 561-569.

(138) W. Hu, A. Miyazaki, H. Tao, A. Itoh, T. Umemura, H. Haraguchi, Anal. Chem. 67 (1995) 3713-3716.

(139) W. Hu, H. Tao, M. Tominaga, A. Itoh, T. Umemura, H. Haraguchi. Int. Symp. Chromatogr., 35th Anniv. Res. Grp. Liq. Chromatogr., Japan, (1995) 765-70.

(140) W. Hu, H. Haraguchi, Anal. Chim. Acta. 285 (1994) 335-341.

(141) W. Hu, K. Tanaka, P.R. Haddad, K. Hasebe, J. Chromatogr. A 884 (2000) 161-165.

(142) W. Hu, P.R. Haddad, K. Hasebe, K. Tanaka, Anal. Commun. 36 (1999) 309-312.

(143) W. Hu, P.R. Haddad, K. Tanaka, K. Hasebe, Analyst 125 (2000) 241-244.

(144) W. Hu, K. Hasebe, M.Y. Ding, K. Tanaka, Fresenius' J. Anal. Chem. 371 (2001) 1109-1112.

(145) M. Macka, P.R. Haddad, J. Chromatogr. A 884 (2000) 287-296.

(146) W. Hu, P.R. Haddad, K. Hasebe, K. Tanaka, P. Tong, C. Khoo, Anal. Chem. 71 (1999) 1617-1620.

(147) M. Chorro, B. Kamenka, S. Faucompre, M. Partyka, M. Lindenheimer, R. Zana, Coll. Surf. A. 110 (1996) 249-261.

(148) W. Hu, A. Miyazaki, H. Haraguchi, Anal. Sci. 11 (1995) 999-1000.

(149) W. Hu, S. Cao, M. Tominaga, A. Miyazaki, Anal. Chim. Acta. 322 (1996) 43-47.

(150) T. Umemura, R. Kitaguchi, K. Inagaki, H. Haraguchi, Analyst 123 (1998) 1767-1770.

(151) T. Umemura, K. Tsunoda, A. Koide, T. Oshima, N. Watanabe, K. Chiba, H. Haraguchi, Anal. Chim. Acta 419 (2000) 87-92.

(152) W. Hu, K. Hasebe, D.M. Reynolds, H. Haraguchi, J. Liq. Chromatogr. Relat. Technol. 20 (1997) 1221-1232.

(153) W. Hu, K. Hasebe, K. Tanaka, J.S. Fritz, S. Inoue, M. Ozeki, Fres. J. Anal. Chem. 370 (2001) 399-402.

(154) G.J. Shen, Z.H. Peng, H.Y. Huang, Y.H. Shi, A.M. Yu, Q.H. Jin, Chem. J. Chinese Uni. 20 (1999) 1538-1541.

(155) W. Hu, K. Hasebe, D.M. Reynolds, T. Umemura, S. Kamiya, A. Itoh, H. Haraguchi, J. Liq. Chrom. Rel. Technol. 20 (1997) 1903-1919.

(156) F. Hofmeister, Arch. Exp. Pathol. Pharmachol. 24 (1888) 247-260.

(157) L.H.N. Cooper, Nature 139 (1937) 284-285.

(158) T. Okada, J.M. Patil, Langmuir 14 (1998) 6241-6248.

(159) T. Masudo, T. Okada, Phys. Chem. Chem. Phys. 1 (1999) 3577-3582.

Experimental

This chapter outlines the instrumentation and chemicals used throughout this work, unless specified in a particular chapter.

2.1 Instrumentation

A Dionex (Sunnyvale, CA, USA) DX 500 IC system was used throughout this study, consisting of a GP40 pump, an AS50 auto-sampler with a 100 µL injection loop, an AD20 UV-Vis absorbance detector and an ED40 electrochemical detector. PeakNet 5.1 (Dionex) Software was used to collect and process the data. The column used throughout this study (L-column, 250 × 4.6 mm i.d., Chemical Inspection and Testing Institute, Tokyo, Japan) was packed with 5 µm ODS material and was housed in a Waters (Milford, MA, USA) 1122/WTC-120 column heater operated at 30°C.

2.2 Reagents and Solutions

Water used throughout this study was prepared in the laboratory using a Millipore (Bedford, MA, USA) Milli-Q water purification system until the resistance was at least 18 MΩ. Prior to use it was filtered through a 0.22 µm membrane filter.

All chemicals used were of analytical reagent grade. General chemicals used are detailed in Table 1.1, and the surfactants used to coat the column are listed in Table 1.2.

Table 2.1 General Chemicals.

Chemical Name	Formula	Supplier
Acetone	CH_3COCH_3	BDH
Acetonitrile	CH_3CN	BDH
Ammonium nitrate	NH_4NO_3	Univar
Calcium chloride	$CaCl_2$	Ajax
Cerous chloride heptahydrate	$CeCl_3.7H_2O$	Aldrich
Cerous perchlorate (40 wt. % soln in water)	$Ce(ClO_4)_3$	Aldrich
Cerous sulfate octahydrate	$Ce_2(SO_4)_3.8H_2O$	Aldrich
Cobalt (II) nitrate	$Co(NO_3)_2$	Ajax
Cobalt (II) perchlorate hexahydrate	$Co(ClO_4)_2.6H_2O$	Aldrich
Cobalt (II) sulfate heptahydrate	$CoSO_4.7H_2O$	Sigma
Copper (II) nitrate hydrate	$Cu(NO_3)_2$	Aldrich
Copper (II) perchlorate hexahydrate	$Cu(ClO_4)_2.6H_2O$	Aldrich
Copper (II) sulfate pentahydrate	$CuSO_4.5H_2O$	Aldrich
Magnesium chloride	$MgCl_2$	BDH
Magnesium perchlorate hexahydrate	$Mg(ClO_4)_2.6H_2O$	Aldrich
Mercuric chloride	$HgCl_2$	BDH
Perchloric acid	$HClO_4$	Ajax
Potassium ferricyanide	$K_3Fe(CN)_6$	May and Baker
Potassium ferrocyanide	$K_4Fe(CN)_6$	Ajax
Potassium iodide	KI	Aldrich
Potassium nitrate	KNO_3	BDH
Silver nitrate	$AgNO_3$	Aldrich
Sodium bicarbonate	$NaHCO_3$	BDH
Sodium bromide	$NaBr$	Aldrich
Sodium chlorate	$NaClO_3$	BDH
Sodium chloride	$NaCl$	Aldrich
Sodium cyanate	$NaCNO$	Aldrich

Sodium hydroxide	NaOH	Ajax
Sodium iodate	$NaIO_3$	Hopkins and Williams
Sodium iodide	NaI	Aldrich
Sodium molybdate	Na_2MoO_4	Aldrich
Sodium nitrate	$NaNO_3$	Ajax
sodium nitrite	$NaNO_2$	Ajax
Sodium perchlorate	$NaClO_4$	Aldrich
Sodium tungstate	Na_2WO_4	BDH
Thallium nitrate	$TlNO_3$	BDH
Zinc chloride	$ZnCl_2$	Aldrich

Table 2.2 Surfactants used for coating the column and/or capillary.

Chemical Name	Formula	Supplier
3-(N,N-dimethylmyristylammonio)propanesulfonate (C14SB)	$C_{19}H_{41}NO_3S$	Fluka
N-tetradecylphosphocholine (C14PC)	$C_{19}H_{42}NO_4P$	Anatrace Inc.
Tetradecyltrimethylammonium chloride (TTACl)	$C_{17}H_{38}ClN$	Fluka
Tetradecyltrimethylammonium bromide (TTABr)	$C_{17}H_{38}BrN$	Aldrich
Sodium dodecylsulfate (SDS)	$C_{12}H_{25}NaO_4S$	Aldrich

2.3 Production of Ce(ClO$_3$)$_3$

Ce(ClO$_3$)$_3$ was produced using a glass ion-exchange column packed with analytical reagent grade Amberlite IRA-400 PS-DVB gel resin (BDH), of capacity 1.4 eq L^{-1}, in the hydroxide form. The resin was converted to the ClO$_3^-$ form by flushing with excess 1.4 M NaClO$_3$. Approximately 18 mL of 0.25 M Ce(ClO$_4$)$_3$ was passed through the column and many fractions of effluent were collected Ce(ClO$_3$)$_3$ and purity was tested against ClO$_3^-$ and ClO$_4^-$ standards on a Dionex IC instrument with an AS11 column. Fractions were then combined and concentrated by rotary evaporation.

2.4 Column Coating Procedure

The void volume, V$_0$, of the packed ODS column was measured in order to calculate retention factors (*k'*) by injecting 10 µL of a 0.27 mM NaNO$_3$ aqueous solution. The column was then coated with the surfactant, following the method detailed by Hu *et al.* [1], by pumping a 30 mM solution through it at a flow rate of 1 mL min^{-1}, with the effluent monitored by UV detection at 210 nm. A sharp increase in the absorption indicated the breakthrough of the surfactant and saturation of the stationary phase. The surfactant loading, Q, on the column was calculated by:

$$Q = (V_b - V_0) \times C \qquad (2.1)$$

where V$_b$ is the breakthrough volume and C is the concentration of the coating solution.

The column was then equilibrated with 0.3 mM of the surfactant, which was also added to all mobile phases to ensure a stable surface coating.

Columns were stripped and recoated approximately every 3 months. Stripping involved flushing the column with a 70% acetonitrile solution at 1 mL min^{-1} for 30 minutes, followed by Milli-Q water for >4 hours.

2.5 References

(1)   W. Hu, P.R. Haddad, Chromatographia 52 (2000) 543-551.

The Behaviour of Anions on a Sulfobetaine-type Stationary phase

3.1 Introduction

The analysis of anions in real samples has dominated investigations into ZIC, with particular focus on those with high ionic strength matrices. The development of these applications brought to light characteristics of the technique that have revealed a puzzling separation mechanism. The main discoveries were a unique selectivity (as shown by the retention sequence in Equation 3.1), an indifference to high ionic strength matrices [1] and the ability to separate ions with a pure water mobile phase [2].

$$IO_3^- \sim MoO_4^{2-} \sim SO_4^{2-} \sim WO_4^{2-} < Cl^- < Fe(CN)_6^{4-} < NO_2^- < CNO^- < Br^- < NO_3^- <$$

$$ClO_3^- < Fe(CN)_6^{3-} < I^- < ClO_4^- \tag{3.1}$$
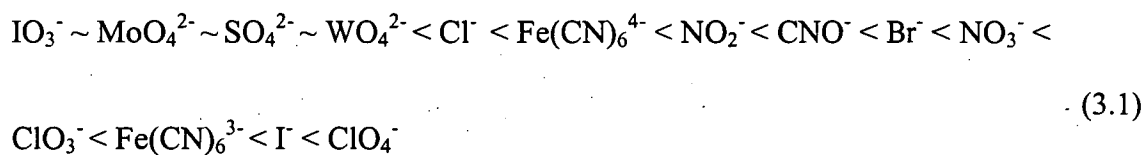
In the case of a sample containing multiple cations and anions, a water mobile phase resulted in a peak for most of the possible combinations of anions and cations in the sample. These complex chromatograms could be overcome if a solution of a suitable electrolyte was used as the mobile phase, which resulted in a single peak for each analyte [1]. With increasing electrolyte concentration an initial increase in retention was observed, but above 5 mM there was no further effect on retention. This behaviour was evident for mobile phases comprising $NaHCO_3$, $NaCl$ or Na_2SO_4 [3]. However,

recent work by Jiang and Irgum [4] showed that increasing the concentration of

$NaClO_4$ in the mobile phase resulted in a decrease in the retention of analyte anions.

This provided an important insight into the determination of the true mechanism of

separation.

Finally, the zeta potential existing at a zwitterionic surface has received some attention

in the literature. The use of zwitterionic surfactants as electro-osmotic flow (EOF)

modifiers in capillary electrophoresis (CE) has revealed that the zeta potential

established at the surface of a zwitterionic surfactant-coated capillary could be

modulated by the addition of different anions to the electrolyte [5]. It was suggested

that different electrolyte anions became incorporated to different extents into the

zwitterionic layer and this in turn altered the zeta potential and hence the EOF. The

existence of such a zeta potential has also been suggested by the calculations of Patil

and Okada [6] and the experimental data of Iso and Okada [7]. Such processes of

anion incorporation into the zwitterion in CE are similar to those governing retention in

ZIC, thus measurements of zeta potential can give further information about the ZIC

retention mechanism.

Despite the previous studies discussed above, the lack of a systematic and

comprehensive set of analyte retention data covering a wide range of mobile phase

compositions and analytes has made it difficult to fully characterise ZIC and to develop

a mechanism which applies under all conditions. The detailed effects of the mobile-

phase cation and anion on the retention of analyte anions are still not well known and

the nature of the stationary phase has not yet been examined fully. The aims of the present study have been to address the deficiencies in the existing retention data by acquiring a systematic data set, to study in detail the zeta potential characteristics of zwitterionic surfaces in contact with various electrolytes using EOF (and hence zeta potential) measurements determined by CE, and to use this information to develop a new, comprehensive retention mechanism for ZIC.

3.2 Experimental

3.2.1 Instrumentation

Details of the IC instrument are given in Chapter 2.

A Beckman Coulter 2050 CE system with a UV absorbance detector was used for the electro-osmotic flow measurements. Data acquisition was performed on a Beckman P/ACE Station Version 1. ODS capillaries (Supelco) with an inner diameter of 50 μm, outer diameter of 363 μm and total lengths of 47 or 27 cm (40 cm or 20 cm to the detector) were used.

3.2.2 Column Coating Procedure

The column coating method is outlined in Section 2.3. The surfactant loading was 1.20 $\times$ 10^{-3} mol of C14SB per column. New ODS capillaries (Supelco) were rinsed with water for 10 min, 30 mM surfactant for 20 min at low pressure (34.5 mbar; breakthrough at 8.5 min) and 0.3 mM surfactant for 30 min at high pressure (1379

mbar). Prior to each run, the capillary was rinsed for 2 min with 0.3 mM surfactant, then 3 min with the running electrolyte (also containing 0.3 mM surfactant).

3.2.3 Determination of the EOF

The method used for the determination of the EOF (measured as the electro-osmotic mobility, μ_{eo}) was the three-injection method of Williams and Vigh [8]. In this method, the same neutral marker is pressure injected three times, with an injection time, t_{inj}. The first injection, N1, is moved through the capillary for a set time using the same low pressure as the injection. This provides a reference point for the position of the second injection, N2. Both N1 and N2 are moved through the capillary for the same time and pressure as described above. A voltage is then applied, which moves the peaks either further towards or away from the detector, depending on whether the electrophoretic mobility is positive or negative. After the third injection, N3, all three peaks are pushed past the detector.

The position of N2 in the capillary, L_{init}, can be calculated using equation 3.2

$$L_{init} = (t_{N2} - t_{N1} - t_{inj}/2)v_m \tag{3.2}$$

where v_m is the pressure mobilisation velocity,

$$v_m = \frac{L_d}{t_{N3} + t_{in}/2 - t_d} \tag{3.3}$$

and L_d is the length to the detector and t_d is the time delay between the final pressure

mobilisation step and the start of data acquisition.

The position of N2 after the electrophoretic step is calculated via:

$$L_{final} = (t_{N3} - t_{N2} - t_{inj}/2)v_m \qquad (3.4)$$

The distance the neutral markers moved during the application of the voltage, L_{eo}, is

therefore

$$L_{eo} = L_{final} - L_{init} \qquad (3.5)$$

The electro-osmotic mobility, μ_{eo}, can then be calculated via:

$$\mu_{eo} = \frac{L_{eo}L_t}{V_{prog}(t_{migr} - t_{ramp-up}/2 - t_{ramp-down}/2)} \qquad (3.6)$$

where V_{prog} is the voltage applied during the electrophoretic step, and $t_{ramp-up}$ and $t_{ramp-down}$ are the time it takes for the voltage to change between 0 to V_{prog}. The time length

of pressure and voltage steps, as well as the magnitude and direction of the voltage,

were varied depending on the direction and magnitude of the EOF and the capillary

length. The three-injection method is very versatile in this respect and also offers

highly precise and accurate measurements of EOF, with the ability to measure even a

very slow EOF in a short time.

Injections were 1 s with 30 s pressure steps between injections. The separation voltage

was approximately 200V cm^{-1} of capillary.

Conditions used in the CE system were maintained as close as possible to those used on the IC system, although it was necessary to buffer the CE system to stabilise the EOF. A low concentration buffer containing ions with a low propensity for inclusion into the zwitterion (1 mM H_2CO_3/HCO_3^-, pH = 6.4) was used, and prepared fresh daily. Surfactant (0.3 mM) was included in the buffer, except with the cerium salts as electrolytes (for the C14SB-coated capillary) due to precipitation. The neutral marker was acetone and direct UV detection was performed at 280 nm.

3.3 Results and Discussion

3.3.1 Modulation of the Surface Charge

The EOF characteristics (and indirectly, the zeta potentials) of an adsorbed layer of the zwitterionic surfactant C14SB (and for comparison a mono-functional anionic surfactant (dodecylsulfate, DDS) and a cationic surfactant (tetradecyltrimethylammonium, TTA)) on a ODS capillary were studied by measuring the EOF in a series of CE experiments. A range of background electrolytes (BGEs) containing different anions and cations but constant salt concentrations was used, and the results for these EOF measurements and the calculated zeta potentials are summarised in Table 3.1. As expected, the cationic surfactant in combination with 25 mM NaCl as BGE gave an anodic EOF and a positive zeta potential (42.5 mV). Replacing the BGE anion with citrate, while maintaining Na^+ as the BGE cation, resulted in a decreased EOF, probably due to strong electrostatic interaction of citrate

Table 3.1 Electro-osmotic flow measurements and calculated zeta potentials obtained with various background electrolytes on a fused silica capillary coated with a zwitterionic (C14SB), cationic (TTA) or anionic (DDS) surfactant.

Electrolyte	EOF ($\times 10^{-9}$ m^2/Vs)	% RSD (n = 5)	Zeta Potential* (mV)
Zwitterionic Surfactant			
NaCl (25 mM)	23.9	0.6	-30.6
MgCl$_2$ (25 mM)	10.4	1.8	-13.3
CeCl$_3$ (25 mM)	-31.4	0.6	40.2
NaClO$_4$ (25 mM)	41.7	0.3	-53.4
Mg(ClO$_4$)$_2$ (25 mM)	23.9	0.7	-30.6
Ce(ClO$_4$)$_3$ (25 mM)	-9.1	2.6	11.7
NaCl (25 mM)	23.9	0.6	-30.6
NaCNO (25 mM)	25.9	0.4	-33.2
NaClO$_4$ (25 mM)	41.7	0.3	-53.4
CeCl$_3$ (25 mM)	-31.4	0.6	40.2
Ce(ClO$_4$)$_3$ (25 mM)	-9.1	2.6	11.7
Cationic Surfactant			
NaCl (25 mM)	-33.2	2.8	42.5
CeCl$_3$ (25 mM)	-25.7	4.5	32.0
Trisodium citrate (5.4 mM)	-8.2	2.1	10.5
NaCl (125 mM)	-26.2	1.2	33.5
Anionic Surfactant			
NaCl (25 mM)	50.6	0.6	-64.8
NaClO$_4$ (25 mM)	51.9	1.0	-66.5

*Calculated using the Helmholtz equation

with the quaternary ammonium group of the surfactant. Experiments with a capillary coated with the typical anionic surfactant resulted in the expected cathodic EOF and a negative zeta potential (-64.8 mV) with 25 mM NaCl as BGE. Replacement of the BGE ion having the same charge as the surface (shown in Table 3.1 with ClO_4^-) had little effect on the EOF and zeta potential.

Substantial EOF values and zeta potentials were observed when the capillary was coated with the zwitterionic C14SB and used in combination with the different BGEs. The 25 mM NaCl BGE gave a net negative zeta potential (-30.6 mV) and a cathodic EOF of 23.9×10^{-9} m^2 $(V \cdot s)^{-1}$ (Table 3.1), whilst the 25 mM $NaClO_4$ BGE gave a cathodic EOF of 41.7×10^{-9} m^2 $(V \cdot s)^{-1}$ and a larger negative zeta potential (-53.4 mV). Baryla and Lucy [5] reported that cathodic EOF values with potassium salts of anions increased according to the following series: SO_4^{2-} < Cl^- < Br^- < I^- < ClO_4^-. This behaviour suggested that these anions interacted more strongly with the quaternary ammonium group on the zwitterion than did the cation with the sulfonate group, resulting in an overall negative zeta potential. The more strongly the anion interacted with the quaternary ammonium group, the more effectively it reduced the effective charge on this group and resulted in the overall zeta potential becoming more negative.

The effect of the electrolyte cation was studied using Na^+, Mg^{2+} and Ce^{3+} salts of Cl^- and ClO_4^-. For both anions, the Mg^{2+} salt resulted in a significantly lower cathodic EOF and lower negative zeta potential than the Na^+ salt. This may be attributed to stronger interaction of Mg^{2+} with the sulfonate group, leading to an effective reduction

in the charge of this group and therefore a reduction in the overall negative zeta potential. The Ce^{3+} salt interacted even more strongly, changing the zeta potential from -30.6 mV for NaCl to 40.2 mV for $CeCl_3$. For ClO_4^- salts, the zeta potential was altered from -53.4 mV for $NaClO_4$ to 11.7 mV for $Ce(ClO_4)_3$. Thus, both the charge on the metal cation as well as the chemical nature of the anion had a major effect on the zeta potential of the zwitterionic coating.

The experimental measurements performed using CE with an ODS capillary coated with a surfactant can be considered to be analogous to the situation occurring in ZIC using a ODS reversed-phase material coated with a surfactant. While the actual loading of the adsorbed surfactant will differ between CE and ZIC, the above results show clearly that in the CE case there is sufficient adsorbed surfactant to interact with the ions in the BGE. The CE data can therefore validly be used to assist in the interpretation of the mechanism which applies in the ZIC case.

3.3.2 Ability of the Mobile Phase Ion to Completely Mask the Surface Charge

The results in Table 3.1 show that the zwitterionic C14SB used in combination with $CeCl_3$ as the BGE resulted in a very similar zeta potential (40.2 mV) to that for the cationic surfactant in combination with NaCl (42.5 mV). This suggests that Ce^{3+} may completely mask the sulfonate charge, effectively leaving a surface similar to that of the cationic surfactant. Similarly, C14SB used in combination with $NaClO_4$ as the BGE resulted in a zeta potential of –53.4 mV, which is in the range of that for an anionic surfactant used in combination with NaCl (-64.8 mV). However, if Ce^{3+} was to

interact so strongly with the sulfonate part of the zwitterion that the negative charge was completely masked, the resultant surface would be expected to act as an anion-exchanger, or in the case of the $NaClO_4$ electrolyte as a cation-exchanger. Indeed, this has been suggested by Patil and Okada [6]. Plots of log k' *versus* log [mobile phase] should therefore show slopes consistent with ion-exchange elution behaviour. The data in Table 3.2 show the expected slope of -1.0 for the elution of nitrate from the anion-exchange column formed by coating reversed-phase silica with a cationic surfactant, using either sodium chloride or sodium perchlorate as the mobile phase. However, with a zwitterionic column there was very little change in log k' as the mobile phase concentration was increased and there was also almost no difference in behaviour between Na^+ and Ce^{3+} salts, except where chloride was the mobile-phase anion (as will be discussed later in Section 3.3.3.1, cation effects on retention on the C14SB system were not great, and were significantly decreased when the nature of the mobile-phase anion was such that its interaction with C14SB was dominant). Thus, there was no evidence of a conventional ion-exchange mechanism operating with the zwitterionic stationary phase regardless of the type of mobile phase used.

Some salt effects might be expected to occur in the log k' *versus* log [mobile phase] plots in that the amount of adsorbed surfactant might alter as the [mobile phase] was changed. However this will increase the ion-exchange capacity of the column, which will affect the linearity of the plots, rather than the slope, because the y-intercept term would vary for each mobile phase concentration. The data showed excellent linearity, suggesting that the capacity of the column was essentially constant for the experiments

Table 3.2 Slopes of plots of log k' versus log [mobile phase] for various surfactants and mobile phases. r^2 values ranged 0.92 to 0.97, except for NaCl with the zwitterionic surfactant, where $r^2 = 0.54$, a result of the low *k'* range.

	Slope	
	Mobile phase anion	
	Cl^-	ClO_4^-
Cationic Surfactant (Mobile phase cation: Na^+)	-0.96	-1.00
Zwitterionic surfactant (Mobile phase cation: Ce^{3+})	-0.11	-0.2
Zwitterionic surfactant (Mobile phase cation: Na^+)	0.09	-0.2

conducted. It can also be pointed out that similar retention effects and slopes for plots

of log k' *versus* log [mobile phase] were observed by Hu *et al.* [1] for mobile phases

which did not contain zwitterion and for which the ion-exchange capacity of the

column was therefore constant.

The lack of a contributing ion-exchange mechanism is supported by the selectivity

observed for C14SB in combination with a $CeCl_3$ BGE. For example, SO_4^{2-} had a high

retention on the cationic surfactant in combination with a NaCl electrolyte, as expected

for an ion-exchange mechanism. However, it was eluted very early with the C14SB

surfactant in combination with a $CeCl_3$ electrolyte. This is consistent with a chaotropic

selectivity that is characteristic of ZIC.

3.3.3 Elution Effects

The elution behaviour of a range of inorganic anions (Br^-, I^-, $Fe(CN)_6^{4-}$, NO_2^-, NO_3^-,

IO_3^-, $Fe(CN)_6^{3-}$, MoO_4^{2-} and WO_4^{2-}) on the sulfobetaine-coated column was studied as a

function of mobile phase concentration for the SO_4^{2-}, Cl^-, CNO^-, ClO_3^- and ClO_4^- salts

of H^+, Na^+, Mg^{2+} and Ce^{3+}.

3.3.3.1   Effect of the Mobile-Phase Anion and Cation on Anion Retention

The effect of the mobile-phase anion on the retention of four representative anions is

shown in Figure 3.1, where the mobile phase counter cation is Na^+. The mobile-phase

anion is increasingly polarisable from SO_4^{2-} through to ClO_4^-, resulting in a significant

Figure 3.1 Effect of the mobile-phase anion species on the retention of analytes using a mobile phase containing 10 mM (with respect to the anion) Na^+ salts. Conditions: column, ODS modified with C14SB; flow rate, 1.0 mL min-1; detection, direct UV at 214 nm; sample, 100 µL containing 1.0 mM of each anion.

reduction in analyte retention, from a capacity factor of over 50 to less than 5 for iodide. This supports the observations of Okada *et al.* [6] and suggests that the diminished retention was due to competitive displacement between the mobile-phase and analyte anions.

Patil and Okada [6] have noted that ZIC is primarily a method for separating anions and they considered that the type of counter-cation in the mobile phase had almost no effect on the separation. This conclusion was based on the use of monovalent mobile-phase cations. This effect was therefore examined using divalent and trivalent cations and the results shown in Figure 3.2 were obtained for mobile phases with Cl^- as the mobile-phase anion. It can be seen that increasing the charge on the counter-cation, and hence its interaction with the negative charge on the stationary phase, caused an increase in analyte anion retention. Figure 3.3 shows that despite a highly competitive mobile-phase anion, ClO_4^- (see Figure 3.1), an increased charge on the mobile-phase cation can still influence the retention of the analyte anion. This increase was most obvious and significant with the analyte, I^-, however the percentage increase in retention of each of these analyte anions was similar. This suggests that the increase in retention was brought about by a decrease in repulsion from the stationary phase, with this effect being equal for all analytes. Similarly, despite a highly shielding mobile-phase cation such as Ce^{3+}, which results in an overall positive zeta potential, the mobile-phase anion can exert such a competitive influence that retention of anions was still diminished (see Figure 3.4). This is supported by the fact that the cation charge
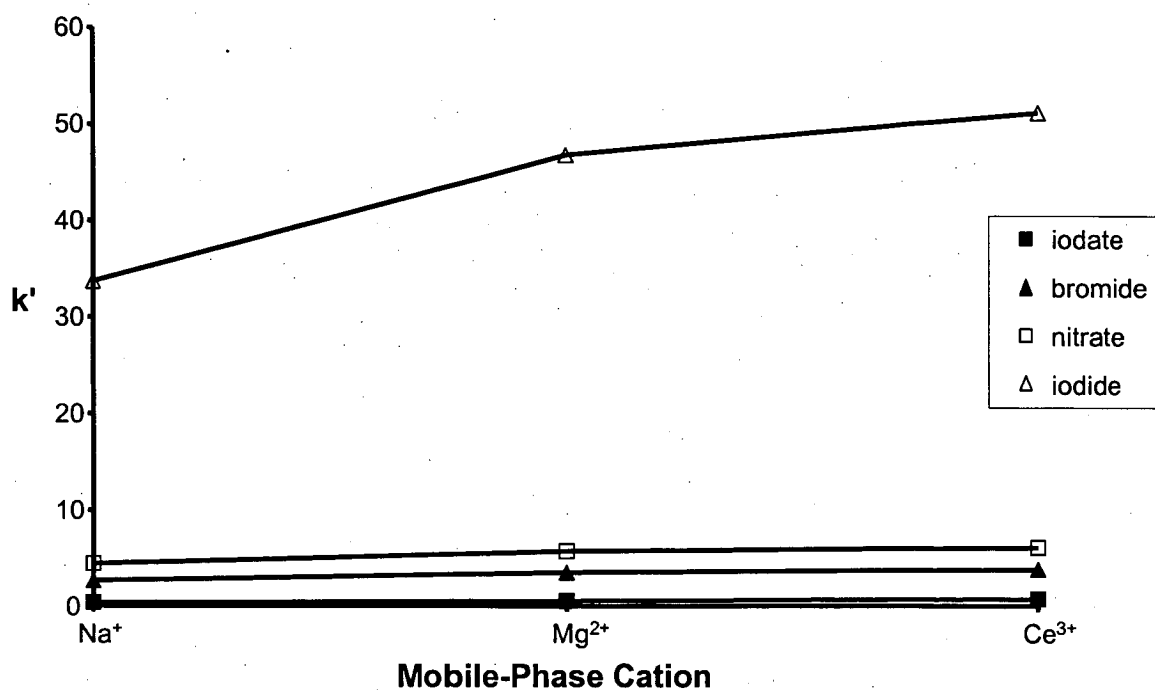
Figure 3.2 Effect of the mobile-phase cation charge on the retention of analytes using a mobile phase containing 10 mM (with respect to the cation) Cl⁻ salts. Other conditions as described in Figure 3.1.
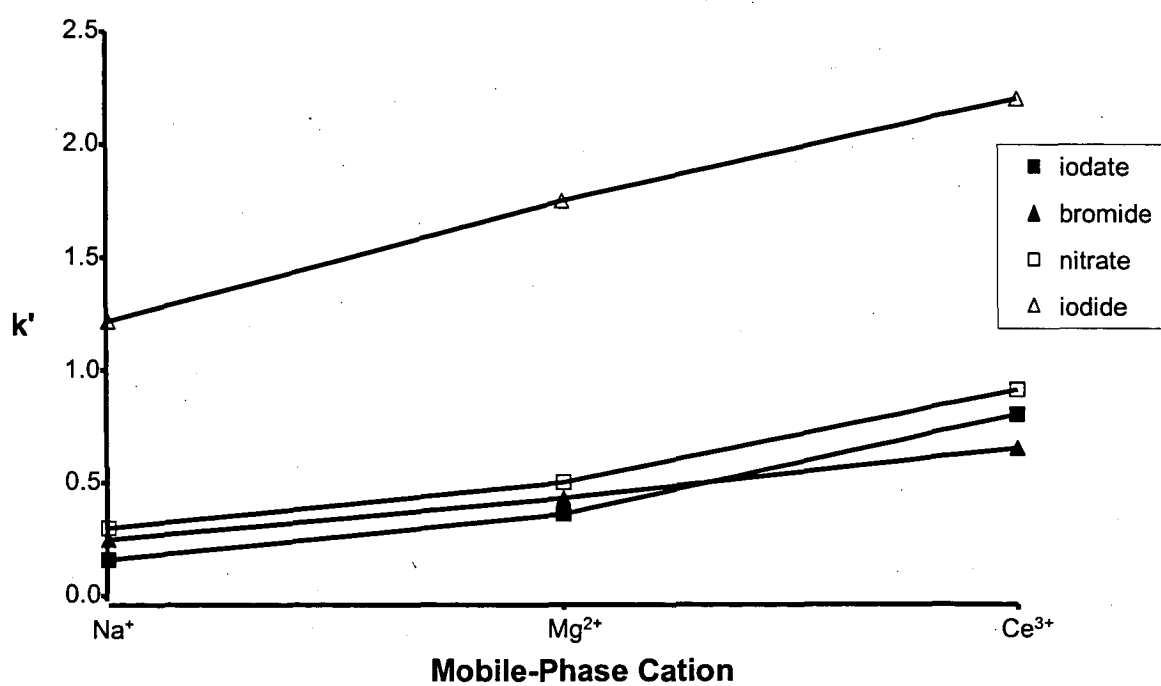
Figure 3.3 Effect of the mobile-phase cation species on the retention of analytes using a mobile phase containing 10 mM (with respect to the cation) ClO_4^- salts. Other conditions as described in Figure 3.1.
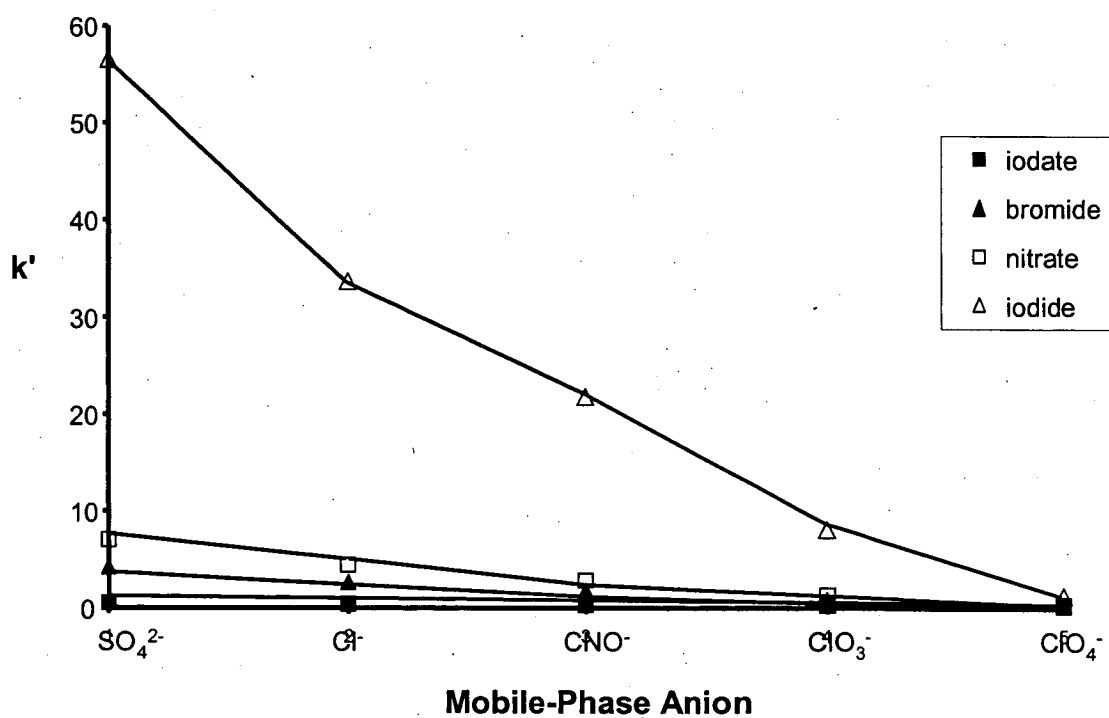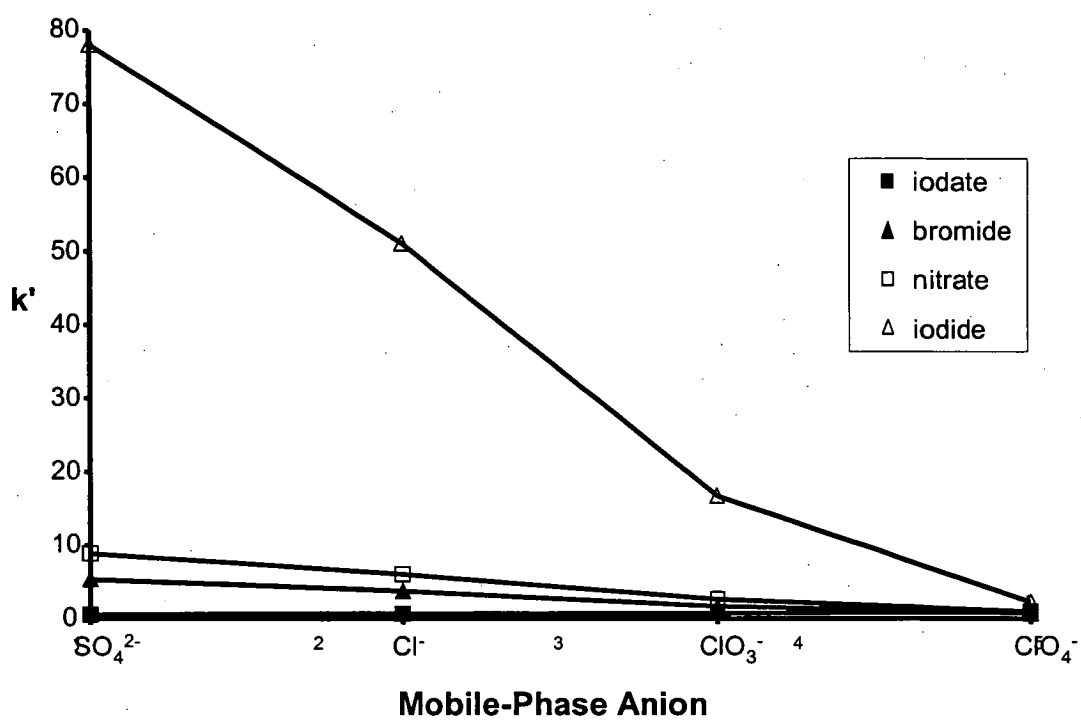
Figure 3.4 Effect of the mobile-phase anion species on the retention of analytes using a mobile phase containing 10 mM (with respect to the anion) Ce^{3+} salts. Other conditions as described in Figure 3.1.

had a great effect on the zeta potential, but a comparatively small effect on the retention of anions. This is discussed further in the next section.

3.3.3.2   Effect of the Zeta Potential on Retention

In the ion-exchange separation of inorganic anions where interaction with the stationary phase is dominated by electrostatic effects, the retention of analyte anions should significantly increase as the zeta potential becomes increasingly positive, be small when the surface charge is neutral, and negligible for negative potentials. However, in ZIC increasingly positive zeta potentials had little effect on the retention of analyte anions and neutral potentials still resulted in high retention (see Figure 3.5), since although the zwitterionic surface is intrinsically neutral it consists of strong charges. In ZIC, as the zeta potential becomes increasingly negative, an electrostatic effect takes over, thereby diminishing retention significantly.

This suggested that retention was due largely to a direct (short-range) chaotropic interaction with the inner positive charge, while repulsive electrostatic effects dominated at negative zeta potentials through suppression of partition into the stationary phase, and subsequently suppression of interaction of analytes with the inner charge. Electrostatic effects do not contribute significantly to k', which is evident in that while the cation charge had a great effect on the zeta potential (see Table 3.1) it had a comparatively small effect on k' (see Figure 3.2). This assumption is further supported by the low retention ($k' = 2.2$) observed for iodide with a $Ce(ClO_4)_3$ mobile phase, which produces a positive zeta potential of 11.7 mV (see Table 3.1).
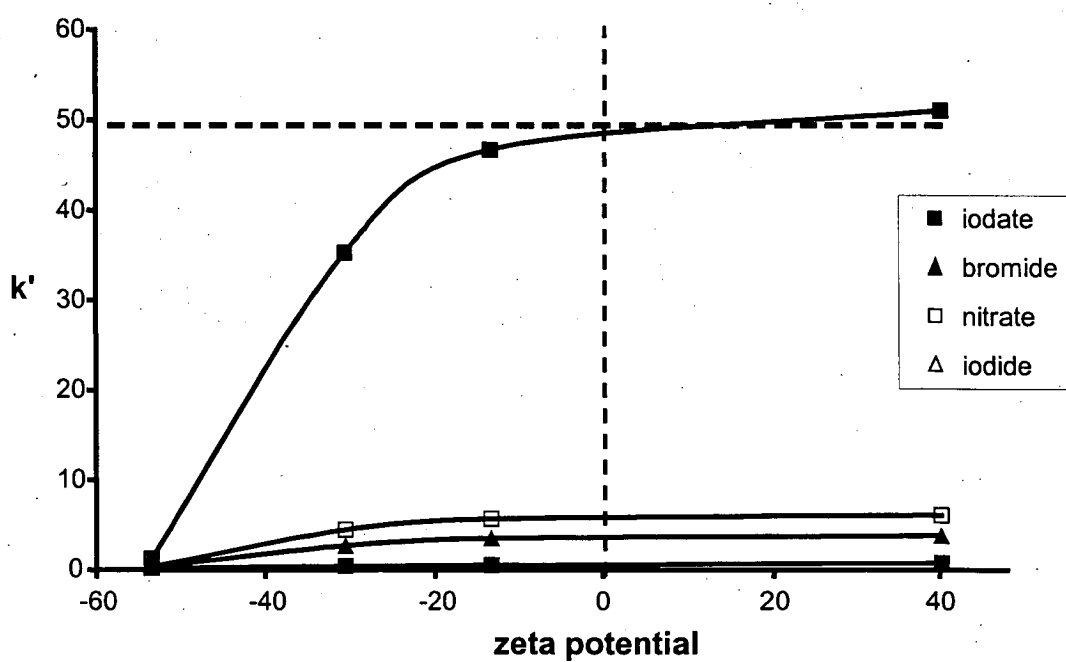
Figure 3.5 Effect of the zeta potential on retention of analytes. Zeta potentials are those determined in Section 3.3.1 and the k' values of the analytes are those determined in Section 3.3.3.1 for the corresponding mobile phases.

3.3.3.3   Effect of the Mobile Phase Concentration on Retention

The elution behaviour for five representative analytes (IO_3^-, NO_2^-, Br^-, NO_3^- and I^-) on the zwitterion-coated column, studied as a function of mobile-phase concentration, is illustrated in Figure 3.6. An abrupt change in k' was observed when the mobile phase was changed from water alone to a low concentration of salt (<1 mM). Further increases in salt concentration resulted in very little further change in k'. In some cases the value of k' decreased significantly as a result of the first addition of salt to the mobile phase (e.g. for IO_3^- as analyte with all mobile phase salts, see Figure 3.6(a)), while in others k' increased when salt was first added (e.g. for I^- as analyte and all mobile phase salts except $NaClO_4$, see Figure 3.6 (e)). The behaviour exhibited was determined by the relative positions of the mobile phase and analyte anions in the ZIC retention order shown in Equation (3.1). When the mobile-phase anion was one that was *less strongly* retained in ZIC than the analyte anion (e.g. SO_4^{2-} as mobile phase, NO_2^- as analyte, see Figure 3.6(b)), then retention of the analyte *increased* compared to that observed in a water mobile phase. On the other hand, a mobile-phase anion retained *more strongly* than the analyte anion (e.g. ClO_4^- as mobile phase, NO_2^- as analyte, see Figure 3.6(b)) caused a *decrease* in retention compared to a water mobile phase. The same trends were evident for all analytes studied, with a small number of anomalous cases discussed later in this section.

Elution effects of Ce^{3+} mobile phases showed similar trends to the Na^+ salts, further supporting the concept that an ion-exchange mechanism does not take place for Ce^{3+}

Figure 3.6 (a) and (b) Effect of the concentration of mobile phases containing various sodium salts on retention times of (a) iodate and (b) nitrite. Other conditions as described in Figure 3.1.

Figure 3.6 (c) and (d) Effect of the concentration of mobile phases containing various sodium salts on retention times of (c) bromide and (d) nitrate. Other conditions as described in Figure 3.1.

(e) iodide

Figure 3.6 (e) Effect of the concentration of mobile phases containing various sodium salts on retention time of iodide. Other conditions as described in Figure 3.1.

mobile phases (as discussed in Section 3.3.2). The elution effects of the same

representative ions (IO_3^-, NO_2^-, Br^-, NO_3^- and I^-) are given as a function of mobile-

phase concentration in Figure 3.7. In this case there was the added lowering of the

repulsion of the outer sulfonate charge due to shielding by the mobile-phase cation,

Ce^{3+}. As there was little interaction and shielding by the Na^+ mobile-phase cation, the

mobile-phase anion dominated the effects on k' (with competitive displacement/direct

chaotropic interaction with the inner functional group). In the case of Ce^{3+} mobile

phases there was a greater contribution of both mobile-phase cation and anion effects.

The behaviour exhibited may still be determined by the relative positions of the

mobile-phase and analyte anions in the ZIC retention order (Equation 3.1), but this

effect may be slightly offset. For example, when the mobile-phase anion was one that

was less strongly retained in ZIC than the analyte anion (e.g. SO_4^{2-} as mobile phase,

NO_2^- as analyte, see Figure 3.7(b)), retention of the analyte increased compared to that

observed in a water mobile phase. However, an initial increase in retention of NO_3^-

was seen with a $Ce(ClO_3)_3$ mobile phase compared with that seen for a water mobile

phase, despite NO_3^- being less strongly retained in ZIC compared with ClO_3^-. Similarly

the small increase in the retention of I^- observed at low concentrations of the $CeClO_4$

mobile phase was not seen for a $NaClO_4$ mobile phase.

Although the same abrupt change in k' is seen when the mobile phase was changed

from water alone to a low concentration of salt (< 1mM), in some cases further

increases in the concentration of Ce^{3+} salts resulted in a significant decrease in k', with
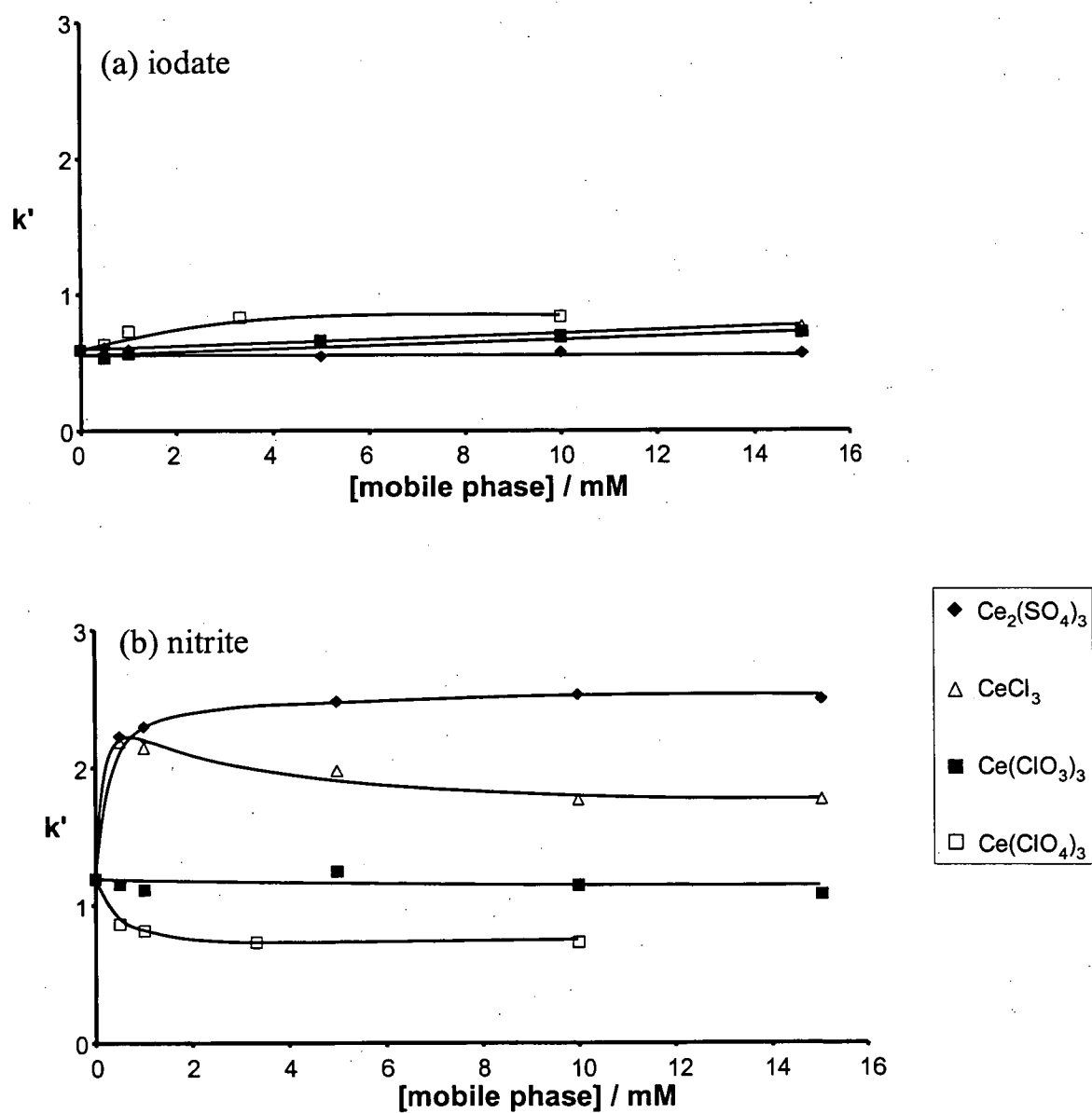
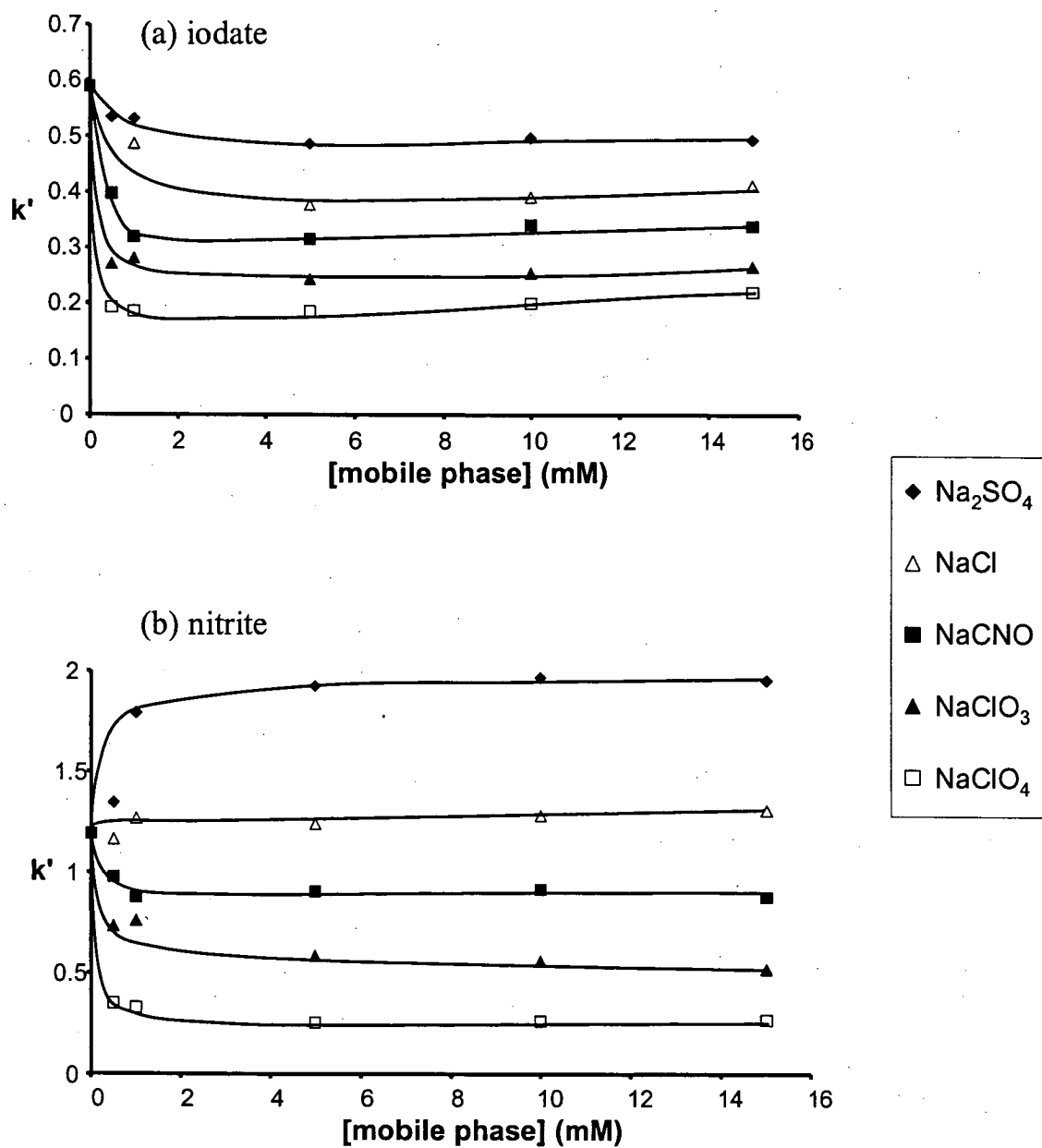**Figure 3.7 (a) and (b)** Effect of the concentration of mobile phases containing various cerium salts on retention times of (a) iodate and (b) nitrite. Other conditions as described in Figure 3.1.
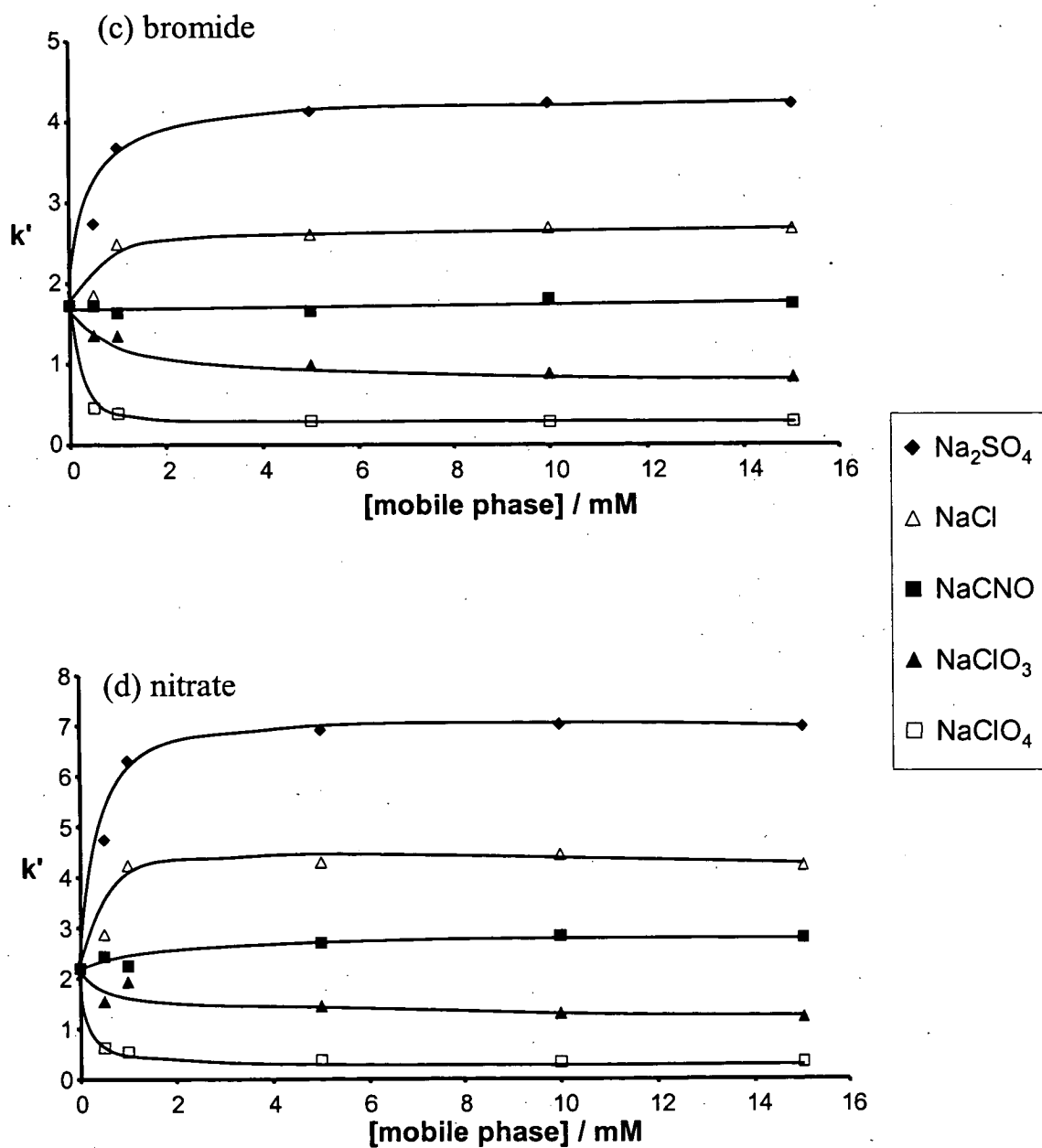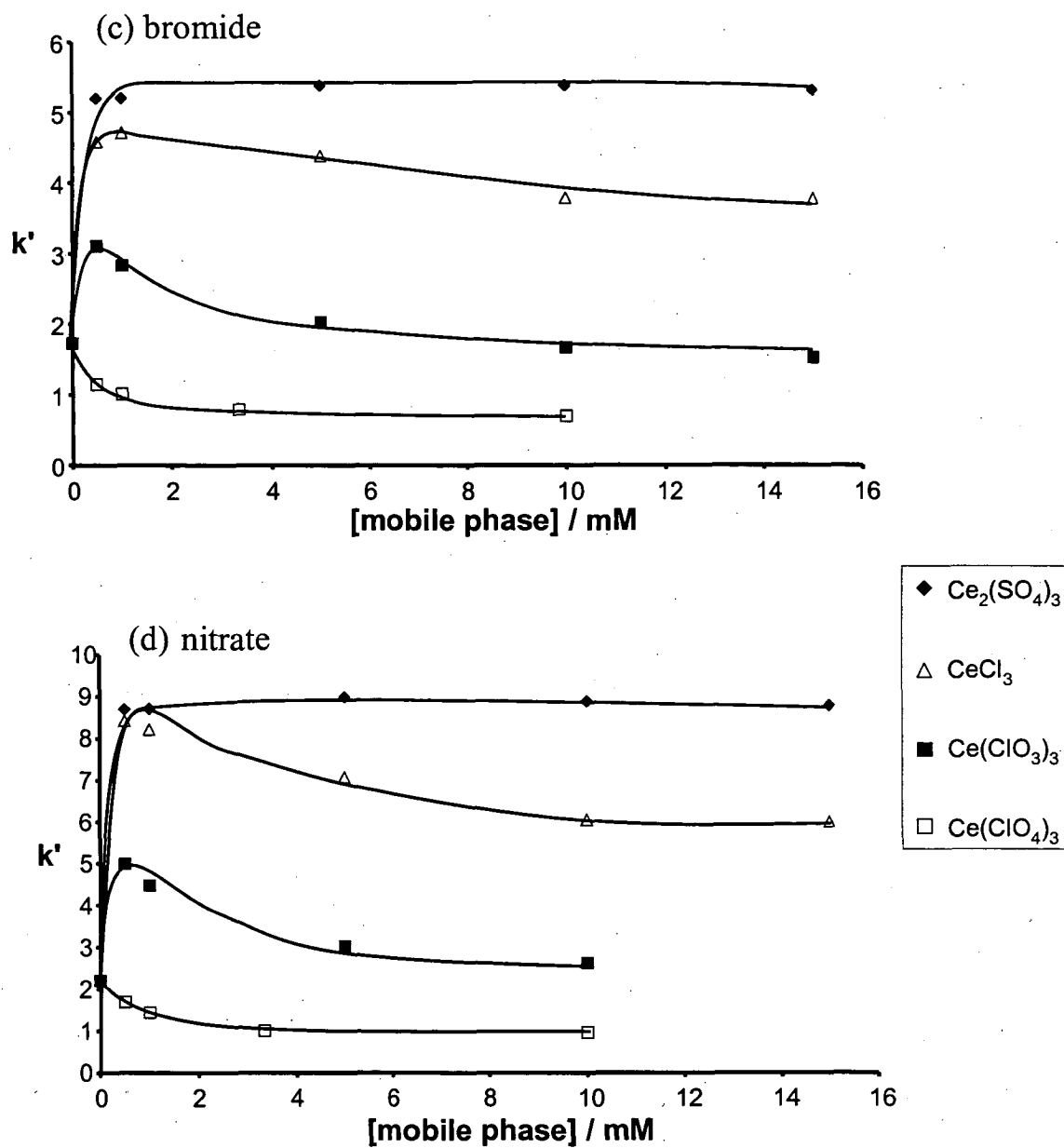
Figure 3.7 (c) and (d) Effect of the concentration of mobile phases containing various cerium salts on retention times of (c) bromide and (d) nitrate. Other conditions as described in Figure 3.1.
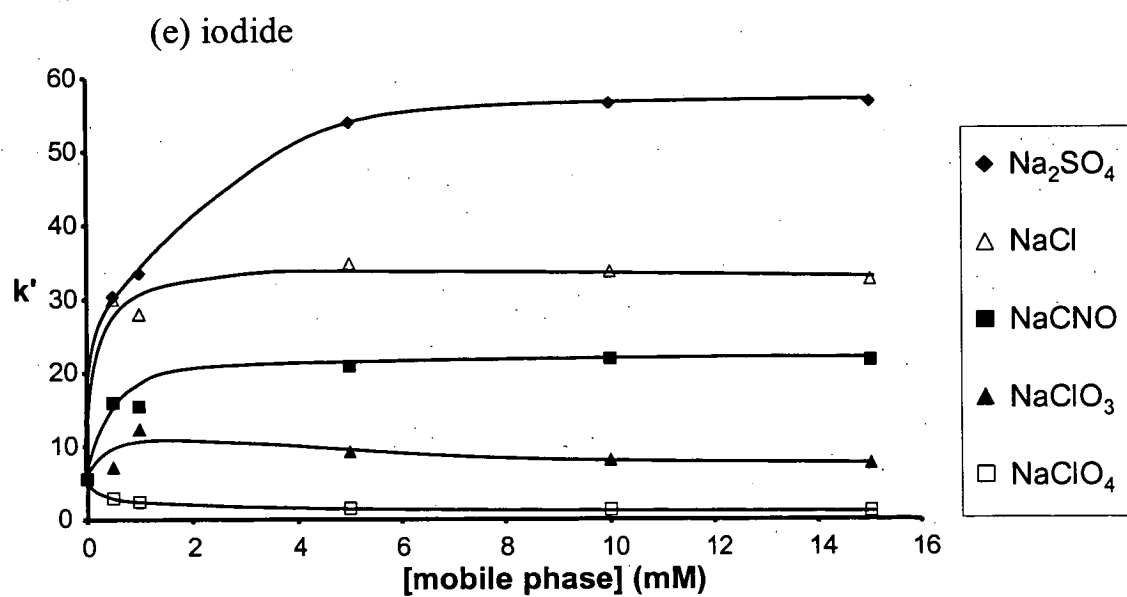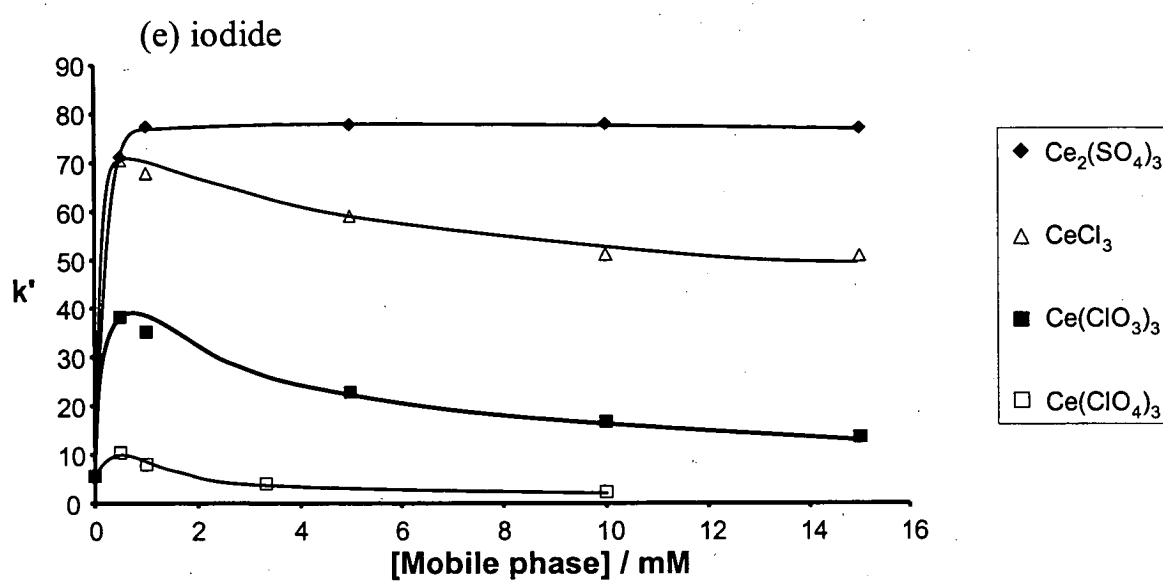
Figure 3.7 (e) Effect of the concentration of mobile phases containing various cerium salts on retention time of iodide. Other conditions as described in Figure 3.1.

little change occurring at concentrations above ~10 mM. This effect will be examined

through analysis of log k' *versus* log [mobile phase] plots in the next section (3.3.3.4).

A small number of special cases did not follow the trends observed for all other

analytes. The effect of increasing the $Ce(ClO_4)_3$ concentration on the retention of

analyte anions is shown in Figure 3.8. While the retention of other weakly retained

anions decreased, the retention of MoO_4^{2-} and $Fe(CN)_6^{4-}$ increased. This may be

attributed to the formation of more highly retained complexes, possibly a mixture of

acids in the case of MoO_4^{2-} (see Figure 3.9) as the pH of $Ce(ClO_4)_3$ was quite low,

ranging from 4.57 (for a 0.5 mM solution) to 3.20 (for a 15 mM solution). Ce^{3+}

complexes may also be responsible for the increased retention of $Fe(CN)_6^{4-}$, as well as

$Fe(CN)_6^{3-}$, which has a greater retention than that of I^- in contrast to that predicted by

Equation 3.1. This is supported in that $Fe(CN)_6^{3-}$ and $Fe(CN)_6^{4-}$ follow expected trends

with a $HClO_4$ mobile phase (see Figure 3.10), indicating no formation of acids, or

complexation (in the absence of Ce^{3+}). Again an increase in the retention of MoO_4^{2-}

was observed with increasing $[HClO_4]$, supporting the formation of MoO_4^{2-} acids. The

large increase in k' observed for NO_2^- can be attributed to HNO_2, which is known to

form at relatively low concentrations of H^+ while other inorganic anions (NO_3^-, Br^-) are

completely ionised at relatively high H^+ concentrations (see Figure 3.11). The increase

in the retention of NO_2^- was less pronounced with increasing $Ce(ClO_4)_3$ concentration

as the pH did not decrease significantly with increasing $Ce(ClO_4)_3$ concentration (see

above). An alternative explanation for these selectivity changes, with particular regard
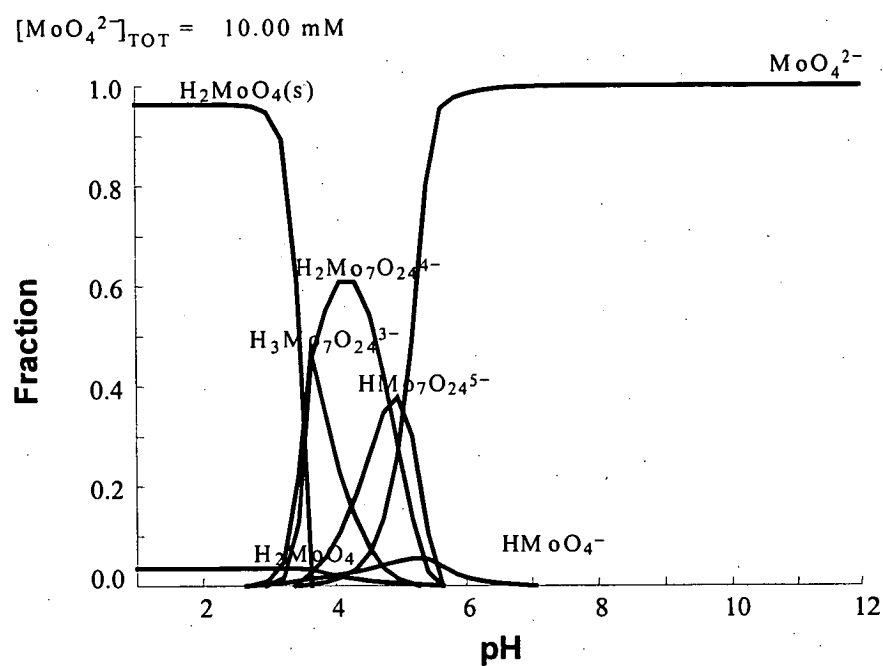
Figure 3.9 Speciation of molybdate with pH, plotted by the Hydra/Medusa program (I. Puigdomenech, Windows program, Stockholm, Version 21).
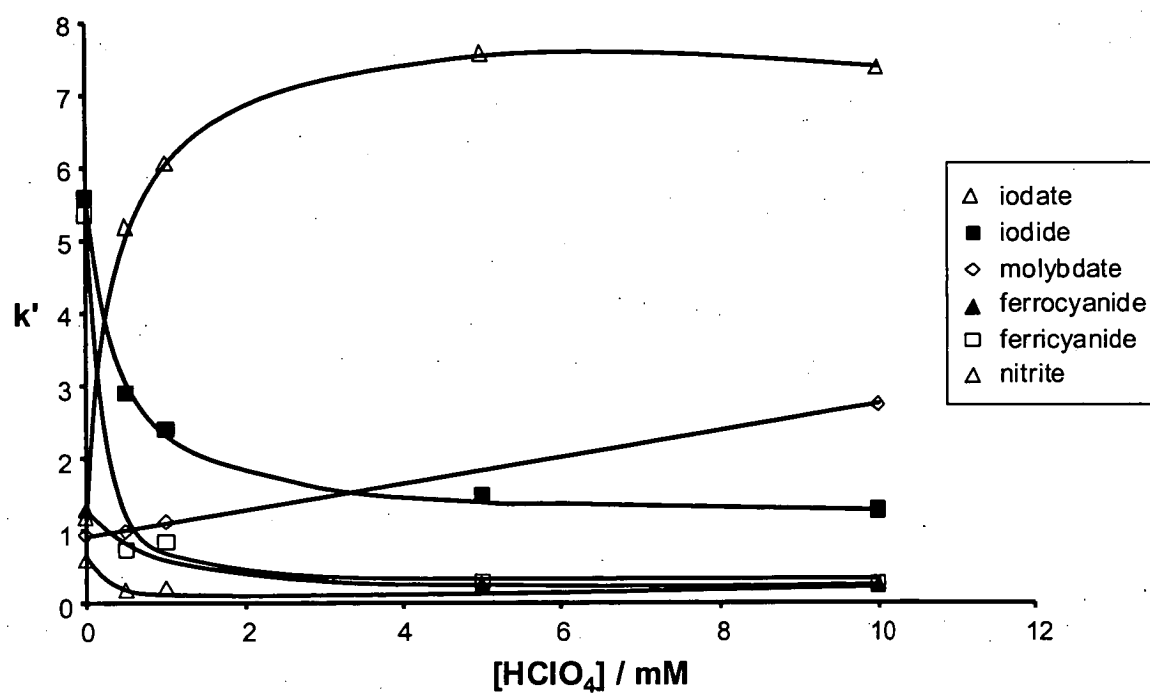
Figure 3.10 Effect of $HClO_4$ concentration on the retention of various analytes. Other conditions as described in Figure 3.1.

(a) $[NO_3^-]_{TOT} = 10$ mM
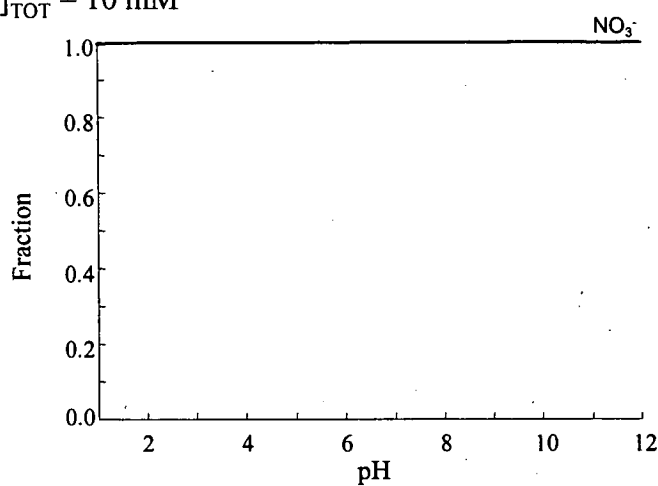
(b) $[Br^-]_{TOT} = 10$ mM
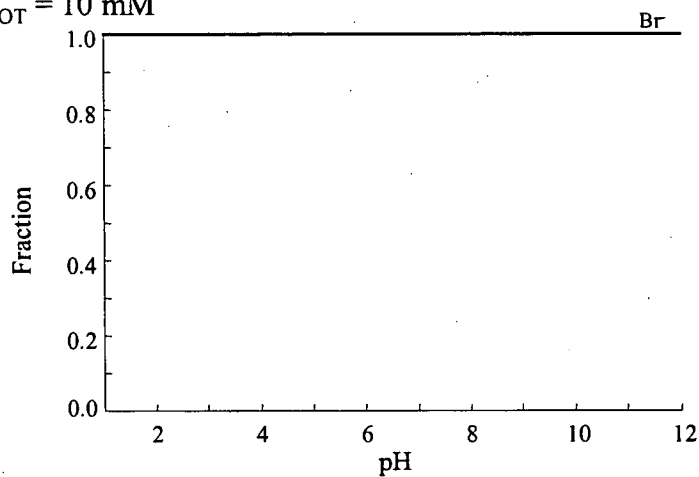
(c) $[NO_2^-]_{TOT} = 10$ mM
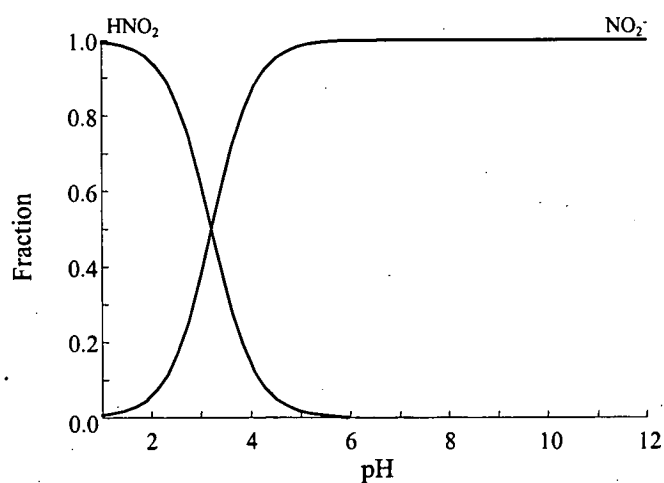
Figure 3.11 Speciation of (a) nitrate; (b) bromide, and (c) nitrite with pH.
Diagrams produced with the Medusa program, as in Figure 3.9.

90

to $Fe(CN)_6^{3-}$ and $Fe(CN)_6^{4-}$, may be that electrostatic effects were stronger with the Ce^{3+} mobile phases and this will be discussed in Section 3.3.3.4, with further analysis of log k' *versus* log [mobile phase] plots.

Nevertheless, the general behaviour seen has not been reported earlier nor predicted to occur in ZIC. Again, these unusual changes in retention are inconsistent with an ion-exchange mechanism.

The data presented in Figures 3.6 and 3.7 have the following implications for practical anion separations. First, analyte retention times may be increased (compared to retention obtained in water mobile phases) by using an anion in the mobile phase which shows weak retention in an ZIC system (e.g. SO_4^{2-}) or by using a highly charged mobile-phase cation, or decreased by using a more strongly retained anion such as ClO_4^-. Second, the analyte retention times are relatively insensitive to further changes in the concentration of the mobile phase. The latter problem can be overcome by using a column coated with a 10:1 mixture of zwitterionic and cationic surfactants, thereby introducing anion-exchange effects to complement the ZIC retention mechanism (see Chapter 5).

3.3.3.4   Interpretation of Log k' *Versus* Log [Mobile Phase] Plots

Hu *et al.* [9] studied the effect of acidic mobile phases (of concentrations between 1-30 mM) in ZIC and suggested that the sulfonate group may be protonated at higher concentrations, resulting in an equilibrium between ZIC and ion-exchange

mechanisms. However, a comparison of $HClO_4$ and $NaClO_4$ mobile phases in this study showed very similar trends depending on the analyte (see Figure 3.12). The behaviour of I^- and $Fe(CN)_6^{3-}$ displayed almost identical trends (Figures 3.12(a) and (b), respectively), while NO_2^- showed markedly different trends (Figure 3.12(c)). This difference was attributed to the formation of HNO_2 as described in the previous section. The slope of the NO_3^- plot (Figure 3.12(e)), became more negative (this was found to be statistically significant utilising a t-test) when the mobile-phase cation was changed from Na^+ to H^+ (–0.2 to –0.27, respectively), which may be a result of an increasing ion-exchange component to the mechanism, as suggested by Hu *et al.* [9]. The Br^- plot (Figure 3.12 (d)) appeared to show a similar trend, though was not statistically significant. It would be expected then that the slope should become increasingly close to –1.0 (the slope expected for an ion-exchange mechanism), as the mobile-phase cation increasingly interacts and shields the outer sulfonate group across the series Na^+ < Mg^{2+} < Ce^{3+}. The slopes for perchlorate mobile phases with increasingly interacting mobile-phase cations are compared in Figure 3.13, for three analytes, NO_3^-, $Fe(CN)_6^{3-}$ and I^-. No change was observed in the slopes for NO_3^- (Figure 3.13 (a)), constant at approximately –0.2. Plots for $Fe(CN)_6^{3-}$ and I^- however, showed a consistent increase in slope, with $Fe(CN)_6^{3-}$ changing from –0.5 to –1.0 and I^- changing from –0.28 to –0.5 (Figure 3.13(b) and (c), respectively). This supports the concept of increased ion-exchange contribution to the separation mechanism when the mobile-phase cation is highly interacting with the outer sulfonate group. The fact that these effects are more pronounced for the more competitive analytes is expected, as shown in Figure 3.2.

(a) ferricyanide
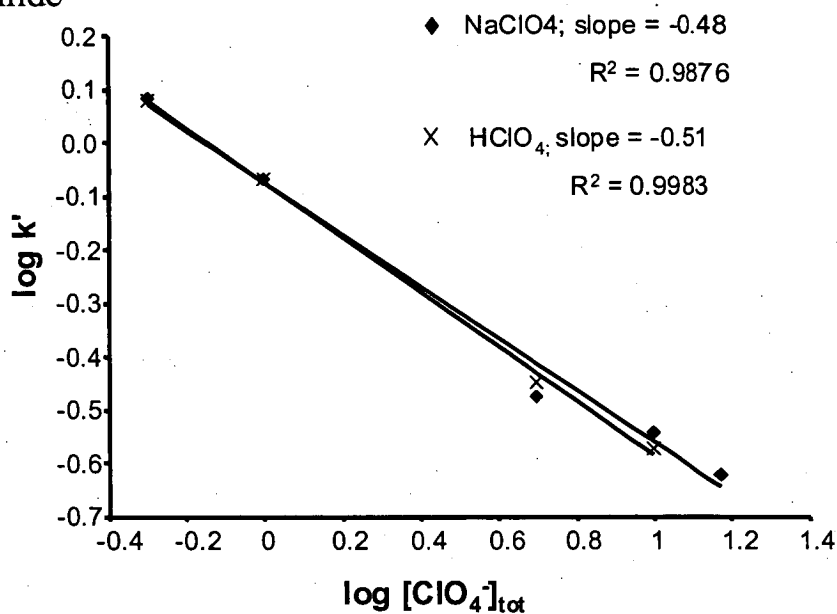
(b) iodide
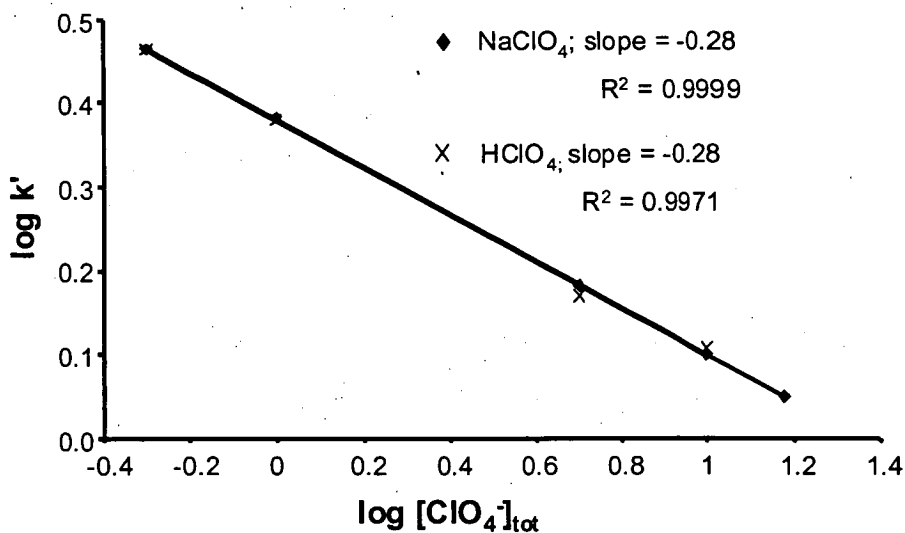
Figure 3.12 (a) and (b) Log k' _versus_ log $[ClO_4^-]$ plots comparing the slopes for $HClO_4$ and $NaClO_4$ of (a) ferricyanide and (b) iodide. Other conditions as described in Figure 3.1.

(c) nitrite
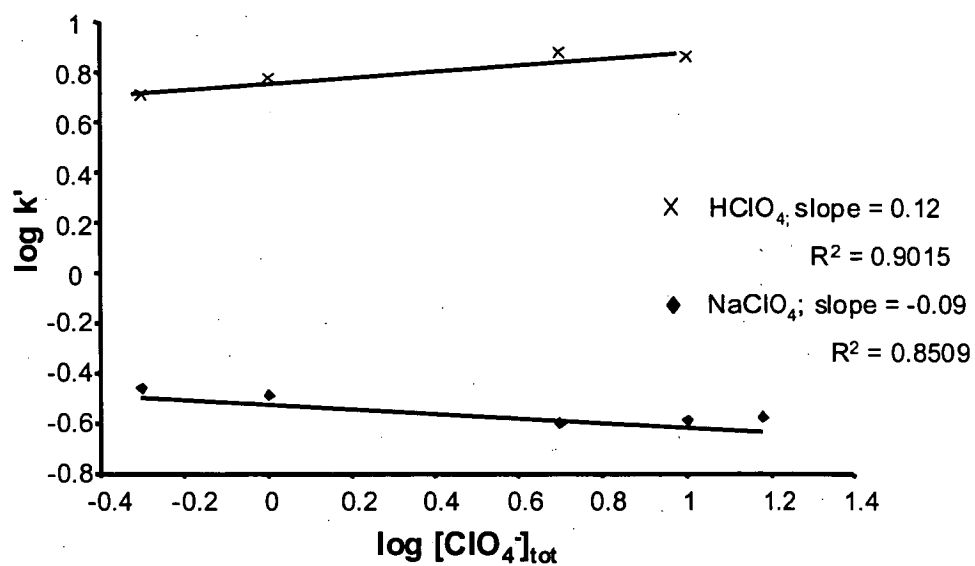
(d) bromide
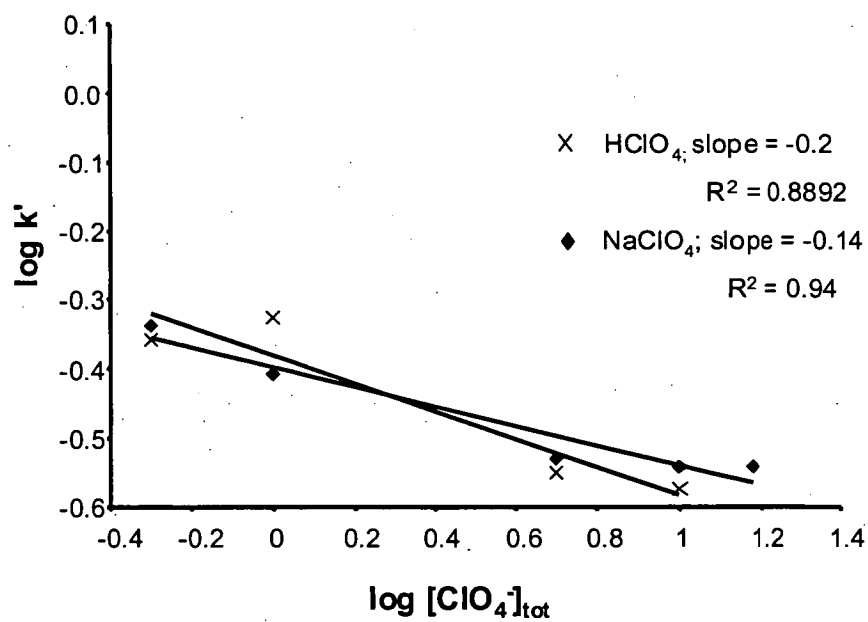
Figure 3.12 (c) and (d) Log k' *versus* log $[ClO_4^-]$ plots comparing the slopes for $HClO_4$ and $NaClO_4$ of (c) nitrite and (d) bromide. Other conditions as described in Figure 3.1.

(e) nitrate
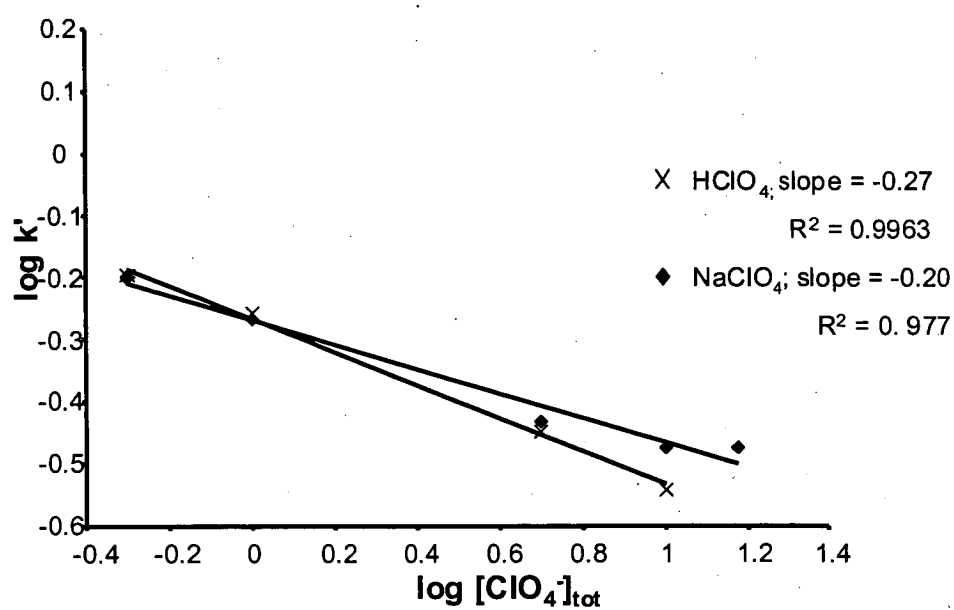
Figure 3.12 (e) Log k' *versus* log $[ClO_4^-]$ plots comparing the slopes for $HClO_4$ and $NaClO_4$ of nitrate. Other conditions as described in Figure 3.1.

(a) nitrate
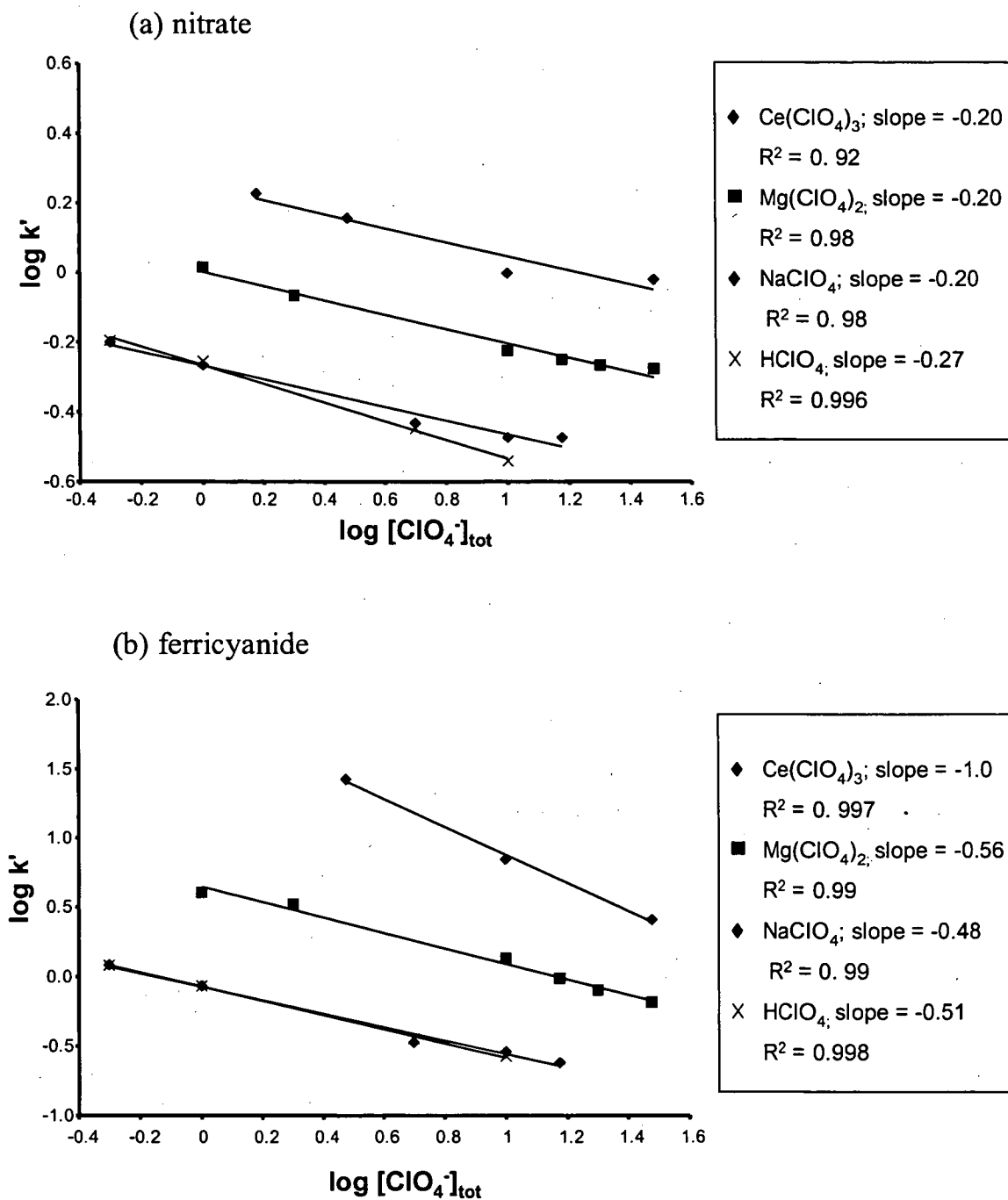
(b) ferricyanide

Figure 3.13 (a) and (b) Log k' *versus* log $[ClO_4^-]$ plots comparing the slopes with varying mobile-phase cation of (a) nitrate and (b) ferricyanide. Other conditions as described in Figure 3.1.

(c) iodide

Figure caption legend:
- ◆ Ce(ClO$_4$)$_3$; slope = -0.52, R^2 = 0. 997
- ■ Mg(ClO$_4$)$_2$; slope = -0.42, R^2 = 0.9957
- ◆ NaClO$_4$; slope = -0.28, R^2 = 0. 9999
- X HClO$_4$; slope = -0.28, R^2 = 0.9971
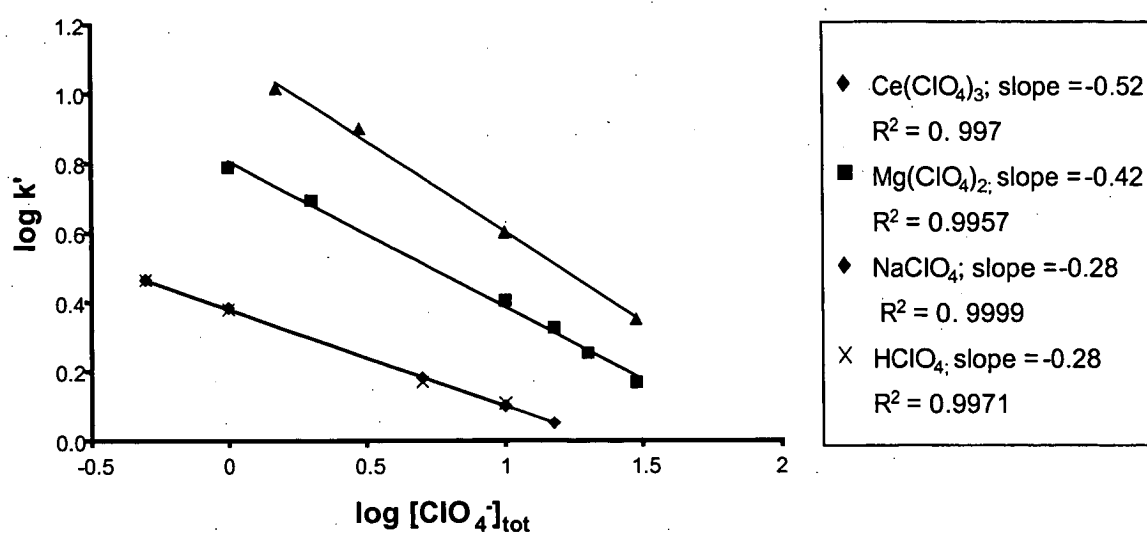
Figure 3.13 (c) Log *k′ versus* log [ClO$_4^-$] plots comparing the slopes with varying mobile -phase cation of iodide. Other conditions as described in Figure 3.1.

3.3.4 Mechanism of Separation

Okada and Patil [10] proposed that there is sufficient flexibility in adsorbed C14SB molecules that in a pure water mobile phase interaction between adjacent adsorbed C14SB molecules can occur (see Figure 3.14(a)). The positive and negative charges of one C14SB molecule are paired with the negative and positive charges, respectively, of a second. A small amount of salt in the mobile phase weakens this pairing of the zwitterion causing a relaxation (disentangling) of the surface morphology (see Figure 3.14(b)). This allows greater accessibility of analyte ions to the functional groups on the C14SB molecule. The rapid initial change in k' values (Figure 3.6) in going from pure water to a 1 or 2 mM concentration of salt in the mobile phase supports this theory of an abrupt change in surface morphology.

It has been suggested [7,11,12] that the selectivity of a zwitterionic stationary phase for anions is a function of the chaotropic character of the anion. Ions such as ClO_4^- are chaotropic, which refers to an increase in entropy resulting from disruption of the water structure surrounding these ions in solution. Chaotropic anions are large with a low charge and have a large number of electrons spread over an appreciable volume such that the electrons are not tightly held by the nucleus. For example, the four equivalent oxygens in perchlorate can bond in all directions with quaternary ammonium groups on the zwitterionic stationary phase. The charge will be effectively distributed among all positive sites to compensate for the negative charge of the perchlorate, leading to diffuse ion-pair formation. This in turn creates a net negative

(a)

(b)
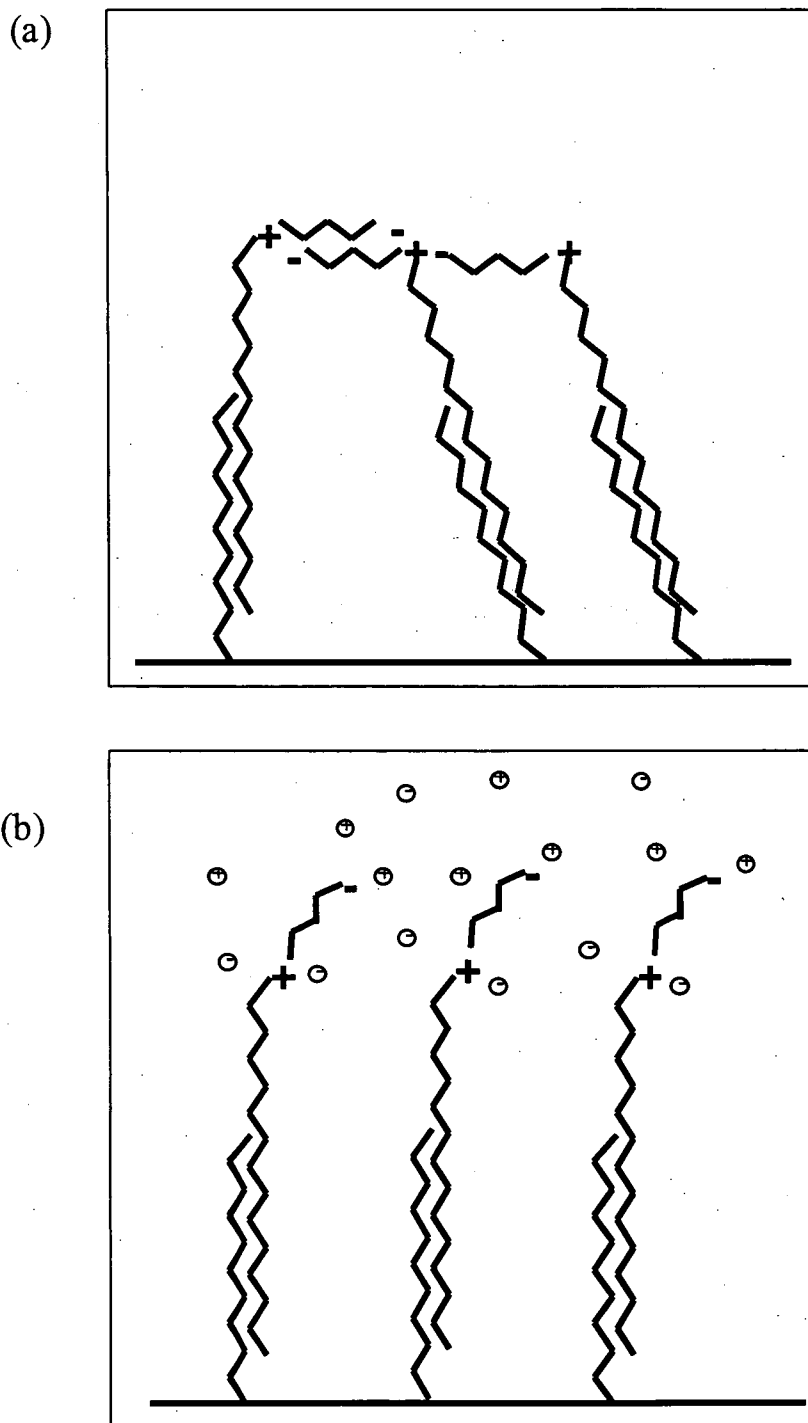
Figure 3.14 Illustration of the surface morphology in (a) water and (b) with the addition of a small amount of electrolyte to the mobile phase. Diagram adapted from [11].

charge on the surface when the counterion of the sulfonic acid group (usually Na^+) is not as tightly bound as the chaotropic anion. This is consistent with the large negative zeta potential observed in CE experiments using $NaClO_4$ as the BGE.

The chromatographic retention of smaller ions such as F^- and SO_4^{2-} is low whereas the retention increases for the series Cl^-, Br^-, I^- because of increased charge distribution. The increasingly negative zeta potential across the series SO_4^{2-}, Cl^- Br^-, I^- and ClO_4^- shown in Table 3.1 and observed also by Baryla and Lucy [5] corresponds to increasing charge distribution and follows the Hofmeister, or chaotropic, series [13]. Hofmeister effects are much greater for anions than cations [14].

The charge on the mobile-phase cation also has some effect on the chromatographic behaviour of anions. Figure 3.2 shows longer retention times for sample anions as the mobile-phase cation is changed from Na^+ to Mg^{2+} to Ce^{3+}. This behaviour may be explained as follows. With a Na^+ salt as the mobile phase the zwitterionic stationary phase has a negative zeta potential (as indicated by the measured EOF values) that exerts a repulsion effect on the analyte anion. Use of a 2+ or 3+ salt reduces the surface negative charge by stronger electrostatic interaction with the sulfonate functional group, making it easier for the analyte anion to approach the positively charged quaternary ammonium groups of the zwitterion.

The proposed retention mechanism comprises two simultaneous effects, one of ion-exclusion and one of chaotropic interaction. The ion-exclusion effect arises as follows. The sulfonate group on the outer part of the zwitterionic stationary phase contributes a

negative charge that repels analyte anions by acting as a Donnan membrane. However, the magnitude of this negative charge (and hence the degree of repulsion created by the Donnan membrane) varies depending on how strongly the mobile-phase cations interact with the sulfonate functional groups and how strongly the mobile-phase anions interact with the quaternary ammonium groups. Strong interaction by the mobile-phase cations decreases the surface negative charge, whilst strong interaction of the mobile-phase anions increases the surface negative charge. In effect, the outer negative charge constitutes a barrier over which an analyte anion must pass in order to approach the quaternary ammonium functional group on the zwitterionic stationary phase. This barrier can be lowered by partial neutralisation of the negative charge on the sulfonate group by a 2+ or 3+ cation, giving increased retention as observed in Figure 3.2.

The other part of the proposed mechanism concerns the interaction of sample anions with the quaternary ammonium functional group of the zwitterion.

The experimental evidence presented here is that separation selectivity follows the order of increasing polarisability, or chaotropic character. The more chaotropic is the analyte anion, the greater will be its retention. Thus, the elution order of anions appears to be determined by "chaotropic selectivity" rather than by electrostatic effects. These effects are illustrated schematically in Figure 3.15.

Figure 3.15(a) shows the zwitterionic stationary phase in equilibrium with the mobile-phase cations and anions and the establishment of the Donnan membrane. The situation occurring with a $NaClO_4$ mobile phase is depicted in Figure 3.15(b). Here

Figure 3.15 Schematic summary of the proposed mechanism. (a) Establishment of the Donnan membrane, (b) use of a NaClO₄ mobile phase, and (c) use of a CeCl₃ mobile phase.

there is a weak interaction between Na^+ and the sulfonate functional group and a strong interaction between ClO_4^- and the quaternary ammonium functional group. These effects combine to establish a relatively strong negatively charged Donnan membrane, which exerts a strong repulsion on analyte anions, especially multiply charged anions like SO_4^{2-}. Those analyte anions that can penetrate the Donnan membrane (and it should be remembered that the charge on this membrane will always be less than in ion-exclusion chromatography where only sulfonate functional groups are present) can undergo chaotropic interactions with the quaternary ammonium functional groups and are therefore retained to various degrees. Figure 3.15(c) shows the situation with a $CeCl_3$ mobile phase, with which there is a strong interaction of Ce^{3+} with the sulfonate groups and a weak interaction of Cl^- with the quaternary ammonium groups. The net result is that the Donnan membrane now becomes weakly positively charged and all analyte anions can penetrate relatively freely. Although under these extreme mobile phase conditions (mobile phase containing a mobile-phase cation as highly interacting as Ce^{3+}) there is a suggestion of increased electrostatic effects (see Section 3.3.3.4), separation of these anions occurs predominantly due to chaotropic interactions with the quaternary ammonium groups.

The proposed mechanism embodies the main elements of the mechanisms suggested previously in that the mobile phase ions are considered to interact with the functional groups in the same manner as suggested in the EDL theory of Hu [15] and there is a surface charge (the Donnan membrane) as suggested by Okada and Patil [10]. However the proposed mechanism is the first to explain the elution order and also the

effects on retention caused by changes in the nature of the mobile-phase anion and cation. This mechanism brings into question the name "Electrostatic Ion Chromatography" that has been applied extensively, since this name suggests a predominance of electrostatic effects in the retention mechanism. It might be more appropriate to use the name "Zwitterionic Ion Chromatography" to refer to ion chromatographic separations in which a zwitterionic stationary phase is employed.

3.4 Conclusions

The comprehensive investigation into the effect of the mobile-phase anion and cation on the retention of analytes and the zeta potential of the (C14SB) ZIC system presented in this chapter has revealed characteristics not seen before. A new retention mechanism is proposed that is based on chaotropic selectivity. Retention in this system is determined by the analyte anion's ability to penetrate the repulsion effects established by a Donnan membrane and to interact chaotropically with the quaternary ammonium group of the zwitterion. Selectivity is determined chiefly by the latter consideration, so that retention follows the Hofmeister (chaotropic) series $IO_3^- < SO_4^{2-} < Cl^- < NO_2^- < CNO^- < ClO_3^- < ClO_4^-$. The proposed mechanism draws on the framework of existing theories of ZIC but provides for the first time an explanation of the effects of the mobile-phase cation on the retention of anionic analytes. The mechanism also offers a coherent explanation for the observation that changing the concentration of a mobile phase can cause the retention of some analytes to increase and others to decrease.

3.5 References

(1) W. Hu, P.R. Haddad, Anal. Commun. 35 (1998) 317-320.

(2) W. Hu, T. Takeuchi, H. Haraguchi, Anal. Chem. 65 (1993) 2204-2208.

(3) W. Hu, P.R. Haddad, K. Hasebe, K. Tanaka, P. Tong, C. Khoo, Anal. Chem. 71 (1999) 1617-1620.

(4) W. Jiang, K. Irgum, Anal. Chem. 71 (1999) 333-344.

(5) N.E. Baryla, C.A. Lucy, Anal. Chem. 72 (2000) 2280-2284.

(6) J.M. Patil, T. Okada, Anal. Commun. 36 (1999) 9-11.

(7) K. Iso, T. Okada, Langmuir 16 (2000) 9199-9204.

(8) B.A. Williams, G. Vigh, Anal. Chem. 68 (1996) 1174-1180.

(9) W. Hu, P.R. Haddad, K. Tanaka, K. Hasebe, Analyst 125 (2000) 241-244.

(10) T. Okada, J.M. Patil, Langmuir 14 (1998) 6241-6248.

(11) T. Umemura, S. Kamiya, A. Itoh, K. Chiba, H. Haraguchi, Anal. Chim. Acta. 349 (1997) 231-238.

(12) K. Irgum, University of Umeå, Sweden, personal communication, May 2000.

(13) M.G. Cacace, E.M. Landau, J.J. Ramsden, Q. Rev. Biophys. 30 (1997) 241-277.

(14) K.D. Collins, M.W. Washabaugh, Q. Rev. Biophys. 18 (1985) 323-422.

(15) W. Hu, Langmuir 15 (1999) 7168-7171.

Mechanistic Studies on the Separation of Cations on a Phosphocholine Stationary Phase

4.1 Introduction

Although the stationary phase in ZIC is bi-functional, it has predominantly been used for the separation of anions [1-3]. The stationary phase is most commonly created by adsorption of a sulfobetaine-type zwitterionic surfactant onto a hydrophobic chromatographic support material, such as a reversed phase ODS column [4]. The sulfobetaine-type surfactant used, for example 3-(N,N-dimethylmyristyl-ammonio)-propanesulfonate (C14SB)), has an inner positively charged functional group (quaternary ammonium group) and an outer negatively charged functional group (sulfonate group) separated by three methylene groups. The resultant chromatographic system has an ability to separate anions with a unique selectivity, whilst cations can only be separated into groups of analytes with the same charge [5]. ZIC has great analytical potential but its development and application has been hindered due to a seemingly complex mechanism of separation.

Proposed mechanisms of separation in ZIC have been derived from studies of the retention behaviour of anions on sulfobetaine-type stationary phases [6-8] (see Chapter 3).

Investigations into ZIC have increasingly extended to the analysis of cations [9]. As mentioned earlier, it was found that the sulfobetaine-type system used for the analysis of anions was not very effective for the separation of cations, as only separation into charge groups was possible [5,10]. Hu and Haddad [10] suggested that this problem may be overcome by using stationary phases in which the positions, spacing or acid-base strength of the charged functional groups on the zwitterion were varied. Altering the acid-base strength of the functional groups [11] or utilising a mixture of anionic and zwitterionic surfactants on the stationary phase [12] allowed the separation of cations, but this outcome was attributed to the additional ion-exchange interactions introduced into the separation. In an alternative approach, Hu *et al.* [9] investigated the use of a phosphocholine-type surfactant (N-tetradecylphosphocholine (C14PC)) to create the stationary phase. This surfactant is analogous to the C14SB used for the analysis of anions, but the charge positions are reversed to give the surfactant a negative inner charge (phosphonate group) and a positive outer charge (quaternary ammonium) (see Chapter 1 for structure). This study found that while the C14SB showed a higher selectivity for anions, the C14PC displayed a high selectivity for cations. It was also found that addition of electrolyte to the mobile phase diminished the selectivity of the C14PC for anions, analogous to the effect observed on the selectivity of cations using the C14SB surfactant [13].

A comprehensive set of retention data presented previously for the anion system (see Chapter 3) revealed characteristics of ZIC not observed previously and which were of importance to the understanding of the separation mechanism. A similar investigation

of the retention of cations on the C14PC phase is now necessary to determine whether this ZIC system behaves in the same manner as the C14SB system. Anions dominate cations in terms of Hofmeister (chaotropic) effects [14], so it was not known whether the cation system would mirror the trends of the anion system in which direct chaotropic interactions play a major role.

The aims of this chapter are to produce a systematic retention data set to use in conjunction with surface potential data from the literature to reveal the nature of analyte interactions with the inner negative charge and the formation and modulation of the surface potential, and to use this information to develop a separation mechanism for ZIC of cations on a C14PC stationary phase.

4.2 Experimental

4.2.1 Apparatus

The details of the IC instrument are given in Chapter 2.

The column used throughout this study was coated with N-tetradecylphosphocholine, with the procedure for coating also outlined in Chapter 2.

A Varian (Palo Alto, CA, USA) SpectraAA-800 system was used for peak identity confirmation of K, Li (AES mode) and Ag (AAS mode) due to the many system peaks observed when indirect UV and conductivity detection was employed. The peak identity of NH_4^+ was confirmed by the post-column addition of Nessler's Reagent (an

alkaline solution of potassium tetraiodomercurate(II)), producing a yellow/orange precipitate where NH_4^+ was present [15]. Tl^+ peaks were identified by the post-column addition of NaI, whereby a yellow precipitate (TlI (s)) indicated the presence of Tl^+ [16].

4.2.2 Reagents

Nessler's reagent was prepared according to literature methods [15].

4.3 Results and Discussion

4.3.1 Proposed Mechanism

With a water mobile phase the opposite charges of adjacent zwitterionic molecules may interact, resulting in a tangled surface morphology. This interaction decreases with the addition of salt to the mobile phase, due to shielding of the charges on the zwitterion by electrolyte ions of opposite charge. This then unfurls the entangled zwitterion molecules and allows greater accessibility of ions on the charges of the zwitterionic stationary phase. This proposal is analogous to the anion system (see Figure 3.14).

Figure 4.1(a) illustrates the equilibration of mobile-phase anions and cations with the charges on the C14PC zwitterion. The outer positive charge on the zwitterion (the quaternary ammonium group) acts as a Donnan membrane. This charge is effective in repelling analyte cations, but the charge is reduced due to the close proximity of the negative phosphonate group. The magnitude and sign of the overall charge on the
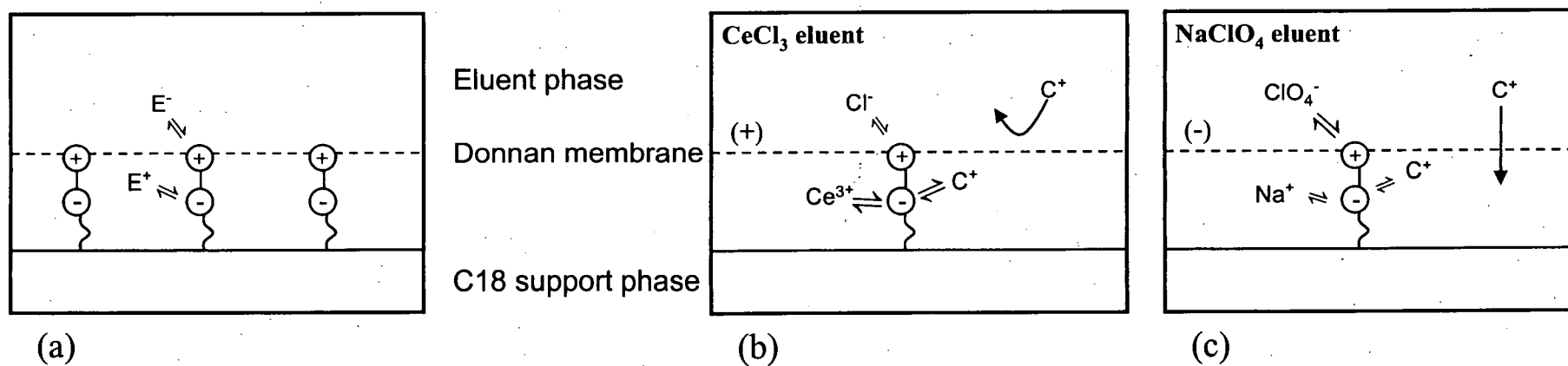
Figure 4.1 Schematic representation of the proposed mechanism for the phosphocholine stationary phase cation system. (a) Establishment of the Donnan membrane, (b) use of a CeCl₃ mobile phase, (c) use of a NaClO₄ mobile phase.

Donnan membrane depends on the interaction and shielding capability of the mobile-phase anions and cations as they interact with the positive and negative charges on the zwitterion, respectively.

The interaction of cations with the phosphonate group (as observed in this work by increased retention for the C14PC stationary phase using water as mobile phase) was found to increase across the series:

$$K^+ \cong Na^+ < NH_4^+ < Li^+ < Tl^+ < Ag^+ < Ba^{2+} \cong Sr^{2+} < Co^{2+} < Ca^{2+} < Cu^{2+} < Cd^{2+} < Zn^{2+} <$$

$$Ce^{3+} \hspace{8cm} (4.1)$$
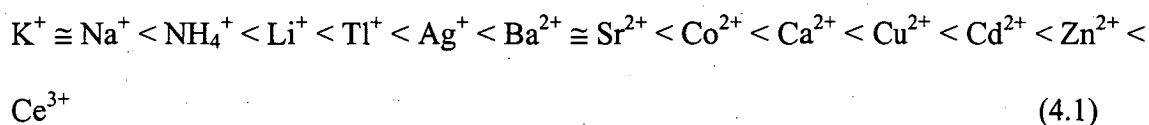
Similarly, the retention times of anions under the same conditions (reflecting interactions of these anions with the quaternary ammonium group) increase across the series:

$$IO_3^- \approx SO_4^{2-} < Cl^- < NO_2^- < CNO^- < Br^- < NO_3^- < ClO_3^- < I^- < ClO_4^- \hspace{1cm} (4.2)$$
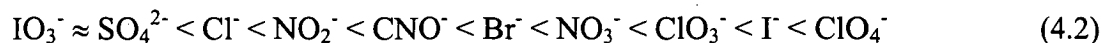
This order follows the general trend of the Hofmeister or chaotropic series [14,17] and reflect the order of increasing polarisability of the analytes. As a consequence, the negative charge on the zwitterion will be shielded to the greatest extent with a Ce^{3+} mobile-phase cation, resulting in a more positive Donnan membrane. The overall Donnan membrane will be most positive when a strongly shielding mobile-phase cation (Ce^{3+}) is combined with a mobile-phase anion (such as Cl^-) that only weakly shields the outer positive charge of the zwitterion. This is illustrated in Figure 4.1(b), where the mobile phase is $CeCl_3$. The Donnan membrane will be least positive (or even negative)

when the mobile-phase anion greatly shields the outer positive charge and the mobile-phase cation only weakly shields the inner negative group, such as when $NaClO_4$ is used as the mobile phase, as illustrated in Figure 4.1(c).

A negative Donnan membrane allows analyte cations to enter the stationary phase (Figure 4.1(c)) while a positive Donnan membrane exerts a repulsive effect on analyte cations (Figure 4.1(b)). In the latter case, analyte cations may still move into the stationary phase if their interaction with the inner charge is sufficiently energetically favourable to overcome this repulsion barrier. Conversely, even if the Donnan membrane is negative, retention may still be small if the nature of the analyte cation (such as Ce^{3+}) does not allow it to interact effectively with the inner charge. Furthermore, analyte cations must compete with mobile-phase cations for interaction with the inner charge and their affinity for the inner negative charge must be comparable or greater than that of the mobile-phase cation for retention to occur.

In Figure 4.1(c), the mobile-phase cation is Na^+ and according to series (4.1), all cations except for K^+ can compete with Na^+ for interaction with the inner negative charge. With little or no repulsion from the Donnan membrane occurring due to the shielding effects of the mobile-phase anion, ClO_4^-, it would be expected that most analyte cations would be retained in this system. It would also be predicted that retention would increase (compared to that in a water mobile phase) with increased mobile phase concentration due to the unfurling of the surface morphology and greater accessibility of the inner charge. In Figure 4.1(b), the analyte cation may overcome the

repulsion of the Donnan membrane if the attraction to the inner charge is sufficient, but it must also compete with Ce^{3+} for interaction with the inner charge. Of the cations listed in the series above, there are none that are more chaotropic than Ce^{3+}, hence it would be expected that all analyte cations would show little retention when the mobile-phase cation is Ce^{3+}.

If the analyte cation lies to the left of the mobile-phase cation in series (1), then its retention should be decreased compared with its retention in a water mobile phase. Additionally, the greater the interaction of the mobile-phase anion with the outer positive charge, the greater the ability of the analyte cation to be retained. With the chaotropic series in mind, the effect of various mobile phases on the retention of analytes can be predicted.

4.3.2 Elution Effects of Analyte Anions

The retention of anions was studied on the phosphocholine stationary phase and it was found that although retention was much less than for cations, the mobile phase still modulated the retention of anions. For example, a $CaCl_2$ mobile phase increased retention of anions while a $NaClO_4$ mobile phase decreased retention compared to that with a water mobile phase (see Figure 4.2). Selectivity of anions on this stationary phase was determined by chaotropic effects, also suggesting that analyte anions interacted directly with the positive charge on the zwitterion, whether that charge was the inner charge (sulfobetaine-type surfactant) or the outer charge (phosphocholine-type surfactant). The fact that interaction, and hence retention, was greater when the
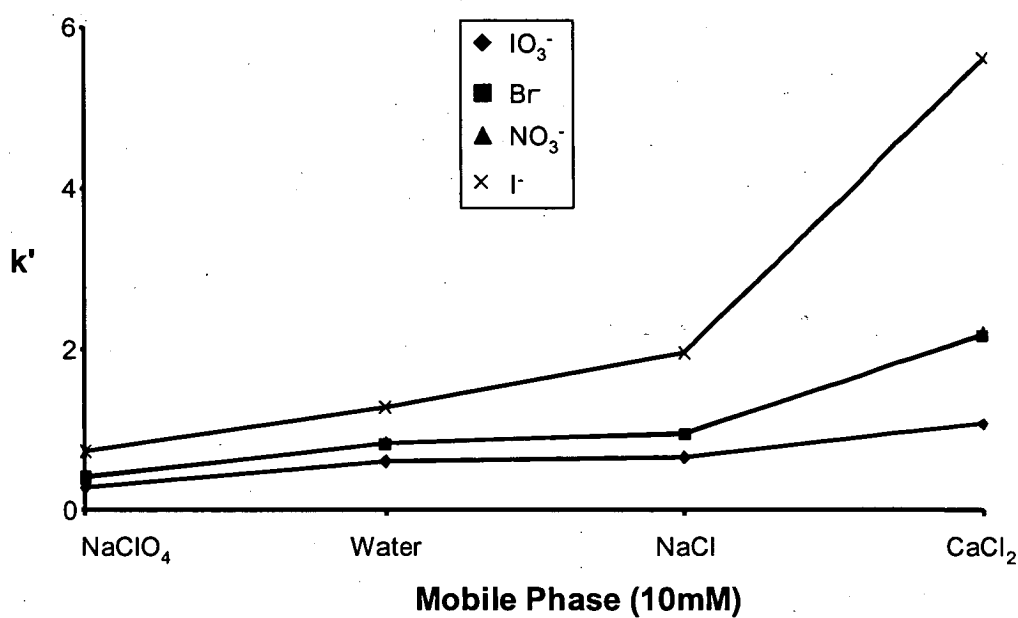
Figure 4.2 Effect of the mobile phase on the retention of anions (IO_3^-, Br^-, NO_3^-, I^-). Conditions: column, ODS modified with C14PC; flow rate, 1.0 mL min^{-1}; detection, direct UV at 210 nm; sample, 100 μL containing 1.0 mM of each anion.

positive charge was the inner charge may be due to the close proximity of the hydrophobic C14 chain. As chaotropic interactions occur most readily with large ions with a low charge, such as ClO_4^- [18], the larger the quaternary ammonium ion, the greater will be its chaotropic interaction with analyte ions. The inner quaternary ammonium group on the sulfobetaine surfactant has a larger hydrophobic moiety, namely the C14 chain, compared to the quaternary ammonium group positioned on the end of the phosphocholine surfactant (next to a two carbon chain). Thus, the sulfobetaine quaternary ammonium group would be expected to have a greater water structure breaking capacity and therefore should associate more readily with analyte ions in solution. This has been demonstrated by Barron and Fritz [19] who found that the relative retention of anions increased as the hydrophobic moiety of trialkylammonium resins was systematically increased.

4.3.3 Zeta Potential Data

According to the mechanism proposed, the mobile-phase anions and cations should together modulate the surface charge of the stationary phase depending on their relative affinities for the opposite charges on the zwitterion. This modulation should be evident in experimentally measured zeta potentials. Iso and Okada [20] determined the effect of various electrolytes on the zeta potential of a phosphocholine-type surfactant through measurement of the electrophoretic mobility of the surfactant micelles in a silica capillary using a capillary electrophoresis system. Their method involved introducing a sample of pyrene and acetone into a capillary filled with electrolyte and

surfactant micelles. Pyrene is partitioned completely into the micelles and therefore migrates with the micelles, while acetone marks the electro-osmotic flow, allowing measurement of the mobility of the micelles and hence the zeta potential. A solution of $NaClO_4$ (160 mM) resulted in a zeta potential of -13.9 mV, supporting the supposition that the ClO_4^- ion shields the quaternary ammonium group to a greater extent than Na^+ shields the inner phosphonate group. A Bu_4NCl solution (80 mM) resulted in a positive zeta potential of 28.4 mV, illustrating the ability of an electrolyte to modulate the zeta potential from negative to positive. In this case, a strong shielding of the negative functionality (phosphonate group) by the Bu_4N^+ ion and weak shielding of the outer positive quaternary ammonium group by the Cl^- mobile phase ion leads to the overall positive zeta potential. These results support the proposed mechanism and are consistent with those obtained on the anion system using C14SB as the zwitterion (see Chapter 3).

4.3.4 Elution Effects of Analyte Cations

The proposed mechanism was further tested by studying the elution behaviour of a range of monovalent inorganic cations, namely K^+, NH_4^+, Li^+, Tl^+ and Ag^+, under varying concentrations of mobile phases containing different anionic and cationic species. Divalent cations (Sr^{2+}, Ba^{2+}, Ca^{2+}, Cd^{2+}, Zn^{2+}) were studied in preliminary investigations but were found to have extremely high retention factors when the mobile-phase cation was monovalent, while Zn^{2+} was found over time to give irreproducible, broad and shouldered peaks.

The mobile-phase anion and cation species (Na^+, Co^{2+}, Cu^{2+}, Ce^{3+}, SO_4^{2-}, NO_3^- and ClO_4^-) were chosen such that they covered a wide range of chaotropic strengths.

The elution effects of the five analytes (K^+, NH_4^+, Li^+, Tl^+ and Ag^+) on a phosphocholine-coated column are shown in Figure 4.3, with increasing concentration of four different mobile phase salts ($NaClO_4$, $Co(ClO_4)_2$, $Cu(ClO_4)_2$ and $Ce(ClO_4)_3$). The $NaClO_4$ mobile phase resulted in an increase in retention compared with that of a pure water mobile phase for all five analytes. This was due to the ability of analyte cations to partition through the negative Donnan membrane (see Fig. 4.1(c)), and the fact that all five analytes can compete to some extent with the mobile-phase cation, Na^+, for the inner negative charge. Thus, the unfurling of the surface morphology with the addition of $NaClO_4$ resulted in a greater ability of these analytes to interact with the inner charge. The greatest increase in retention with the $NaClO_4$ mobile phase was observed for Ag^+ due its great ability to interact with the inner negative charge compared with the other four analytes (see interaction series shown in (4.1)). Ag^+ also has the highest selectivity compared to the mobile-phase cation, Na^+.

The $Co(ClO_4)_2$ mobile phase caused decreased retention for K^+ compared to that of a pure water mobile phase, but increased the retention of Li^+ and Ag^+. According to the chaotropic series, it would be expected that the Co^{2+} ion would compete more strongly for the anionic sites on the stationary phase than the three monovalent analytes. The

Figure 4.3 Effect of the concentration of various perchlorate salts in the mobile phase on the retention of (a) K^+ and (b) NH_4^+. Conditions: detection, indirect conductivity (with AAS used for peak identity confirmation); sample, 100 μL containing 1.0 mM of each cation, other conditions as in Figure 4.2.
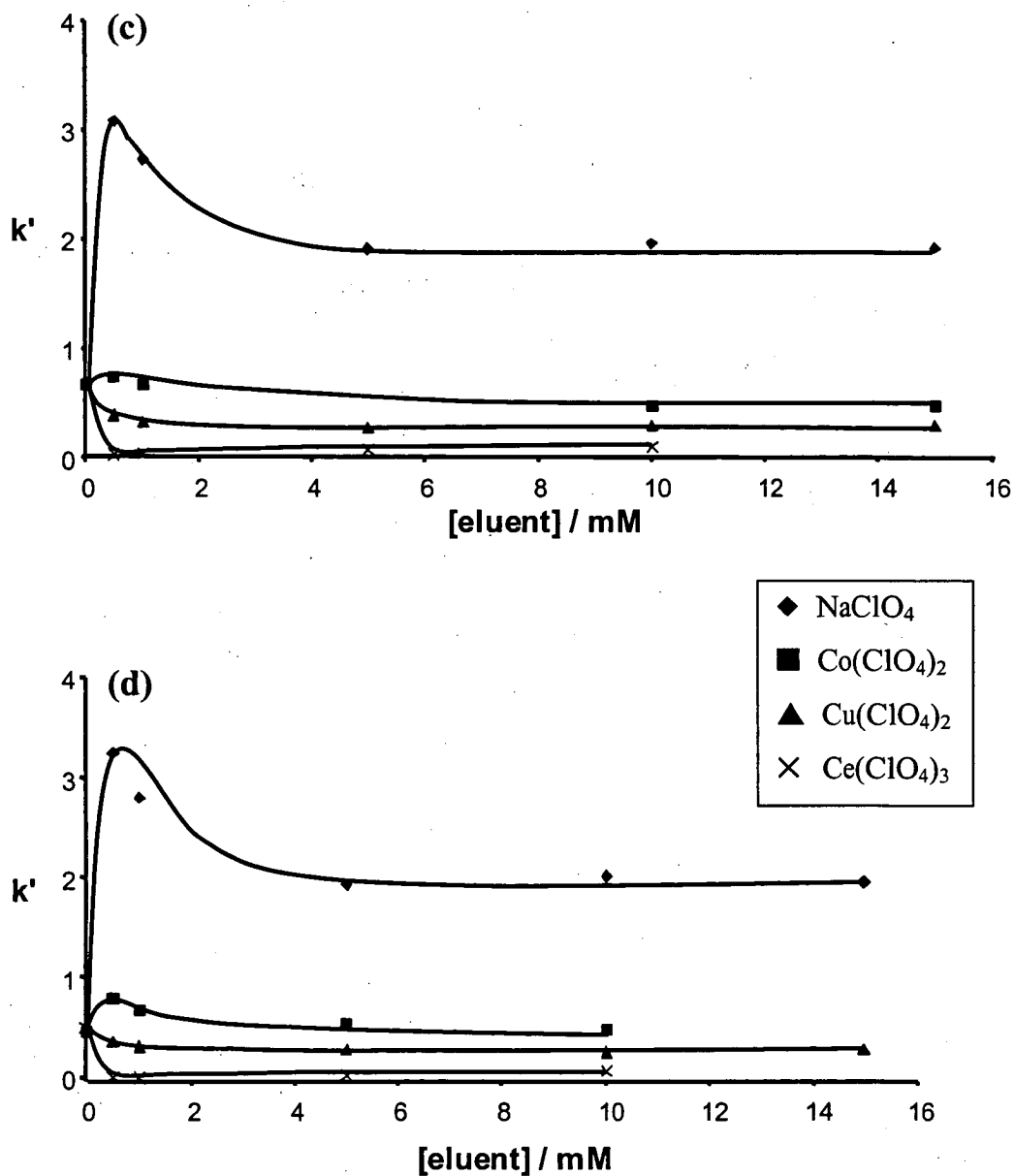
Figure 4.3 continued Effect of the concentration of various perchlorate salts in the mobile phase on the retention of (c) Li+ and (d) Tl^+. Conditions: detection, indirect conductivity (with AAS used for peak identity confirmation); sample, 100 µL containing 1.0 mM of each cation, other conditions as in Figure 4.2.

119
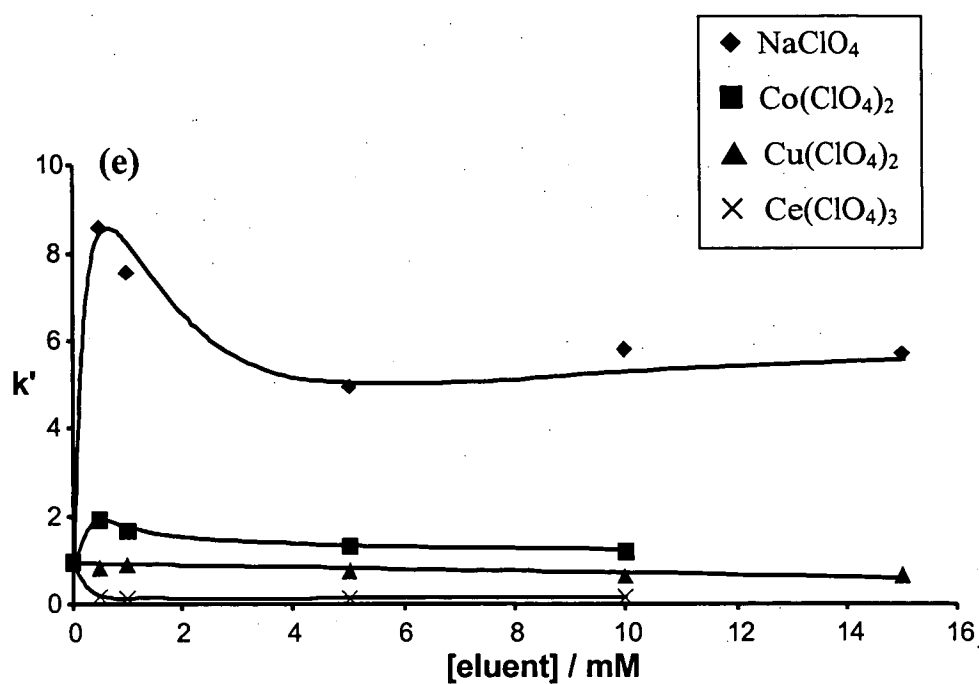
Figure 4.3 continued Effect of the concentration of various perchlorate salts in the mobile phase on the retention of (e) Ag^+. Conditions: column, ODS modified with C14PC; flow rate, 1.0 mL min^{-1}; detection, indirect conductivity (with AAS used for peak identity confirmation); sample, 100 μL containing 1.0 mM of each cation.

analyte cations. At low concentrations of the mobile phase, retention of Li^+ and Ag^+ increased due to greater accessibility of the inner negative charge, however retention decreased at increasingly higher concentrations as the highly chaotropic mobile-phase cation, Co^{2+}, competed effectively for the inner negative charge site. This resulted in a decrease in retention for K^+ and Li^+, but had little effect on the Ag^+ ion. $Ce(ClO_4)_3$ resulted in a decrease in the retention of all analytes due to the strong competition afforded by the highly chaotropic Ce^{3+} ion, which possibly also created a repulsive positively charged Donnan membrane. The same trends were observed for all analytes studied (see Figures 4.3 (d) and (e)) and were consistent with those obtained for the anion system using C14SB (see Chapter 3). The ClO_4^- mobile phases were used to analyse the elution effects in the first instance, due to the greater retention of all analytes compared with SO_4^{2-} mobile phases as a result of the more favourable Donnan membrane formed with the former anion. Trends and conclusions can be drawn with more certainty where the retention factor, k', is significant. The SO_4^{2-} mobile phases (Na_2SO_4, $CoSO_4$, $CuSO_4$ and $Ce_2(SO_4)_3$) were consistent with the elution effects observed for the ClO_4^- salts (shown with three representative analytes, K^+, Li^+ and Ag^+ in Figure 4.4). This suggests that although ClO_4^- (as the mobile phase) shielded the quaternary ammonium group to a great extent, the mechanism of the system was the same. However, the slight decrease in retention (after the initial abrupt increase) with increasing mobile phase concentration (eg. for analyte Ag^+ and a $NaClO_4$ mobile phase) was more pronounced for the ClO_4^- mobile phases than for the SO_4^{2-} mobile phases.
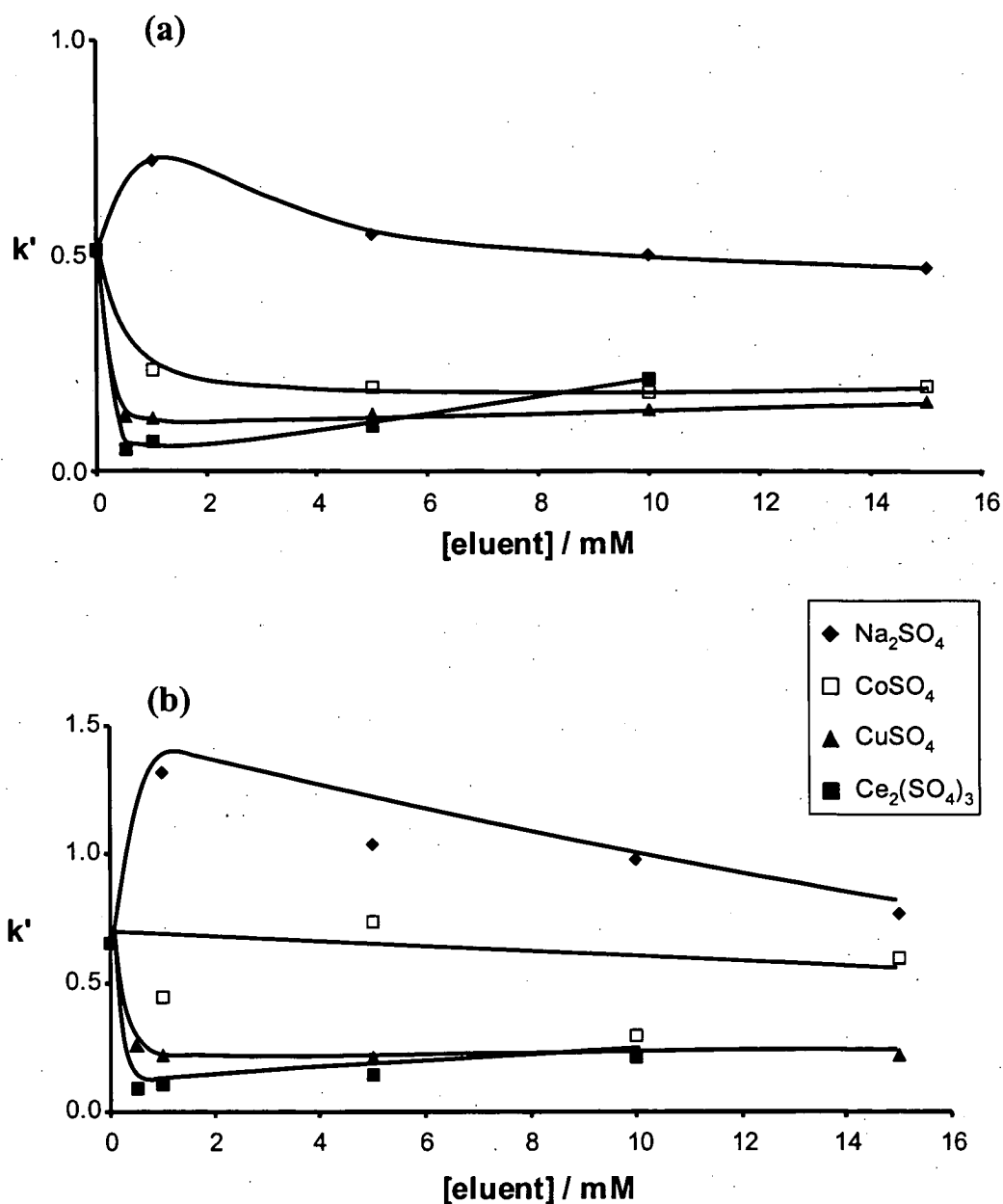
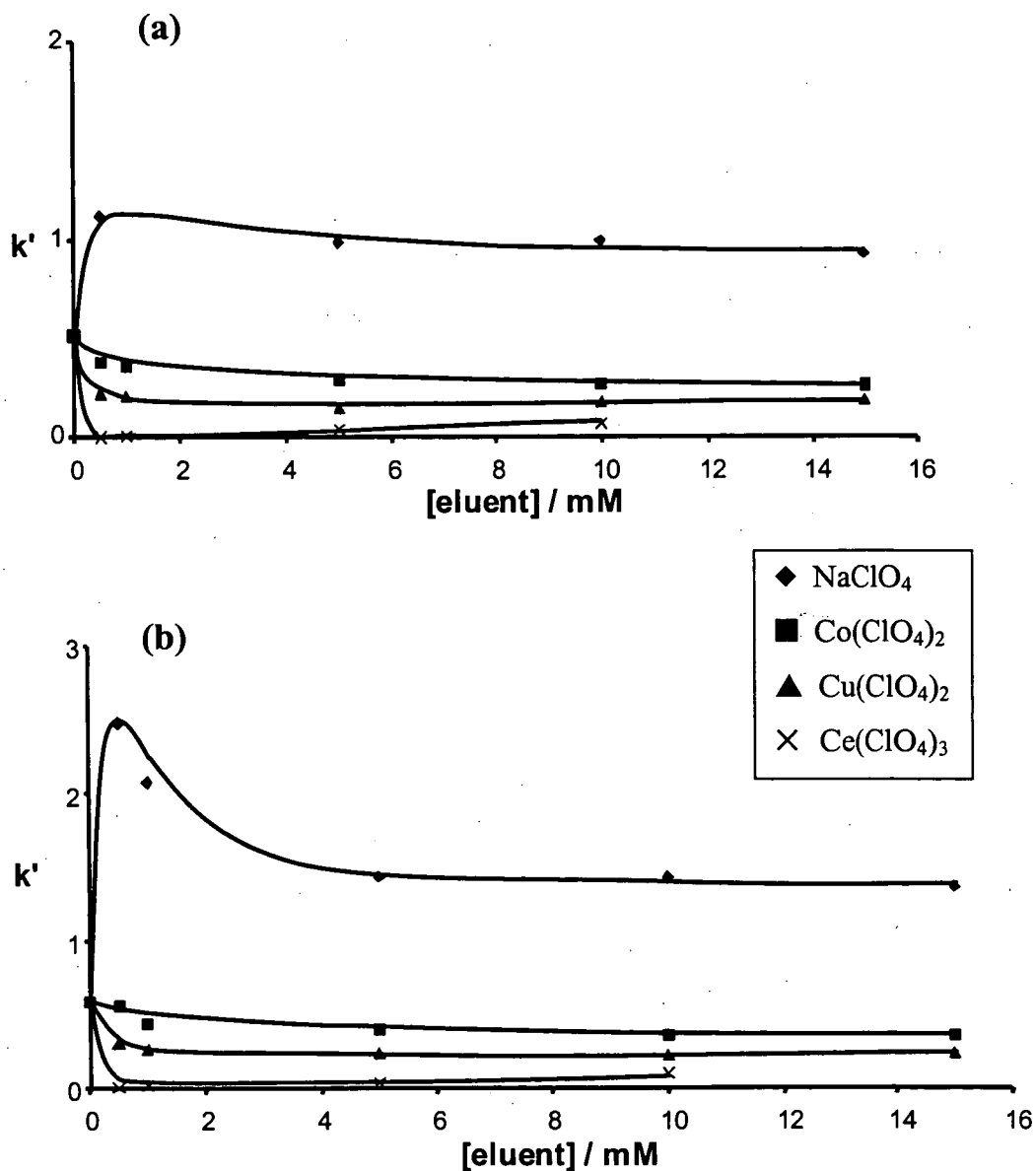**Figure 4.4** Effect of the concentration of various sulfate salts in the mobile phase on the retention of (a) K^+ and (b) Li^+. Conditions: column, ODS modified with C14PC; flow rate, 1.0 mL min^{-1}; detection, indirect conductivity (with AAS used for peak identity confirmation); sample, 100 μL containing 1.0 mM of each cation.

This may have been due to a greater electrostatic effect (as described in Section 3.3.3.4), but the slopes of log k' *versus* log [mobile phase] plots revealed no conclusive evidence of this, given that they were all only slightly negative, and the values of k' for the Ce^{3+} salts were too small to draw definitive conclusions.

Figures 4.5 illustrates the effect of the nature of the mobile-phase cation species on the retention of analyte cations. It is clearly evident that as the affinity of the mobile-phase cation for the inner charge increased, the retention of analyte cations decreased. This supports the proposed mechanism in relation to the competition between the mobile-phase and analyte cations for the inner charge. This effect was observed for both a weakly interacting mobile-phase anion (such as SO_4^{2-}, Figure 4.5 (a)) and a strongly interacting mobile-phase anion (such as ClO_4^-, Figure 4.5 (b)).

The effect of the mobile phase counter-anion species on the retention of analyte cations, for which the mobile-phase cation was the weakly-interacting Na^+, is illustrated in Figure 4.6 (a). There was a marked increase in retention with increasing chaotropic character of the mobile-phase anion, which was particularly evident on changing from NO_3^- to ClO_4^-. Thus, the counter anion can affect the retention of analyte cations. This corresponded directly to a decrease in the repulsive nature of the Donnan membrane as the mobile-phase anion increasingly shielded the outer positive charge, allowing the analyte cation greater access to the inner negative charge. This effect can be seen despite the presence of a strongly competing mobile-phase cation (Cu^{2+}), as illustrated in Figure 4.6 (b). The high affinity of Cu^{2+} for the inner negative
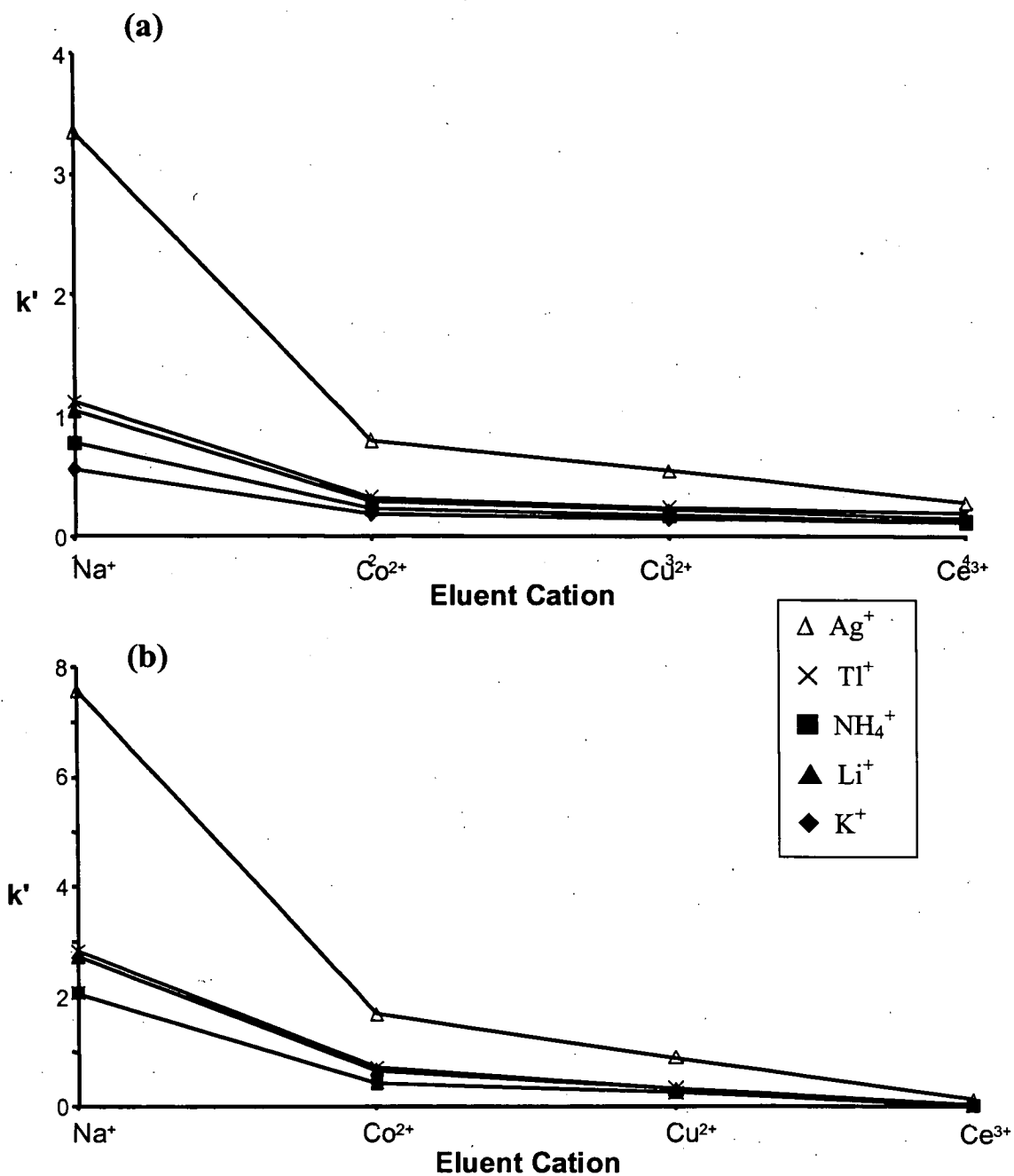
Figure 4.5 Effect of the mobile-phase cation species on the retention of various analytes using mobile phases containing 10 mM (with respect to the cation) (a) SO_4^{2-} salts, and (b) ClO_4^- salts. Other conditions are the same as described in Figure 4.2.
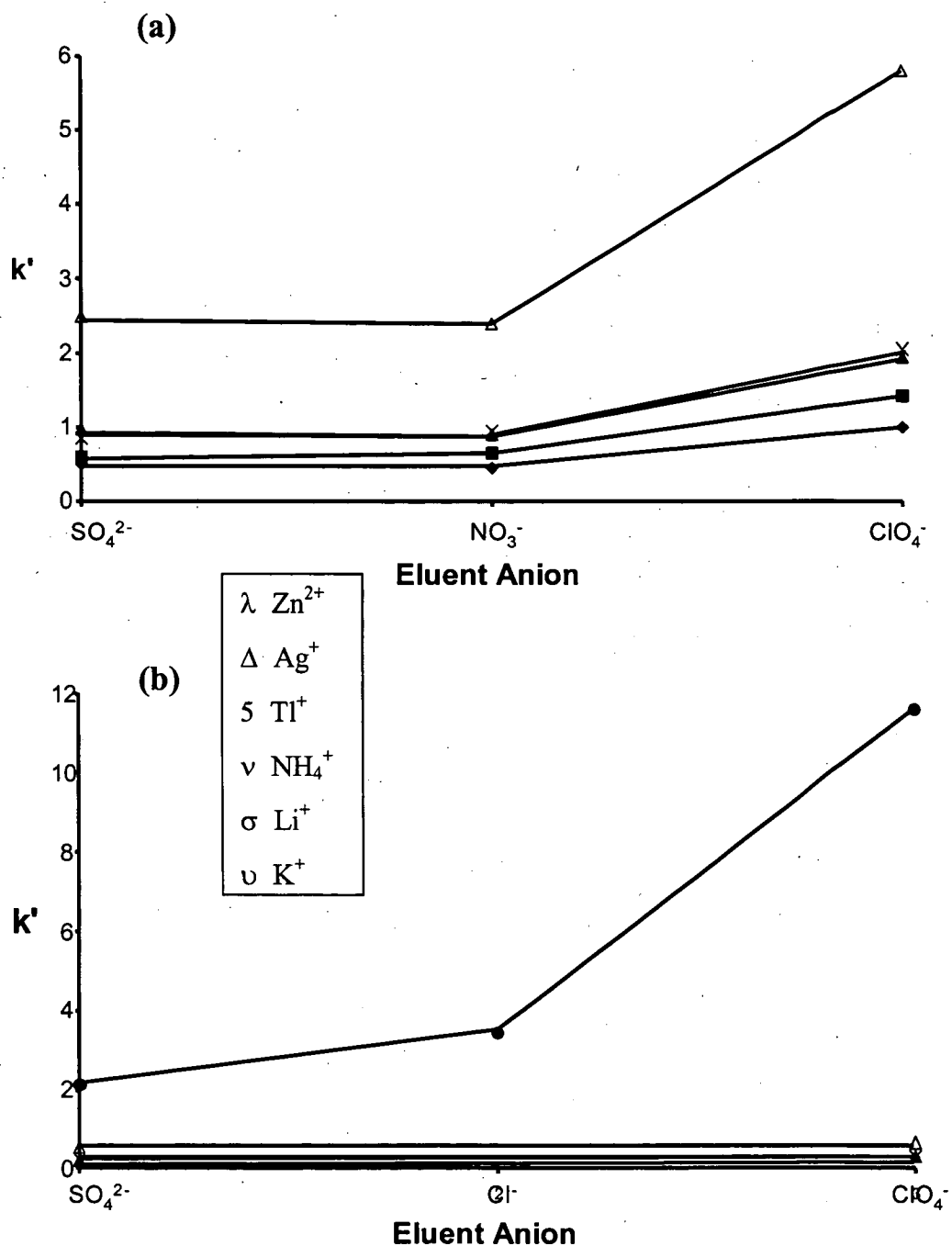
Figure 4.6 Effect of the mobile-phase anion species on the retention of various analytes using mobile phases containing (a) 10 mM (with respect to the anion) Na^+ salts, and (b) 10mM (with respect to the cation) Cu^{2+} salts. Other conditions are the same as described in Figure 4.2.

charge of the stationary resulted in suppression of the effect of the mobile-phase anion

for all analytes except Zn^{2+}, for which a significant increase in retention was noted on

changing the mobile-phase anion from Cl^- to ClO_4^-, due to Zn^{2+} greater affinity for the

stationary phase than Cu^{2+} (see series 4.1 in Section 4.3.1). Again, the results for the

effects of the mobile-phase anion supported the proposed mechanism and were

consistent with the reported mechanism operating in the anion system with C14SB as

the zwitterion.

4.4 Conclusions

This study has confirmed that a phosphocholine surfactant stationary phase has greater

selectivity for cations over anions, although there is also the potential to separate

polarisable anions, depending on the electrolyte added to the mobile phase. The

retention data presented here characterise the effects of the mobile-phase anion and

cation on the retention of cations on a phosphocholine surfactant-coated column. The

data reveal that cations are retained due to the same chaotropic interactions observed

with anions on the sulfobetaine-type surfactant system. The proposed mechanism

explains the elution effects based on both ion-exclusion effects and direct chaotropic

interactions with the inner charge on the zwitterion. The ion-exclusion component,

namely the build up of a Donnan membrane at the outer positive charge that is

dependent on the shielding ability of the mobile-phase anion and cation, is supported

by the elution trends observed, as well as by zeta potential studies reported in the

literature. Shielding and retention at the inner negative charge is determined by the

chaotropic series: $K^+ \cong Na^+ < NH_4^+ < Li^+ < Tl^+ < Ag^+ < Ba^{2+} \cong Sr^{2+} < Co^{2+} < Ca^{2+} <$ $Cu^{2+} < Cd^{2+} < Zn^{2+} < Ce^{3+}$, and by the ability of mobile-phase anions to shield the outer positive charge, which follows the chaotropic series for anions $IO_3^- \approx SO_4^{2-} < Cl^- <$ $NO_2^- < CNO^- < Br^- < NO_3^- < ClO_3^- < I^- < ClO_4^-$.

4.5 References

(1)   W. Hu, S. Cao, M. Tominaga, A. Miyazaki, Anal. Chim. Acta. 322 (1996) 43-47.

(2)   W. Hu, P.R. Haddad, Anal. Commun. 35 (1998) 317-320.

(3)   W. Hu, P.R. Haddad, K. Hasebe, K. Tanaka, P. Tong, C. Khoo, Anal. Chem. 71 (1999) 1617-1620.

(4)   W. Hu, T. Takeuchi, H. Haraguchi, Anal. Chem. 65 (1993) 2204-2208.

(5)   W. Hu, H. Tao, H. Haraguchi, Anal. Chem. 66 (1994) 2514-2520.

(6)   W. Hu, Langmuir 15 (1999) 7168-7171.

(7)   T. Okada, J.M. Patil, Langmuir 14 (1998) 6241-6248.

(8)   J.M. Patil, T. Okada, Anal. Commun. 36 (1999) 9-11.

(9)   W. Hu, P.R. Haddad, K. Hasebe, K. Tanaka, Anal. Commun. 36 (1999) 97-100.

(10)   W. Hu, P.R. Haddad, Trends in Anal. Chem. 17 (1998) 73-79.

(11)   W. Hu, H. Haraguchi, Anal. Chem. 66 (1994) 765-767.

(12)   W. Hu, K. Hasebe, D.M. Reynolds, H. Haraguchi, J. Liq. Chromatogr. Relat. Technol. 20 (1997) 1221-1232.

(13)   Hu, W. *International Ion Chromatography Symposium '98*, September 1998, Osaka, Japan, presentation 57.

(14)   K.D. Collins, M.W. Washabaugh, Q. Rev. Biophys. 18 (1985) 323-422.

(15)   A.I. Vogel. *Vogel's Textbook of Quantitative Chemical Analysis*, 5th ed.; Longman, Scientific and Technical co-published with John Wiley and Sons: New York, 1989.

(16)   *Merck Index*, 11 ed.; Merck and Co., Inc.: Rahway, New Jersey, USA, 1989.

(17) M.G. Cacace, E.M. Landau, J.J. Ramsden, Q. Rev. Biophys. 30 (1997) 241-277.

(18) K. Irgum, University of Umeå, Sweden, personal communication, May 2000.

(19) R.E. Barron, J.S. Fritz, J. Chromatogr. 284 (1984) 13-25.

(20) K. Iso, T. Okada, Stud. Surf. Sci. Catal. 132 (2001) 117-120.

Manipulation of Analyte Selectivity in ZIC

5.1 Introduction

Manipulation of analyte selectivity is a fundamental component of any versatile separation technique. Complex sample matrixes often contain trace amounts of the analyte of interest (resulting in very small peaks) which need to be isolated from large peaks of excess matrix ions. The selectivity of ZIC has advantages over standard ion-exchange separations in the early elution of ions of low polarisability, such as SO_4^{2-} and Cl^-, which in matrices such as seawater can interfere with other analyte peaks. In ion-exchange, SO_4^{2-} is retained strongly, often obscuring I^-. The important characteristic advantage of ZIC is that above a certain concentration of electrolyte in the mobile phase, there is little effect on retention – this prevents self-elution, as seen in standard ion-exchange. On the other hand, it also limits the ability to manipulate selectivity in ZIC.

Common techniques employed in ion-exchange chromatography to vary selectivity have little application in ZIC. For example, the addition of organic modifiers to the mobile phase is limited in ZIC since too high a concentration will strip the zwitterionic surfactant from the stationary phase. The effect of varying the pH of the mobile phase has been explored by Hu *et al.* [1,2], where it has been found that there existed an ability to change the selectivity from $NO_2^- < Br^- < NO_3^-$, to $Br^- < NO_2^- < NO_3^-$ to $Br^- <$

NO_3^- < NO_2^- by altering the pH between 1 to 3. Effectively the retention of NO_2^- was selectively increasing, which is thought to be due to the formation of HNO_2 (see Chapter 3).

As discussed in Chapters 3 and 4, the main means of manipulating the separation selectivity in ZIC is to vary the mobile-phase anion and cation species, however this too is limited. It was discussed (in Chapter 4) that a $CeCl_3$ mobile phase may increase the electrostatic effect on anions and a $NaClO_4$ mobile phase may alter the effect on cations. In this chapter, increasing the ion-exchange component of the separation mechanism by mixing a cationic surfactant with the zwitterion in the coating solution is investigated. This may introduce electrostatic effects and permit the nature of the mobile phase to be used as a variable to control retention. A similar study has been undertaken utilising a mixture of strong anionic and zwitterionic micelles to coat the column to give for the simultaneous separation of anions and cations [3], as well as a mixture of a zwitterionic surfactant containing a weak and strong charge, and an anionic surfactant [4].

Modification of reversed-phase stationary phases with charged surfactants is a well-known, simple and useful method to create a column for ion chromatographic (IC) separations [5,6], where the surfactant used carries either positively-charged groups (eg., cetyltrimethylammonium [7-9]) or negatively-charged groups (eg., eicosanesulfonate [10]). The elution order for a reversed-phase column coated with a cationic surfactant is F^- < Cl^- < SO_4^{2-} < NO_2^- < Br^- < NO_3^- with a monovalent eluting

ion [11], which differs from the order for these anions yielded from a fixed-site strong

ion-exchange column, where the order is $F^- < Cl^- < NO_2^- < Br^- < NO_3^- < SO_4^{2-}$ [5].

This result has been attributed to the fact that the polarisability of the ions contributes

to their retention in the hydrophobic environment arising from the long alkyl chain of

the surfactant [12,13]. Nevertheless, the addition of a cationic surfactant to the

zwitterionic coating mixture would be expected to add ion-exchange character and

selectivity to the retention mechanism.

SO_4^{2-}, HPO_4^{2-}, and F^- are important species (amongst others such as Cl^-, NO_2^-, Br^- and

NO_3^-) in the analysis of water, but as mentioned above they have shown very little or

no retention on the reversed-phase/zwitterionic-surfactant stationary phases when pure

water or an electrolyte solution was used as the mobile phase. Although a good

separation for SO_4^{2-}, HPO_4^{2-}, and F^- can be achieved using a fixed-site quaternary

ammonium-type ion-exchange column such as the IonPac AS4A [6], a mobile phase

with strong competing anions, such as carbonate, is required to avoid impractically

long retention times. In other words, weaker competing anions, such as hydroxide or

tetraborate, are not suitable for this task unless a specialised stationary phase such as

the IonPac AS11 [14] is used. However, the retention times are often lengthy.

A new type of stationary phase is presented in this chapter and is obtained by coating

the ODS stationary phase with a solution of mixed zwitterionic-cationic surfactants.

As opposed to the zwitterion alone on the stationary phase, the stationary phase shows

affinity for multivalent ions and allows their separation, with much shorter retention

times than normal ion chromatography and also permits a weak and suppressible mobile phase to be used. An example analysis of tap water illustrates the successful separation of SO_4^{2-}, HPO_4^{2-} and F^-, with a weak eluting ion and good detection limits.

The effect of the ratio of zwitterionic/cationic surfactant in the coating solution on selectivity was investigated via analysis of the slopes of log k' *versus* log [mobile phase] plots.

5.2 Experimental

5.2.1 Apparatus

Details of the IC instrument used are given in Chapter 2, but included a Dionex anion self-regenerating suppressor (Model ASRS), inserted between the UV-visible detector and the conductivity detector to reduce the conductance of the mobile phase.

5.2.2 Reagents

The tetradecyltrimethylammonium chloride (TTACl) was converted to the hydroxide form by first loading it onto an ODS stationary phase and then conditioning the column with 0.1 mM NaOH solution for 2 h at a flow rate of 1.0 mL min^{-1}. Following this step, the surfactant was removed from the column using 50 mL of 50% acetonitrile/water solution pumped through the column at a flow rate of 1.0 mL min^{-1}. The effluent was collected and heated to 50 °C in an oven for about 8 h in order to

remove the acetonitrile. The resultant tetradecyltrimethylammonium hydroxide (TTAOH) solution was stored in a refrigerator.

Inorganic salts used for preparing the samples in this work were obtained from Wako Chemicals (Osaka, Japan).

5.3 Results and Discussion

5.3.1 Manipulation of Analyte Selectivity

Cationic surfactants having quaternary ammonium functional groups have frequently been used to convert reversed-phase stationary phases into "permanently" or dynamically-coated materials which are suitable for the separation of anions. In the "permanent" coating method the surfactant is absent from any subsequent mobile phase and typical surfactants used for this task are hexadecyltrimethylammonium (HTA), dodecyltrimethylammonium (DTA), cetylpyridinium (CP) and tetradecyltrimethylammonium (TTA) [5]. TTA was chosen as a representative cationic surfactant in the present study because its alkyl-chain was identical to that of C14SB. An ODS column pre-coated to saturation with TTA surfactant was used to study the characteristics of the anion-exchange IC system, employing aqueous NaHCO$_3$ and Na$_2$CO$_3$ mobile phases with suppressed conductivity detection. Figure 5.1 illustrates the separation of 0.1 mM solutions of the Na$^+$ salt of F$^-$, Cl$^-$, NO$_2^-$, Br$^-$, NO$_3^-$, SO$_4^{2-}$ and 0.02 mM HPO$_4^{2-}$ using 25 mM Na$_2$CO$_3$ as the mobile phase. All analytes were separated and F$^-$ was completely resolved from the water-dip. The elution order for
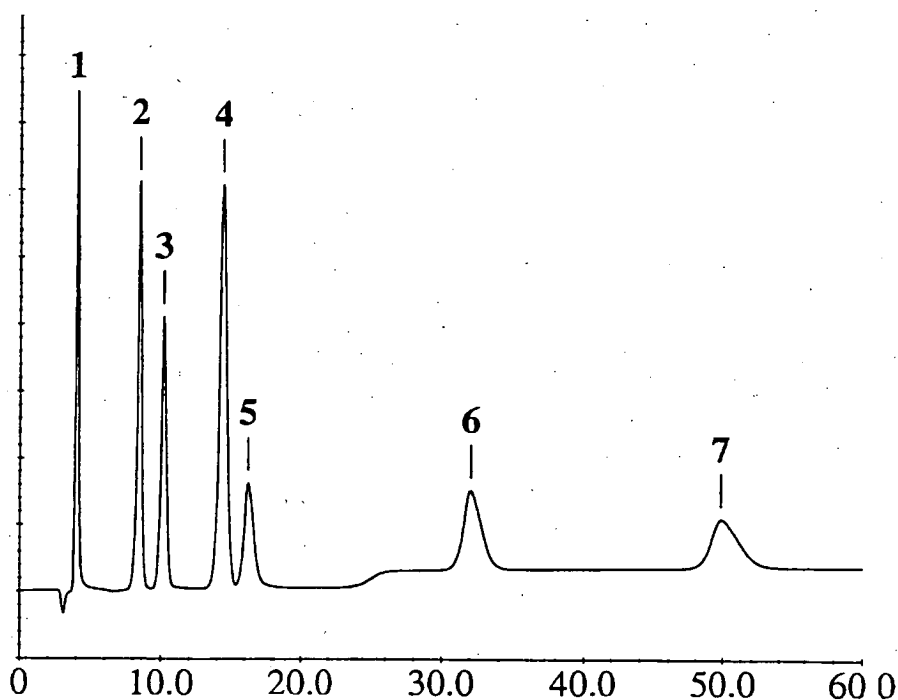
Figure 5.1 Chromatogram of a mixture of F^-, HPO_4^{2-}, Cl^-, SO_4^{2-}, NO_2^-, Br^- and NO_3^- (0.1 mM each, except for HPO_4^{2-} which was present at 0.02 mM) obtained using an ODS column coated with TTA micelles and 25 mM Na_2CO_3 as the mobile phase. Detection: suppressed conductivity; sample injection volume: 100 μL; flow rate: 1.0 mL min^{-1}. Peaks: 1 = F^-, 2 = Cl^-, 3 = HPO_4^{2-}, 4 = NO_2^-, 5 = SO_4^{2-}, 6 = Br^-, and 7 = NO_3^-.

these analyte ions was $F^- < Cl^- < HPO_4^{2-} < NO_2^- < SO_4^{2-} < Br^- < NO_3^-$ for the Na_2CO_3

mobile phase and $F^- < Cl^- < NO_2^- < Br^- < HPO_4^{2-} < NO_3^- < SO_4^{2-}$ for the $NaHCO_3$

mobile phase. The earlier elution of the divalent analytes with a CO_3^{2-} eluting anion is

a result of a more favourable stoichiometric exchange process, where comparatively

two HCO_3^- ions are required to exchange one divalent analyte. These retention orders

are typical of that observed for anion-exchange stationary phases having semi-

permanent functional groups. Very polarisable analytes (eg. I^- and SCN^-) were not

eluted from the TTA-coated column even when the effluent was monitored for more

than 20 hours, as they bind too strongly to the quaternary ammonium group.

Figure 5.2 details the same separation with a column coated with just the C14SB

surfactant. No separation of F^-, SO_4^{2-} and HPO_4^{2-} was achieved.

Three C14SB/TTA mixed surfactant solutions were prepared with different molar

ratios of these two surfactant species and were used as the column coating solutions.

The molar ratios of C14SB/TTA were 10:1, 8:2, and 10:10 (mM/mM) with the same

ODS column used for all, coated to saturation with these surfactant mixtures.

Separation of the same mixture of anions used in Figure 5.1 was undertaken and it was

observed that for columns coated with the C14SB/TTA ratio of 10:1 and a mobile

phase consisting of sodium tetraborate, good separation was achieved with a shorter

analysis time (see Figure 5.3). The elution order was found to be $F^- < HPO_4^{2-} < SO_4^{2-} <$

$Cl^- < NO_2^- < Br^- < NO_3^-$, which is similar to that seen in ZIC. The same elution order

was observed for the 8 mM/2 mM C14SB/TTA coatings.
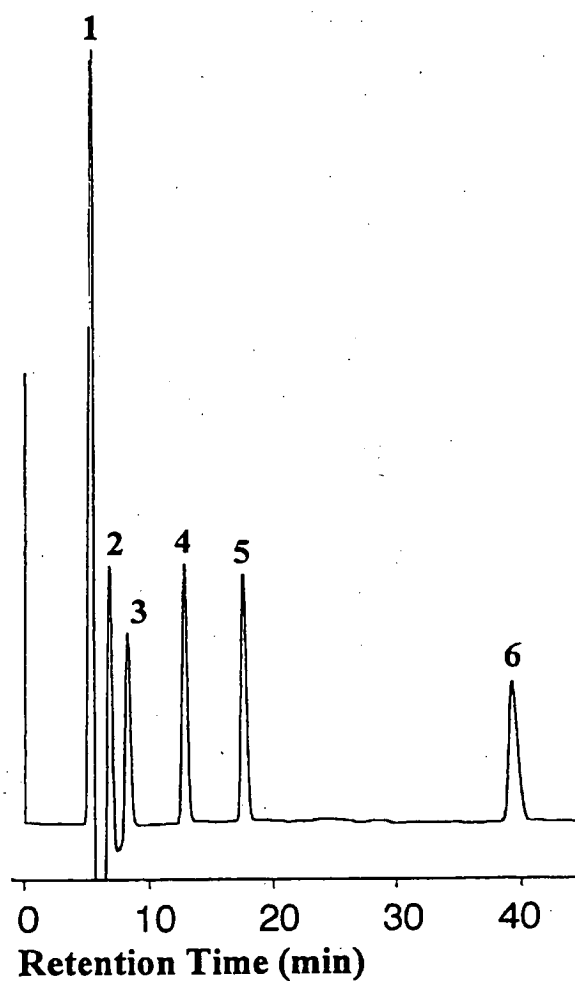
Figure 5.2 Chromatogram of a mixture of F^-, HPO_4^{2-}, Cl^-, SO_4^{2-}, NO_2^-, Br^- and NO_3^- (0.1 mM each, except for HPO_4^{2-} which was present at 0.02 mM) obtained using an ODS column coated with C14SB micelles and 10 mM $NaHCO_3$ as the mobile phase. Other conditions as in Figure 5.1.

Peaks: $1 = F^-$, HPO_4^{2-}, SO_4^{2-}, $2 = Cl^-$, $3 = NO_2^-$, $4 = Br^-$, $5 = NO_3^-$, $6 = I^-$.
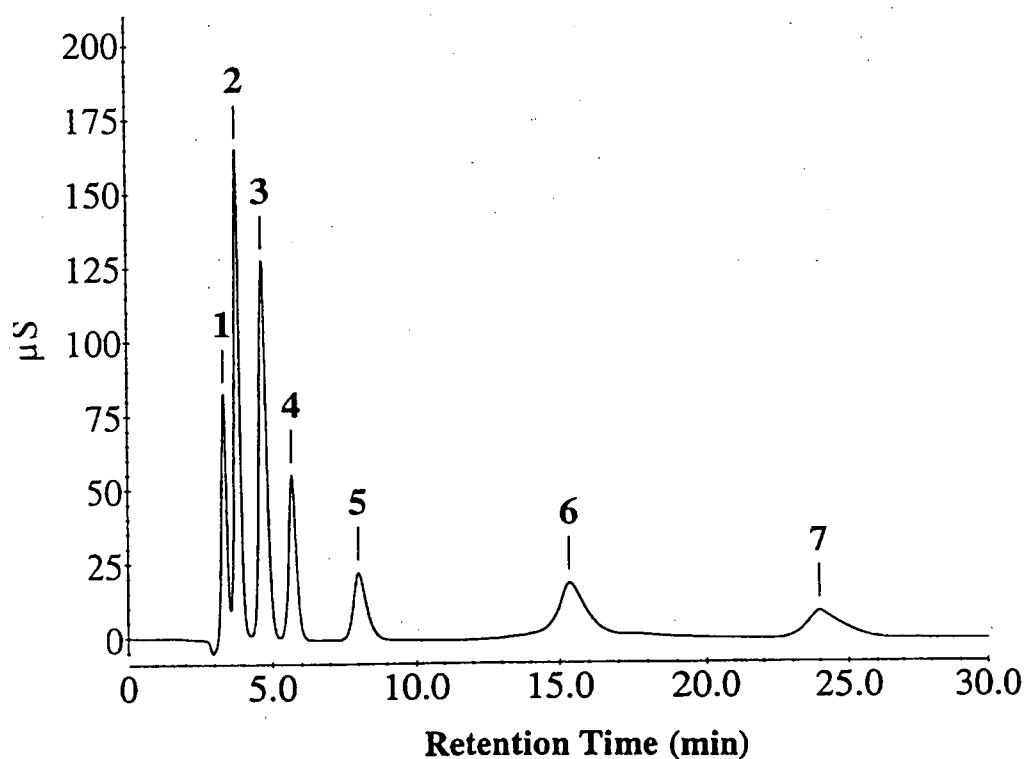
Figure 5.3 Chromatogram of a mixture of F^-, Cl^-, NO_2^-, Br^-, NO_3^-, HPO_4^{2-}, and SO_4^{2-} (1.0 mM of each species) using a mixed zwitterionic/cationic surfactant mixture of C14SB/TTA (20 mM/2 mM); mobile phase: 5 mM sodium tetraborate. Other conditions were as described in Figure 5.1. Peaks: 1 = F^-, 2 = HPO_4^{2-}, 3 =SO_4^{2-}, 4 = Cl^-, 5 = NO_2^-, 6 = Br^-, and 7 = NO_3^-.

Better resolution of the F^-, HPO_4^{2-} and SO_4^{2-} peaks was obtained for the column coated with 10:10 (mM/mM) C14SB/TTA, as shown with a Na_2CO_3 mobile phase in Figure 5.4. The elution order in this case was $F^- < HPO_4^{2-} < Cl^- < SO_4^{2-} < NO_2^- < Br^- < NO_3^-$. The changes in elution order can be attributed to the addition of ion-exchange interactions to the retention mechanism.

5.3.2 Application to the Analysis of Tap Water

The detection limits on the column coated with a 10:10 (mM/mM) C14SB/TTA solution, with a 20.0 mM Na_2CO_3 mobile phase and suppressed conductivity for F^-, HPO_4^{2-}, Cl^-, SO_4^{2-}, NO_2^-, Br^- and NO_3^- (S/N = 3, sample injection volume of 100 μL) were 0.11, 0.12, 0.12, 0.18, 0.49, 0.49, and 0.52 μM, respectively. The linear calibration range ($r^2 > 0.998$) for all of the model analyte ions extended up to at least 8.0 mM. Recoveries of the model analyte anions added to a tap water sample at the 10-50 μM level were >99.2% for all of the analytes. Relative standard deviation (%RSD) of retention time and peak heights and peak areas for the standard sample containing 0.1 mM each of the model analyte ions was also evaluated by analysis of this sample 15 times under the same conditions and %RSD values for all analytes were less than 0.45%. Baseline separation of F^- from the water-dip was facilitated if the coating solution contained >20% (on a molar basis) of the cationic surfactant was employed for detection of the analyte ions. The analytical performance of the 10/1 (mM/mM) C14SB/TTA coating is given in Table 5.1.
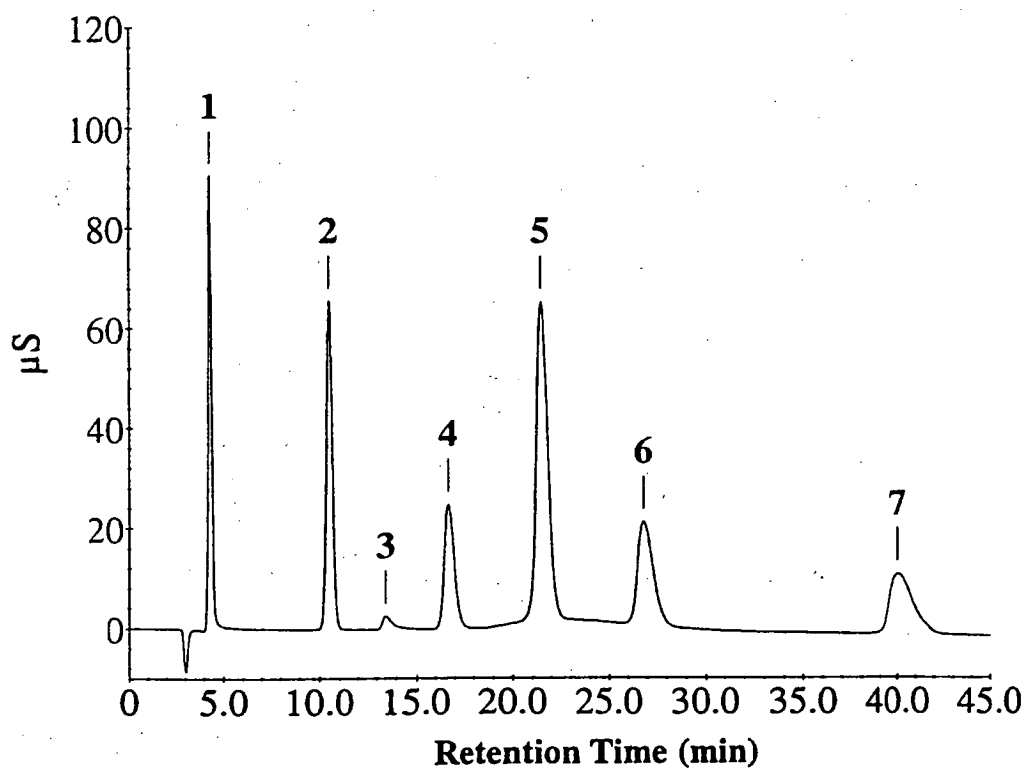
Figure 5.4 Chromatogram of mixture of F^-, HPO_4^{2-}, Cl^-, SO_4^{2-}, NO_2^-, Br^- and NO_3^- (0.1 mM each) obtained using an ODS column coated with C14SB/TTA (10 mM/10 mM) mixed micelles and 20 mM Na_2CO_3 as the mobile phase. Other conditions were as described in Figure 5.1. Peaks: 1 = F^-, 2 = HPO_4^{2-}, 3 = Cl^-, 4 = SO_4^{2-}, 5 = NO_2^-, 6 = Br^- and 7 = NO_3^-.

Table 5.1 Analytical performance data for the separation of common anions on an ODS column coated with mixed 10:1 (mM/mM) C14SB/TTA micelles.

Analyte	Detection Limit (μM)	Detection Limit (ng/L)	Precision (% relative standard deviation, n = 13)		
			Retention time	Peak height	Peak area
F^-	0.08	2	0.6	0.8	1.1
HPO_4^{2-}	0.11	11	0.6	0.8	2.1
SO_4^{2-}	0.09	9	0.7	0.7	1.9
Cl^-	0.007	2	0.7	0.9	2.3
NO_2^-	0.07	3	0.7	0.9	2.5
Br^-	0.07	6	0.8	0.6	1.1
NO_3^-	0.09	6	0.9	1.0	1.7

As a practical application, the 10/10 (mM/mM) C14SB/TTA system was chosen to analyse inorganic anions in tap water in which the levels of F^-, SO_4^{2-}, and Cl^- were found to be 0.09, 0.11, and 0.28 mM, respectively. The same tap water sample was also analysed using a conventional anion-exchange column (IonPac AS14) and the concentrations for F^-, SO_4^{2-}, and Cl^- were found to be 0.09, 0.10, and 0.29 mM, respectively.

5.3.3 Log *k'* *Versus* Log [Mobile Phase] Plots

As mentioned in Chapter 3, an ion-exchange mechanism is characterised by a stoichiometric equilibrium between the solute ion (analyte) and the competing mobile phase ion. The following equation can be derived that relates the retention of an analyte (capacity factor, *k'*) with the concentration of the competing ion (E_M^{y-}), and the relative charges of the analyte (*x*) and competing ion (*y*) [5]:

$$\log k_A^{'} = C_1 - \frac{x}{y}\log[E_M^{y-}] \qquad\qquad (5.1)$$

A plot of log *k'* *versus* log [E_M^{y-}] should give a straight line with a slope of $-x/y$, which means monovalent competing and analyte ions should result in a slope of −1. Deviations from this can be a result of assumptions made in the derivation, in particular that activity effects are negligible, which can be significant especially for multivalent analytes [5]. Deviations may also be attributed to the contribution of a mechanism other than ion-exchange to the retention of analytes, although some differences

between analytes may be due to activity effects (eg. for $Fe(CN)_6^{3-}$ and $Fe(CN)_6^{4-}$, see Section 3.3.3.3).

To evaluate the separation mechanism involved in this system, plots of log k' *versus* log [mobile phase] were constructed and the slopes of the resultant plots are listed in Table 5.2. Only UV-absorbing anions are included, given that a UV detector was used for these plots. Plots for the ZIC system in combination with a Na_2CO_3 or $NaHCO_3$ mobile phase were linear with positive slopes observed for all analytes, indicating that a mechanism other than ion-exchange was operative. When mixed surfactants having a molar ratio of 10:1 of C14SB/TTA were used as the column coating solution, the slopes for F^-, Cl^-, NO_2^-, SO_4^{2-} and HPO_4^{2-} were still positive, indicating that the ZIC mechanism was the chief contributor to the separation of these ions. For the molar ratio of 8:2 (mM/mM) C14SB/TTA the slopes for the monovalent ions were slightly less negative than those observed for the TTA surface, indicating the ZIC mechanism still made a small contribution to the separation. Slopes for the divalent anions were largely negative with values of −1.11 and −1.22 for HPO_4^{2-} and SO_4^{2-}, respectively, which are slightly larger than those observed for the TTA stationary phase, indicating no contribution from the ZIC mechanism in the separation of these ions.

A Na_2CO_3 mobile phase was employed to study the 10:10 (mM/mM) molar ratio-coated stationary phase. With this mobile phase a slope of less than −0.5 and −1 would be expected for monovalent and divalent analytes, respectively, for a hydrophobic exchange site such as that created by semi-permanently-coated TTA. Indeed, the

Table 5.2 Slopes of plots of log k' versus log [mobile phase] for stationary phases coated with different surfactants.

Analyte	TTA	C14SB[b]	C14SB	C14SB/TTA (10 mM/1 mM)	C14SB/TTA (8 mM/2 mM)	C14SB/TTA (10 mM/10 mM)	C14SB	C14PC
	Eluent: NaHCO$_3$ 10-50 mM	Eluent: NaHCO$_3$ 1-20 mM	Eluent: Na$_2$CO$_3$ 1-20 mM	Eluent: NaHCO$_3$ 10-50 mM	Eluent: NaHCO$_3$ 6-23 mM	Eluent: Na$_2$CO$_3$ 20-70 mM	Eluent: CeCl$_3$ 0.5-15 mM	Eluent: NaClO$_4$ 0.5-15 mM
F$^-$	-0.56	-	-	0.11	-0.46	-0.24	-	-
Cl$^-$	-0.60	-	-	0.06	-0.49	-0.16	-	-
NO$_2^-$	-0.61	0.11	0.29	0.03	-0.56	-0.19	-0.07	-
Br$^-$	-0.55	0.20	0.36	-	-0.67	-0.14	-0.07	-0.05 (K$^+$)
NO$_3^-$	-0.61	0.27	0.37	-	-0.56	-0.18	-0.11	-0.18 (NH$_4^+$)
HPO$_4^{2-}$	-0.98	-	-	0.24	-1.11	-0.84	-	-0.15 (Li$^+$)
SO$_4^{2-}$	-1.08	-	-	0.23	-1.22	-0.82	-	-0.15 (Tl$^+$)
I$^-$	-	0.50	0.51	-	-	-	-0.10	-0.13 (Ag$^+$)

slopes for SO_4^{2-} and HPO_4^{2-} with the Na_2CO_3 mobile phase are close to -1 (-0.82 and

-0.84, respectively), and slopes for the monovalent anions ranged between -0.14 and

-0.24.

5.3.4 The Mechanism

The changing slopes of the log k' *versus* log [mobile phase] plots illustrate the effect of

adding a monovalent surfactant to the zwitterionic surfactant in the coating mixture. In

the ZIC system, adding electrolyte to the mobile phase either abruptly increases or

decreases the retention of analytes. This is due to the unfurling of the surface

morphology on the addition of a small amount of salt, allowing ions to interact directly

with the inner charge through short-range, chaotropic interactions. Further increases in

electrolyte concentration have little effect on analyte retention as the mobile phase ions

cannot compete with analyte ions via long-range electrostatic interactions as they do in

ion-exchange. It is only a certain localised concentration of ions that compete with the

analyte ion. Thus, the slopes of log k' *versus* log [mobile phase] for ZIC are close to

zero. The addition of a monovalent surfactant to the stationary phase creates a site for

long-range electrostatic interactions. This type of interaction is much stronger than

short-range chaotropic interactions, as can be seen in the difference in the retention

time for I^- on the zwitterionic ZIC system compared with that on the monovalent

system, with retention times of approximately 40 minutes and over 20 hours

respectively, with a similar mobile phase. Thus, even at low levels of TTA added to

the C14SB coating solution a change in selectivity is observed. In particular, analytes

that are weakly chaotropic, but are highly charged (i.e. HPO_4^{2-} and SO_4^{2-}) are affected greatly by electrostatic effects and therefore experience a significant increase in retention compared with the ZIC system. As well as the change in selectivity, the increasingly negative slopes (of the log k' *versus* log [mobile phase]) with increasing TTA molar ratio correspond to the contribution of an ion-exchange mechanism whereby increasing the concentration of mobile-phase ions allows greater competition with analyte ions, due to long-range electrostatic effects. Thus, it can be concluded that the mechanism dominating retention of an analyte depends on the nature of that analyte. If it is small and highly charged, retention will be governed largely by electrostatic effects, whereas if it has a small charge spread over a large volume retention will be largely dominated by chaotropic effects. Therefore, the more chaotropic an analyte, the less negative its slope and vice versa.

The ability of a mobile-phase cation such as Ce^{3+} to completely mask the outer sulfonate charge on the C14SB zwitterion, or analogously ClO_4^- to mask the outer positive charge on the C14PC zwitterion, was discussed in Section 3.3.2 and further in Section 3.3.3.4. The slopes for these systems are included in Table 5.2. It was concluded in Section 3.3.3.4 that under these extreme conditions, electrostatic effects may play a greater role in retention and results obtained in this chapter give a good indication of the effect on slopes with just a small contribution of ion-exchange to the mechanism. The slopes shown for the Ce^{3+}/C14SB and ClO_4^-/C14PC systems agree with this conclusion. In this case it can be seen not so much as a contribution of an ion-

exchange mechanism but a greater contribution of long-range electrostatic effects to the system.

In Section 3.3.2 it was concluded that no ion-exchange occurs in ZIC as there was no difference observed between $NaClO_4$ and $Ce(ClO_4)_3$ mobile phases with C14SB. However, this may be because ClO_4^- shields the quaternary ammonium group such that retention is very low for all analytes, regardless of the mobile-phase cation, hence the slope is unchanged. However, there is a significant difference between the slopes of NaCl and CeCl$_3$ mobile phases with C14SB (0.09 and -0.11, respectively), as both charges on the zwitterion are shielded to a similar extent with a NaCl mobile phase. On the other hand with CeCl$_3$, the sulfonate charge is shielded to a much greater extent than the quaternary ammonium group. Selectivity changes are in agreement with this theory, as it can be seen that the multivalent ions are increasingly retained compared with monovalent ions, when the mobile-phase cation is changed from Na^+ to Ce^{3+} (see Section 3.3.3.3).

Thus it should be possible to separate Cl^- and F^- with a Ce^{3+} mobile phase in a reasonable run time. Moreover the mixed-surfactant system has the major advantage of being able to be used with a suppressible mobile phase.

5.4 Conclusions

Manipulation of the separation selectivity in ZIC remains its greatest limitation. However, stationary phases formed by semi-permanently coating an ODS column with

a solution of mixed zwitterionic and cationic surfactants provides a means to manipulate the selectivity in ZIC by introducing an ion-exchange component to the mechanism, where the greatest effect is seen with small, highly-charged analytes. Selectivity can be manipulated by varying the ratio of cationic/zwitterionic surfactants in the coating solution, but at higher proportions of the cationic surfactant a mobile phase of greater eluting power is needed, resulting in greater baseline noise and higher detection limits.   Thus, manipulation of the selectivity is at the cost of reduced sensitivity. However, even at low molar ratios of cationic/zwitterionic surfactant ion-exchange effects dominate the separation of divalent anions, due to the greater strength of long-range electrostatic effects compared with short-range chaotropic interactions.

5.5 References

(1)   W. Hu, P.R. Haddad, K. Tanaka, K. Hasebe, Analyst 125 (2000) 241-244.

(2)   W. Hu, K. Hasebe, M.Y. Ding, K. Tanaka, Fresenius' J. Anal. Chem. 371 (2001) 1109-1112.

(3)   W. Hu, K. Hasebe, D.M. Reynolds, H. Haraguchi, J. Liq. Chromatogr. Relat. Technol. 20 (1997) 1221-1232.

(4)   W. Hu, A. Miyazaki, H. Haraguchi, Anal. Sci. 11 (1995) 999-1000.

(5)   P.R. Haddad, P.E. Jackson. *Ion Chromatography: Principals and Applications.*, Elsevier, Amsterdam: 1990.

(6)   J. Weiss. *Ion Chromatography,* 2nd ed.; VCH Verlagsgesellschaft mbH and VCH Publishers , Inc.: Mannheim and New York, 1995.

(7)   D.J. Barkley, T.E. Dahms, K.N. Villencuve, J. Chromatogr. 395 (1987) 631-640.

(8)   F.G.P. Mullins, Analyst 112 (1987) 665-671.

(9)   T. Takeuchi, E.S. Yeung, J. Chromatogr. 370 (1986) 83-92.

(10)   R.M. Cassidy, S. Elchuk, Anal. Chem. 54 (1982) 1558-1563.

(11)   I. Molnar, H. Knauer, D. Wilk, J. Chromatogr. 201 (1980) 225-240.

(12)   R.E. Barron, J.S. Fritz, J. Chromatogr. 316 (1984) 201-210.

(13)   R.E. Barron, J.S. Fritz, J. Chromatogr. 284 (1984) 13-25.

(14)   Dionex Corporation, Dionex Product Selection Guide, 1997/1998, Sunnyvale, USA.

Mathematical Modelling of the Separation

Mechanism

6.1 Introduction

The models described in Chapters 3 and 4 are phenomenological, qualitative descriptions of the separation mechanism that are essential to understanding and further developing ZIC. Translating that information into something useable and effective for solving day to day separation problems requires a fully quantitative mathematical model. This may be in the form of a hard model, based on the theory of the phenomenological model, or a "soft" empirical model such as that provided by an artificial neural network (ANN). The former is useful in that fundamental constants are determined describing various parameters in the system, but to develop such a model, the system must be well understood. However, when relationships between variables are difficult to predict, a soft model may be an effective alternative method to predict selectivity and retention behaviour.

There are two types of hard models for ion-exchange and similar systems, namely stoichiometric and non-stoichiometric [1]. Stoichiometric models are developed by manipulating the equations for a series of chemical equilibria describing variables in the system, to reach the final retention equation. Non-stoichiometric models describe retention without the formation of chemical complexes and are based on the premise

that retention is influenced largely by electrostatic effects. Stahlberg [1] states that a proper model for electrostatic interaction must first be formulated before other interactions can be taken into account, and if retention varies significantly with the ionic strength of the mobile phase, then electrostatic interactions must be considered.

The mathematical model published by Okada and Patil [2] is of the non-stoichiometric type and assumes that there are two ZIC retention mechanisms (namely, ion-pair and partition) based on Poisson-Boltzmann theory. They concluded that in water, small, well-hydrated ions interact with the zwitterionic surface via a partition mechanism and large, poorly hydrated ions interact via an ion-pair mechanism (directly interacting with the charge on the zwitterion opposite to that of the analyte). They also suggested that the retention of the analyte, in this case iodide, was affected by the nature of the mobile-phase anion, but not the mobile-phase cation. However, their study compared only monovalent mobile-phase anions and cations.

An artificial neural network (ANN) is a computer program that simulates the functioning of the brain, in particular the way that it can learn from information and past problems such that it can understand and solve new, unknown problems. There are a variety of different networks that come with an ANN computer package, but the most commonly used is the Multilayer Perceptron network. Each network consists of a number of neurons, or nodes, which are the basic processing units, and are grouped into layers. There may be many nodes in a layer and many layers in a network. All Multilayer Perceptron networks have an input layer, with a node for each input variable

(i.e. concentration, pH, ionic strength, etc) and one output layer, with a node for each output variable (i.e. k' for five different analytes would require five nodes). Between these two layers there must be at least one hidden layer, which uses an algorithm to manipulate the input data to calculate the output data. The number of nodes required in the hidden layer, and the number of hidden layers, is determined by experimentation. A data set is required to "train" the network, such that it has develops mathematical equations that can predict the output data for new input data.

The aim of this chapter was to apply a mathematical hard model to the data of Chapter 3, based on the approach of Okada and Patil [2] but modified to more closely represent the model proposed in Chapter 3. As a second attempt at quantitation of the model, an ANN was applied.

6.2 Experimental

6.2.1 Hard Model

The data employed were those determined in Chapter 3, where the column used had an entire surface area of 790 m^2, and a molecular density of the zwitterionic surfactant on the surface of 1.52 μmol·m^{-2}. Calculations were performed using the mathematical programming package, MathCad Plus Version 6.0 (Cambridge, MA).

6.2.2 Soft Model

The Artificial Neural Network (ANN) program used was Trajan Version 3.0 (Trajan Software Ltd., Durham, U.K). A Pentium II 350 MHz, 64 Mb RAM, 4 Gb HDD computer was used for all computations, which required just minutes to complete.

6.3 Results and Discussion

6.3.1 Hard Model Approach

A schematic of the hard model approach to modelling a system is shown in Figure 6.1. Experimental data are entered into the mathematical model, from which parameters are determined. This leads to a functional equation that can be used for new experimental conditions, from which retention data can be calculated and then cross-checked with the experimental data. If a good agreement is not achieved, then these new experimental results are used to recalculate the parameters until the calculated data are approximately equal to experiment, resulting in a good working model. Typically, linear regression is used to calculate the parameters in a hard model, where regression analysis estimates or predicts one variable from knowledge of its relationship with another variable. If this relationship is unclear linear regression is not applicable, which was the case in this study. Instead, MathCad was used to generate values for the parameters of interest and to explore their relationships.
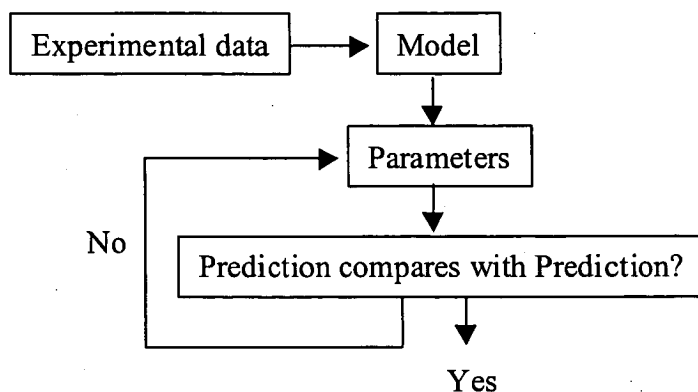
Figure 6.1 Schematic representing the hard modelling process.

6.3.1.1   Derivation of the Model

Figure 6.2 illustrates the electrostatic potential profile as well as the parameters required for the modelling of the C14SB system. The electrostatic potentials ψ_{in} and ψ_{out} (equivalent to the experimental zeta potential, determined via EOF measurements, see Section 3.3.1) are constant under the set conditions, whereas $\psi_{dipolar}$ and $\psi_{outside}$ are distance dependent. The symbols +d and -d refer to the distance from and into the dipole layer, respectively. K_{SC} and K_{NA} are the ion association constants describing the equilibria between the sulfonate group and mobile-phase cation, and between the quaternary ammonium group and the mobile-phase anion, respectively. The derivation of the equations discussed below is based on that by Okada and Patil [2]. However, their model considered only the effect of the mobile-phase anion, so it has been modified to include both anion and cation effects, in order to be consistent with the model proposed in Chapter 3. Mono-, di- and trivalent mobile-phase cations and
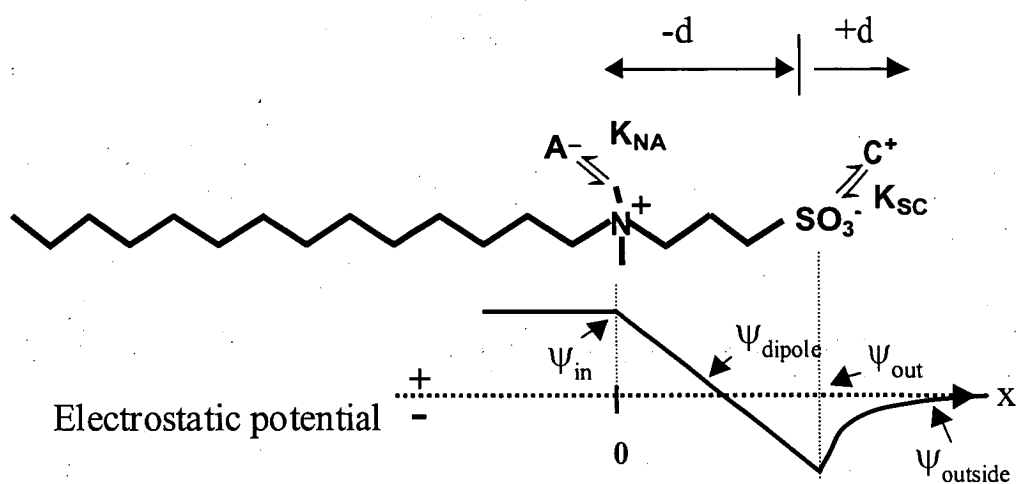
Figure 6.2 Schematic diagram of a DDAPS molecule indicating the parameters required for development of the mathematical model (adapted from [2]).

monovalent mobile-phase anions are considered, with necessary modifications to the Okada and Patil approach being marked with an asterisk.

The equations derived for this model are based on the Poisson-Boltzmann equation (Equation 6.1), which describes the charge of the electrostatic potential, ψ, in space (or distance, x, from the surface) and is a function of the charge density, ρ, in the medium, of permittivity, ε, assumed here as being equal to that of water. No Stern layers were assumed, such that interactions with the charges on the zwitterion occurs at the charged planes.

$$\frac{d^2\psi}{dx^2} = -\frac{\rho}{\varepsilon_o \varepsilon} \tag{6.1}$$

The charge density of the surface is dependent on the charge of the ions (z_i), the bulk concentration of those ions (n_i) and the overall electrostatic potential, ψ, thus equation 6.1 can be rewritten as:

$$\frac{d^2\psi}{dx^2} = -\frac{F}{\varepsilon_o \varepsilon} \Sigma z_i n_i^* \exp\left(-\frac{z_i F\psi}{RT}\right) \tag{6.2}$$

This equation can distinguish between the behaviour of ions of different charge, but cannot distinguish between ions of the same charge that differ in their chemical nature. Standard chemical potential terms, μ^o, which are equal to the Gibbs' free energy of transfer of an ion from aqueous solution to the stationary phase ($\Delta G = zF\psi$, where F is

Faraday's constant), can be included in the equation (see Equation 6.3). Hence, it can

be concluded that selectivity between like-charged analytes is due to differences in

their chemical potential.

$$\frac{d^2\psi}{dx^2} = -\frac{F}{\varepsilon_o\varepsilon}\Sigma z_i n_i^* \exp\left(-\frac{z_i F\psi - \Delta\mu^0}{RT}\right) \tag{6.3}$$

In this case, the stationary phase is assumed to be planar. The Debye-Hückel

approximation [3] can be applied when the strength of the electrostatic interaction

between charged bodies and ions in the system is small compared with the thermal

energy of ions. That is, if $|z_i F\psi| \ll RT$, the exponential term can be expanded

resulting in a linearised, second order Poisson-Boltzmann equation. Some boundary

conditions must be specified in order to apply the approximation. Firstly, at the

surface, the electrostatic potential depends on the surface charge density, σ, and

permittivity of the medium, given by:

$$\frac{d\psi}{dx}\Big|_{x=0} = -\frac{\sigma}{\varepsilon_o\varepsilon} \tag{6.4}$$

where σ is the surface charge density, which is dependent on the amount of

zwitterionic surfactant (e.g. C14SB) adsorbed onto the stationary phase. At distance,

+d (i.e. the distance from the sulfonate group of C14SB), the electrostatic potential, ψ,

depends on the charge, σ_{dip}, at the outer surface, and is determined by the interaction

and shielding of the positive and negative charge on the zwitterion by the mobile-phase anion and cation, respectively. This condition is described in Equation 6.5.

$$\frac{d\psi}{dx}\bigg|_{x=+d} = -\frac{\sigma_{dip}}{\varepsilon_\circ \varepsilon} \tag{6.5}$$

Electroneutrality must be maintained, with the electrostatic potential moving into the stationary phase being equal to that moving out into the bulk solution, i.e.:

$$\psi\big|_{x=+d} = \psi\big|_{x=-d} \tag{6.6}$$

That is,

$$\int_0^d \sum z_i n_i^0 \exp\!\left(\frac{-z_i F \psi_{(x)}^{dipolar} - \Delta\mu_i^0}{RT}\right) dx = -\int_d^\infty \sum z_i n_i^0 \exp\!\left(\frac{-z_i F \psi_{(x)}^{outside}}{RT}\right) dx \tag{6.7}$$

where, according to the Gouy-Chapman model, the right hand side of Equation 6.7 is equal to:

$$-\int_d^\infty \sum z_i n_i^0 \exp\!\left(\frac{-z_i F \psi_{(x)}^{outside}}{RT}\right) dx = \frac{\sinh\!\left(\dfrac{F\psi_{out}}{2RT}\right)\sqrt{8RT\varepsilon_0 \varepsilon n^0}}{F} \tag{6.8}$$

Equation 6.7 must be modified to take into account the reduction of the effective charges on the zwitterion due to shielding by the mobile-phase anion and cation:

$$\int_0^d \sum z_i n_i^0 \exp\left(\frac{-z_i F \psi_{(x)}^{dipolar} - \Delta\mu_i^0}{RT}\right) dx - \frac{\sigma K_{NA} n^0 \exp\left(\frac{F\psi_{in}}{RT}\right)}{1 + K_{NA} n^0 \exp\left(\frac{F\psi_{in}}{RT}\right)} =$$

$$-F \int_d^\infty \sum z_i n_i^0 \exp\left(\frac{-z_i F \psi_{outside}}{RT}\right) dx - \frac{\sigma K_{SC} n^0 \exp\left(\frac{F\psi_{out}}{RT}\right)}{1 + K_{SC} n^0 \exp\left(\frac{F\psi_{out}}{RT}\right)}$$

(6.9)

Finally, the electrostatic potential must approach zero with increasing distance from the surface:

$$\frac{d\psi}{dx}\bigg|_{x=\infty} = 0$$

(6.10)

According to these boundary conditions, and applying the Debye-Hückel approximation, Equation 6.3 can be simplified to:

$$\frac{d^2\psi}{dx^2} = \frac{\kappa^2}{z_a^2 z_c + z_c^2 |z_a|} \left\{ (M_a - M_c)\frac{RT}{F} + \left(|z_a| M_a + z_c M_c\right)\psi \right\}$$

(6.11)*

where,

$$M_a = \exp\left(\frac{\Delta\mu_a^\circ}{RT}\right)$$

(6.11a)

$$M_c = \exp\left(\frac{\Delta\mu_c^\circ}{RT}\right);$$

(6.11b)

$$\kappa = \left(\frac{F^2 \sum_i z_i^2 n_i^\circ}{\varepsilon_0 \varepsilon R T} \right)^{0.5}$$

(6.11c)*

This equation can be integrated to obtain,

$$\frac{d\psi}{dx} = -\left(\alpha \psi^2 + \beta \psi + C \right)^{0.5}$$

(6.12)

where

$$\alpha = \frac{\kappa^2}{z_a^2 z_c + z_c^2 |z_a|} \left(|z_a| M_a + z_c M_c \right)$$

(6.12a)*

$$\beta = \frac{2 F n^\circ}{\varepsilon_0 \varepsilon} \left(M_a - M_c \right)$$

(6.12b)

and C is the integral constant, which can be calculated from the boundary condition at the inner surface described in Equation 6.4:

$$C = \left(\frac{\sigma}{\varepsilon_0 \varepsilon} \right)^2 - \alpha \psi_{in}^2 - \beta \psi_{in}$$

(6.13)

6.3.1.2   Modelling Trends of the Zeta Potential

The zeta potential can be calculated by solving Equation 6.9 to obtain $\psi_{dipolar}$ as a function of x:

$$\frac{1}{\sqrt{\alpha}}\left(\sinh^{-1}\frac{\psi_{dipolar}+\dfrac{\beta}{2\alpha}}{\sqrt{\dfrac{C}{\alpha}-\dfrac{\beta^2}{4\alpha^2}}}-\sinh^{-1}\frac{\psi_{in}+\dfrac{\beta}{2\alpha}}{\sqrt{\dfrac{C}{\alpha}-\dfrac{\beta^2}{4\alpha^2}}}\right)=x \qquad (6.14)$$

where C is calculated using equation 6.13.

No solvation changes were considered, in other words, the analytes were assumed to interact directly with the zwitterionic charges and form ion associates. The electrolyte concentration was set to be 25 mM, with surfactant molecules assumed to be fully extended and the distance between the positive and negative charge on the zwitterion calculated to be 0.4 nm. Calculations of the inner and outer zeta potential (ψ_{in} and ψ_{out}, respectively), with an assumed surfactant molecular density of 1.2 μmol m^{-2}, are given in Table 6.1, for 1:1, 2:1 and 3:1 cation:anion charged electrolytes (see Table 6.1 (a), (b) and (c), respectively), and show the effect on the zeta potential with varying K_{SC} and K_{NA} values. From left to right across the table, increasing K_{SC} values resulted in an increasingly more positive inner potential, ψ_{in}, as the mobile-phase cation increasingly shields the outer sulfonate group (i.e. changing from a Na$^+$ to Ce^{3+} mobile phase). This resulted in an increasingly more positive outer potential (the measured zeta, or electrostatic, potential, ψ_{out}), which follows experimental observations. It can be seen that the zeta potential may be positive when K_{SC} is large enough, which also supports the experimental results (i.e. ζ (CeCl$_3$) = + 40.2 mV). Reading down the column,

Table 6.1 (a) Data generated for calculations of the inner and outer electrostatic potential for different values of K, for a 1:1 monovalent electrolyte mobile phase, with a surface molecular density of 1.2 μmol m^{-2}.

	$K_{SC} = 10^{-5}$		$K_{SC} = 10^{-4}$		$K_{SC} = 10^{-3}$		$K_{SC} = 10^{-2}$		$K_{SC} = 10^{-1}$	
K_{NA}	ψ_{in}	ψ_{out}	ψ_{in}	ψ_{out}	ψ_{in}	ψ_{out}	ψ_{in}	ψ_{out}	ψ_{in}	ψ_{out}
$(\times 10^{-6})$	$(\times 10^{-3})$	$(\times 10^{-3})$	$(\times 10^{-3})$	$(\times 10^{-3})$	$(\times 10^{-3})$	$(\times 10^{-3})$	$(\times 10^{-3})$	$(\times 10^{-3})$	$(\times 10^{-3})$	$(\times 10^{-3})$
0.10	58.04	-7.725	58.69	-7.057	63.69	-1.948	107	42.33	127.2	62.95
0.40	58.02	-7.741	58.67	-7.072	63.67	-1.963	106.9	42.27	127.1	62.94
1.60	57.94	-7.802	58.59	-7.133	63.59	-2.023	106.6	42.01	126.8	62.87
6.40	57.63	-8.045	58.28	-7.375	63.27	-2.257	105.1	41.01	125.5	62.6
25.6	56.45	-8.961	57.11	-8.285	62.06	-3.14	100.2	37.43	121.4	61.54
102.4	52.59	-11.99	53.24	-11.29	58.14	-6.01	87.85	27.61	111.5	57.89
409.6	43.2	-19.38	43.88	-18.6	48.82	-12.84	68.43	11.49	94.82	49.41
1638	27.61	-31.63	28.39	-30.63	33.68	-23.76	48.4	-3.328	73.91	36.77
6554	8.051	-46.52	9.004	-45.16	14.91	-36.61	29.48	-14.07	51.45	22.32
26210	-13.14	-61.54	-11.96	-59.7	-5.373	-49.24	9.302	-25.01	28.55	6.784
104900	-34.48	-75.02	-33.04	-72.63	-25.77	-60.5	-10.61	-35.35	8.033	-6.409

Table 6.1 (b) Data generated for calculations of the inner and outer electrostatic potential for different values of K, for a 2:1 (C:A) electrolyte mobile phase, and a surface molecular density of 1.2 μmol m^{-2}.

	1.2 μmol m^{-2}							
	$K_{SC} = 10^{-4}$		$K_{SC} = 10^{-3}$		$K_{SC} = 10^{-2}$		$K_{SC} = 10^{-1}$	
K_{NA}	ψ_{in}	ψ_{out}	ψ_{in}	ψ_{out}	ψ_{in}	ψ_{out}	ψ_{in}	ψ_{out}
$(\times 10^{-6})$	$(\times 10^{-3})$	$(\times 10^{-3})$	$(\times 10^{-3})$	$(\times 10^{-3})$	$(\times 10^{-3})$	$(\times 10^{-3})$	$(\times 10^{-3})$	$(\times 10^{-3})$
0.10	56.78	-8.16	60.17	-4.587	82.34	18.79	100.7	38.17
0.40	56.75	-8.174	60.14	-4.6	82.26	18.73	100.6	38.15
1.60	56.67	-8.23	60.06	-4.651	81.95	18.51	100.4	38.04
6.40	56.32	-8.449	59.71	-4.85	80.78	17.64	99.26	37.64
25.6	55.04	-9.264	58.43	-5.587	76.99	14.85	95.64	36.22
102.4	50.99	-11.82	54.42	-7.874	68.25	8.544	86.82	32.39
409.6	41.83	-17.51	45.44	-12.83	54.85	-0.18	72.38	25.61
1638	27.64	-25.74	31.61	-19.84	40.57	-5.958	54.7	17.32
6554	10.68	-34.26	15.04	-27.06	23.77	-12.29	35.84	8.368
26210	-0.006865	-0.04133	-2.16	-33.27	6.662	-18.35	17.23	-1.117
104900	-0.02306	-0.04619	-0.0179	-37.91	-0.008509	-23.47	2.679	-7.385

Table 6.1 (c) Data generated for calculations of the inner and outer electrostatic potential for different values of K, for a 3:1 (C:A) electrolyte mobile phase, and a surface molecular density of 1.2 μmol m^{-2}.

	1.2 μmol m^{-2}							
	$K_{SC} = 10^{-2}$		$K_{SC} = 10^{-1}$		$K_{SC} = 5 \times 10^{-1}$		$K_{SC} = 1$	
K_{NA}	ψ_{in}	ψ_{out}	ψ_{in}	ψ_{out}	ψ_{in}	ψ_{out}	ψ_{in}	ψ_{out}
$(\times 10^{-6})$	$(\times 10^{-3})$	$(\times 10^{-3})$	$(\times 10^{-3})$	$(\times 10^{-3})$	$(\times 10^{-3})$	$(\times 10^{-3})$	$(\times 10^{-3})$	$(\times 10^{-3})$
0.10	70.59	8.8	86.55	26.51	95.35	36.27	98.94	40.26
0.40	70.54	8.765	86.48	26.48	95.28	36.26	98.86	40.25
1.60	70.32	8.625	86.23	26.38	95	36.19	98.57	40.2
6.40	69.52	8.101	85.28	25.99	93.94	35.95	97.45	40.02
25.6	66.87	6.413	82.12	24.69	90.5	35.1	93.85	39.36
102.4	60.33	2.557	74.4	21.45	82.29	32.75	85.42	37.41
409.6	50.02	-1.79	61.62	16.3	69.01	28.51	72.01	33.6
1638	36.39	-5.94	45.71	10.27	52.94	23.11	55.98	28.51
6554	20.73	-10.35	28.65	3.658	36.43	17.11	39.78	22.77
26210	5.575	-14.4	12.87	-2.515	21.07	10.2	25.21	16.37
104900	-6.491	-17.46	11.74	-6.724	5.952	-0.273	12.52	8.335

increasing K_{NA} values (i.e. changing from a Cl$^-$ to ClO$_4^-$ mobile phase) resulted in decreased inner potentials, as well as having a large effect on the outer potential (decreasing, eventually becoming negative), again supporting the model.

Comparing the results for 1:1, 2:1 and 3:1 cation:anion mobile phases, larger variations in the zeta potential are calculated for monovalent mobile-phase cations with varying K_{NA} values. This does not support the experimental data (see Table 6.2), which show an increasing difference in zeta potential between mobile-phase anions Cl$^-$ and ClO$_4^-$ as the mobile-phase cation is changed from Na$^+$ to Mg^{2+} to Ce^{3+}.

Table 6.2 Effect of the mobile-phase cation and anion on the zeta potential (ζ).

| | ζ (mV)* | | |
| | Mobile-Phase Cation | | |
Mobile-Phase Anion	Na$^+$	Mg^{2+}	Ce^{3+}
Cl$^-$	-30.6	-13.3	40.2
ClO$_4^-$	-53.4	-30.6	11.7
Increase Factor	1.7	2.3	3.4

*Values from Table 3.1

However, this may be explained by changes in the surfactant molecular density on the column (possible through desorption, or increased adsorption of surfactant molecules present at a low concentration in the mobile phase). The effect on the calculations of increasing the molecular density of the zwitterion molecules on the surface is shown in

Table 6.3 Data generated for calculations of the inner and outer electrostatic potential for different values of K, for a 1:1 (C:A) electrolyte mobile phase, and a surface molecular density of 2.4 μmol m^{-2}.

	$2.4\ \mu mol\ m^{-2}$											
	$K_{SC} = 0$		$K_{SC} = 10^{-5}$		$K_{SC} = 10^{-4}$		$K_{SC} = 10^{-3}$		$K_{SC} = 10^{-1}$		$K_{SC} = 10^{-1}$	
K_{NA}	ψ_{in}	ψ_{out}	ψ_{in}	ψ_{out}	ψ_{in}	ψ_{out}	ψ_{in}	ψ_{out}	ψ_{in}	ψ_{out}	ψ_{in}	ψ_{out}
$(\times10^{-6})$	$(\times10^{-3})$	$(\times10^{-3})$	$(\times10^{-3})$	$(\times10^{-3})$	$(\times10^{-3})$	$(\times10^{-3})$	$(\times10^{-3})$	$(\times10^{-3})$	$(\times10^{-3})$	$(\times10^{-3})$	$(\times10^{-3})$	$(\times10^{-3})$
0.10	104.5	-27.29	104.5	-27.29	106.2	-25.48	115.4	-16.11	137.8	6.821	163.2	32.91
0.40	104.3	-27.39	104.3	-27.39	106.1	-25.58	115.2	-16.19	137.6	6.776	162.8	33.06
1.60	103.7	-27.77	103.7	-27.77	105.5	-25.94	114.6	-16.49	136.6	6.593	161.3	33.59
6.40	101.6	-29.15	101.6	-29.15	103.3	-27.26	112.3	-17.59	133.3	5.869	156.6	34.94
25.6	95.17	-33.4	95.17	-33.4	96.96	-31.33	105.7	-20.93	124.5	3.329	146	36.44
102.4	81.78	-42.67	81.78	-42.67	83.72	-40.1	92.47	-28.04	109.1	-2.143	129	35.31
409.6	62.37	-56.34	62.37	-56.34	64.64	-52.88	73.65	-38.29	89.21	-9.548	107.5	29.84
1638	39.84	-71.61	39.84	-71.61	42.52	-66.89	51.81	-49.51	66.63	-18.43	83.85	21.06
6554	16.02	-86.26	16.02	-86.26	19.13	-80.08	28.56	-60.25	42.92	-27.72	59.45	10.36
26210	-8.192	-99.16	-8.192	-99.16	-4.717	-91.55	4.79	-69.99	19.05	-36.93	35.22	-1.398
104900	-32.28	-109.8	-0.03228	-109.8	-28.5	-101	-18.83	-78.57	-4.191	-45.82	13.16	-11.49

Table 6.3, for a 2.4 μmol m^{-2} density and a 1:1 (valency) cation:anion electrolyte in the mobile phase. As expected, greater zeta potentials are observed, but the general trends remain the same. The effect of the surfactant molecular density with different mobile phases is discussed further in Section 6.3.1.3.

6.3.1.3   Calculation of k' and the Zeta Potential

According to the following derivation, retention due to ψ_{out}, is ignored, with k' assumed to be dominated by ψ_{in}. However, in the previous section it was shown that ψ_{in} and ψ_{out} affect each other, and this dependency is noted in Figure 6.3, hence ψ_{out} indirectly affects k'. This was deemed to be a good first approximation to the current model.

The chromatographic retention factor of an analyte (k') is defined as:

$$k' = \frac{A}{V_0} \cdot K \tag{6.15}$$

where A and V_0 are the total surface area and void volume of the column.
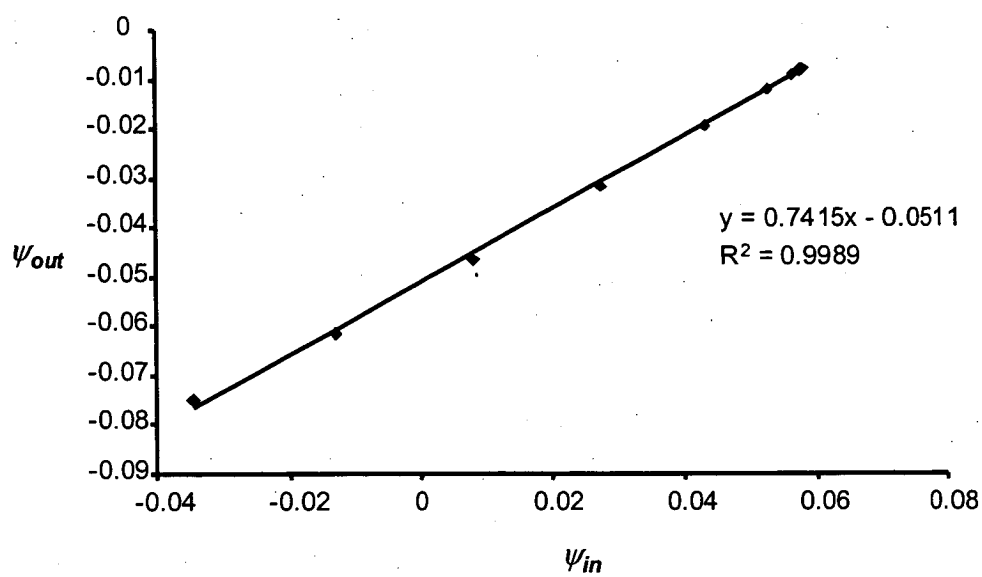
Figure 6.3 Dependence of the outer potential, Ψ_{out}, on the inner potential, Ψ_{in}, shown here for a 1:1 electrolyte mobile phase, where, $K_{SC} = 10^{-5}$.

The association constant for the interaction of an analyte anion with the inner quaternary ammonium group, K_{NA}, is defined by:

$$K_{NA} = \frac{\Gamma_{N-analyte}}{\partial n^0_{analyte}}$$

(6.16)

Where $\Gamma_{N-analyte}$ is the surface concentration of the quaternary ammonium group forming ion pairs with the analyte, and $\Gamma_{N-analyte}/\partial n^0_{analyte}$ is the limiting slope of the adsorption isotherm of the analyte.

Therefore retention due to this phenomenon is equal to:

$$k'_{N-analyte} = \frac{A}{V_0} \cdot \left(\frac{\Gamma_{N-analyte}}{\partial n^0_{analyte}} \right)$$

(6.17)

Similarly, retention due to the repulsion/attraction of the zeta potential, is given by:

$$k'_{\psi_{out}} = \frac{A}{V_0} \int_0^d \left(\exp\left(-\frac{z_A F \psi_{dipole}}{RT} \right) - 1 \right) dx$$

(6.18)

Combining the two contributions to the retention (combining Equations 6.17 and 6.18), gives:

$$k' = \frac{A}{V_0} \left\{ \int_0^d \exp\left(\frac{F \psi_{dipolar}}{RT} \right) dx + \left(\frac{\partial \Gamma_{N-analyte}}{\partial n^0_{analyte}} \right) \right\}$$

(6.19)

Table 6.4 details the calculated k' values of I^- (with assumed $K_{N\text{-}analyte}$ = 1.8 M^{-1}), where

K_{SC} and K_{NA} were varied until the calculated k' approached the experimental k', shown

in Table 6.3. The aim of this was to determine reasonable K_{SC} and K_{NA} values for Na$^+$,

Mg^{2+}, Ce^{3+}, Cl$^-$ and ClO$_4^-$ mobile-phase ions, which are shown in the second and third

columns. It can be seen that a good correlation was achieved, producing theoretically

acceptable K_{SC} and K_{NA} values. It was found that K_{SC} had little effect on retention

where the mobile-phase cation was Na$^+$, over the concentration range of 0 - 0.1 M^{-1} .

This agrees with experiment and the proposed model, since Na$^+$ exhibits very little

shielding of the outer sulfonate group. For the mobile-phase anion, Cl$^-$, both K_{NA} and

ΔG are important, indicating that Cl$^-$ only just overcomes the repulsion of the Donnan

membrane in order to interact with the inner charge, while ClO$_4^-$, Mg^{2+} and Ce^{3+}

interact with the charges on the zwitterion strongly enough that their interaction

overcomes repulsion, hence K_{NA} (or K_{SC}) dominates, for these ions. Despite this good

correlation, obtaining appropriate values that explain all the data proved difficult. For

example, the same parameters cannot explain the large increase in retention for I^-, from

a k' of 5.59 to 35.29 when the concentration of NaCl is changed from 1 to 15 mM,

respectively, when other anions show a much smaller increase. Also, application of

these K values to the calculation of the zeta potential, or ψ_{out}, resulted in a poor

correlation between experimental and calculated zeta potentials (see Table 6.5).

Table 6.4 Retention factors for I⁻ calculated assuming a molecular density of 1.52 μmol m⁻². $K_{N-analyte}$ is assumed to be 1.8 M⁻¹ for I⁻.

Mobile Phase (25mM)	Experimental k'^*	K_{SC} (M⁻¹)	K_{NA} (M⁻¹)	Calculated k'
NaCl	33.7	0-0.1	0.01	29.4
			ΔG=1.5kJmol⁻¹	
NaClO₄	1.26		5	2.52
MgCl₂	46.72	1.5		46.4
CeCl₃	51.08	3		53.1
Ce(ClO₄)₃	2.24			3.23

*Data from Section 3.3.3

Table 6.5 Calculation of the zeta potential for various mobile phases, using K_{NA} and K_{SC} values determined in Table 6.4.

	Experimental ζ / mV*	Calculated ζ / mV
NaCl	-30.6	-8.1
NaClO₄	-53.4	-55.7
MgCl₂	-13.3	+3.4
CeCl₃	+40.2	+10.1
Ce(ClO₄)₃	+11.7	-8.6

*Data from Table 3.1

A change in the surface density of surfactant molecules with different mobile phases was explored as a possible explanation for this discrepancy, with results being shown in Table 6.6. It can be seen that the surface molecular density can be altered to obtain a calculated zeta potential that correlates well with the experimental zeta potential, for all mobile phases (except $Ce(ClO_4)_3$). This suggests that the nature of the mobile phase may affect the zwitterionic coating.

The addition of electrolyte to the system may cause a change in the amount of surfactant adsorbed on the stationary phase, either by salting-out and increasing the amount, or electrostatic repulsion between surfactant molecules resulting in a decreased adsorbed amount.

Table 6.6 Calculation of the zeta potential for various mobile phases, using K_{NA} and K_{SC} values determined in Table 6.4, with varying surfactant molecular densities.

Mobile Phase	Experimental ζ / mV*	Calculated ζ / mV With varying surfactant molecular densities (μmol m^{-2})				
		1.2	1.5	2.6	3.0	3.4
NaCl	-30.6		-8.1	-25.4	-34.6	
NaClO$_4$	-53.4		-55.7			
MgCl$_2$	-13.3		+3.4	-7.1	-10.6	-13.9
MgClO$_4$	-30.6			-26.4	-27.8	
CeCl$_3$	40.2	+42.9	+10.1			
Ce(ClO$_4$)$_3$	11.7	-7.5	-8.6	-10.5		

*Data from Table 3.1

The latter case may become significant with a $NaClO_4$ mobile phase (due to the resultant high zeta potential), while a $MgCl_2$ mobile phase would have a combined effect where decreased adsorption would occur due to a relatively high zeta potential, as well as increased adsorption due to the multivalent ion causing greater salting out than a monovalent ion [4]. Hence for $NaClO_4$ and $CeCl_3$, the assumption of low densities gives calculated zeta potentials close to that seen in experiment, while higher assumed densities are suitable for a NaCl mobile phase. The high density indicated for the $MgCl_2$ mobile phase indicates that the salting-out effect dominates any repulsion effect, similar to $Mg(ClO_4)_2$, which is observed to have a relatively low overall zeta potential. Hu [5] stated that coating the column with a coating solution containing the zwitterion and $NaHCO_3$ results in a more efficient coating than if the coating solution contained Na_2CO_3. It was considered that a study on the effect of the mobile phase on the surfactant molecular density on the column may be a worthwhile study, but this was not undertaken due to the lack of a clear relationship between the zeta potential and molecular surface density (due to the two opposing phenomena). Even if it were relatively straightforward, this effect could prohibitively increase the complexity of the calculations.

It was at this point that the hard model approach was abandoned, and the usefulness of a soft model was investigated.

6.3.2 Soft Model Approach – Artificial Neural Network

As shown in Section 6.3.1, the development and modelling of mechanisms such as that in ZIC can be complex, and indeed it is usually not possible to explain all experimental data with chromatographic data alone (hence the investigation into the surface potential in Chapter 3). The hard model approach described above was largely hindered by a lack of accurate equilibrium values, the complexity inherent in both the mobile-phase anion and cation effects on retention of anionic analytes, and also due to the possibility of a change in the surface adsorption.

Thus, Artificial Neural Networks (ANN's) were investigated for their applicability in predicting the retention behaviour of analytes in ZIC. As soft models are empirical, they produce no useful insight into the theoretical mechanism of separation nor useful parameters, such as equilibrium constants, nevertheless, they may still be a valid tool for the prediction of retention and selectivity.

6.3.2.1   Modelling

ANN's require a training data set and a test data set, where data may be numeric or non-numeric. Non-numeric data can be difficult to model, thus it is desirable to convert nominal-valued variables to numeric ones. The variables under study in this case are the mobile phase concentration, and the nature of the mobile-phase cation and anion. The former consists of numeric data, i.e. 0.5-15 mM; the nature of the cation

can be described in terms of cation charge, such as 1, 2 and 3 for Na^+, Mg^{2+} and Ce^{3+}, respectively. The nature of the anion creates a challenge as they are all monovalent anions, and must be described according to some numeric system. The most credible approach is to assign a rating to each based on expert knowledge, for example, each anion could be represented by its ΔG value, or association constant (K_{ass}). However, it is recommended to keep the ANN as simple as possible, and only increase the complexity if required, so as a first approximation, the mobile-phase anions were assigned the values 0, 1, 2, 3 and 4 for SO_4^{2-}, Cl^-, CNO^-, ClO_3^- and ClO_4^-, respectively. Implicit in this assignment is that CNO^- is midway between SO_4^{2-} and ClO_4^-, and in terms of polarisability, this is a satisfactory approximation.

The most common type of network architecture (Multilayer Perceptrons) and algorithm (back propagation) were used. Conversion, scaling and normalisation of the data were performed automatically. The automatic network designer was used as a starting point, with the number of nodes in the hidden layer being varied until the best network was achieved (shown in Figure 6.4, with 15 nodes in the hidden layer). Only five analytes were included (IO_3^-, NO_2^-, Br^-, NO_3^-, I^-) since a training data set should discard as many outliers and missing data points as possible. The water mobile phase data were also omitted, since their inclusion resulted in poor correlation ($r^2 < 0.7$). Other parameters included a learning rate of 0.6 and a momentum of 0.3. The training was continued for 5000 epochs (calculations and comparisons between calculated and

experimental data), until the verification error just started increasing to avoid

overtraining. The training and test data sets are given in Tables 6.7 and 6.8.
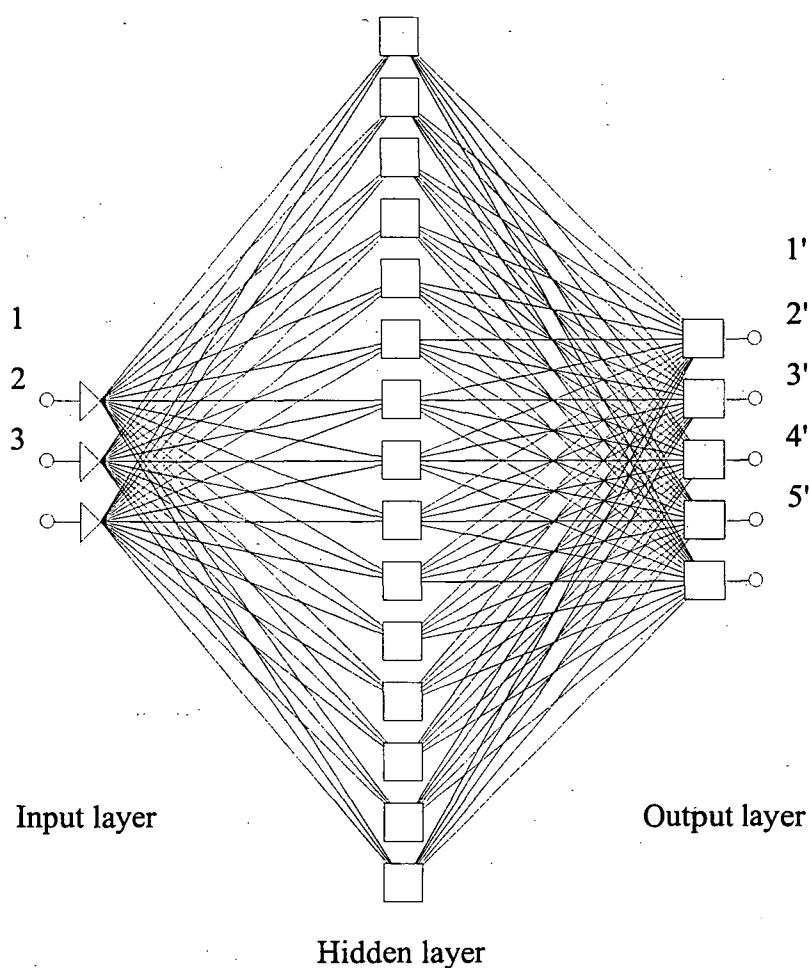

Figure 6.4 Schematic of the three-layer ANN network used in this study, containing 3
input nodes, 15 hidden layer nodes and 5 output nodes.
Input layer: 1 = mobile phase concentration; 2 = cation charge; 3 = anion species.
Output layer: retention factors of 1' = IO_3^-; 2' = NO_2^-; 3'= Br^-; 4'=NO_3^- and 5'=I^-.

Table 6.7 Data set used to train the Artificial Neural Network.

Input Variables			Output Variables				
Concentration	Cation	Anion	iodate	nitrite	bromide	nitrate	iodide
0.5	1	0	0.53	1.35	2.74	4.7	30
0.5	3	0	0.61	2.23	5.2	8.7	71.2
0.5	1	1	0.4	1.16	1.85	2.87	30
0.5	2	1	0.54	1.7	3.4	6.14	49.4
0.5	3	1	0.59	2.19	4.59	8.42	71
0.5	1	2	0.4	0.977	1.72	2.42	16
0.5	1	3	0.27	0.73	1.35	1.54	7.2
0.5	3	3	0.53	1.15	3.1	4.99	38.2
0.5	1	4	0.19	0.35	0.46	0.63	2.92
0.5	2	4	0.26	0.48	0.72	1.03	6.15
0.5	3	4	0.63	0.86	1.14	1.68	9
1	1	0	0.53	1.79	3.682	6.3	33
1	3	0	0.59	2.3	5.21	8.7	77.4
1	1	1	0.48	1.27	2.49	4.23	28
1	2	1	0.51	1.66	3.46	6.14	49.9
1	3	1	0.58	2.14	4.72	8.21	67.9
1	1	2	0.32	0.88	1.63	2.24	15
1	1	3	0.28	0.76	1.35	1.93	12.3
1	3	3	0.56	1.11	2.83	4.47	35.2
1	1	4	0.18	0.33	0.39	0.54	2.42
1	2	4	0.27	0.44	0.62	0.86	4.93
1	3	4	0.73	0.82	1	1.43	7
10	1	0	0.5	1.97	4.229	7.03	56.5
10	3	0	0.58	2.53	5.38	8.88	78
10	1	1	0.39	1.28	2.68	4.44	33.7
10	2	1	0.5	1.6	3.47	5.67	46.7
10	3	1	0.69	1.77	3.78	6.04	51.08
10	1	2	0.34	0.913	1.8	2.83	21.8
10	1	3	0.25	0.56	0.88	1.29	8.06
10	3	3	0.7	1.14	1.66	2.62	16.7
10	1	4	0.2	0.26	0.28	0.34	1.26
10	2	4	0.4	0.4	0.47	0.54	1.79
10	3	4	0.83	0.73	0.69	0.95	2.24
15	1	0	0.49	1.95	4.22	6.97	56.7
15	3	0	0.57	2.5	5.31	8.78	77.1
15	1	1	0.41	1.31	2.67	4.23	32.6
15	2	1	0.5	1.58	3.32	5.4	44.2
15	3	1	0.76	1.77	3.77	6	50.8
15	1	2	0.34	0.87	1.74	2.791	21.6
15	1	3	0.26	0.52	0.82	1.22	7.6
15	3	3	0.72	1.08	1.52		13.58
15	1	4	0.22	0.27	0.28	0.34	1.12
15	2	4	0.41	0.41	0.48	0.53	1.47

Table 6.8 Data set used to test the Artificial Neural Network.

Input Variables			Output Variables				
Concentration	Cation	Anion	iodate	nitrite	bromide	nitrate	iodide
5	1	0	0.49	1.93	4.13	6.91	53.9
5	3	0	0.54	2.48	5.38	8.98	77.8
5	1	1	0.38	1.24	2.6	4.29	34.8
5	2	1	0.5	1.65	3.67	6.05	49.8
5	3	1	0.66	1.98	4.38	7.08	59.02
5	1	2	0.32	0.9	1.65	2.7	20.9
5	1	3	0.24	0.59	0.98	1.44	9.2
5	3	3	0.66	1.24	2.02	3.02	22.8
5	1	4	0.18	0.25	0.29	0.37	1.52
5	2	4	0.41	0.41	0.49	0.6	2.53
5	1	0	0.589	1.192	1.726	2.199	5.589

6.3.2.2   Accuracy of the Model

Figure 6.5 details a plot of calculated *k'* *versus* experimental *k'* for the best obtained

network (described above), with a line of best fit of, $y = 0.9895x - 0.0168$ and $r^2 =$

0.9976. The equation determined for the test set was $y = 0.96x + 0.5$ with an $r^2 = 0.98$.

The slope (0.96 ± 0.02) was not statistically equal to 1, as expected for an accurate

model, and the error in the intercept was large. Again, the high retention of I^- with

increasing Na_2SO_4 and NaCl mobile-phase concentration was underestimated by this

model, reflecting the difficulty in modelling this two-part mechanism (see Section

3.3.4). This error obtained may also be largely due to the difficulty in translating the

mobile-phase anion variable into a numeric form. ΔG values, (-8.16, 2.74, 2.49, 2.2

and 2.04) $\times 10^{-9}$, for SO_4^{2-}, Cl^-, CNO^-, ClO_3^- (approximated) and ClO_4^-, respectively,

calculated from ionic radii [6], were substituted, along with K_{ass} [7] values for both the

mobile-phase anion and cation (some data estimated), with all cases resulting in a

poorer correlation ($r^2 < 0.8$). An attempt to include 8 analytes in the training data set

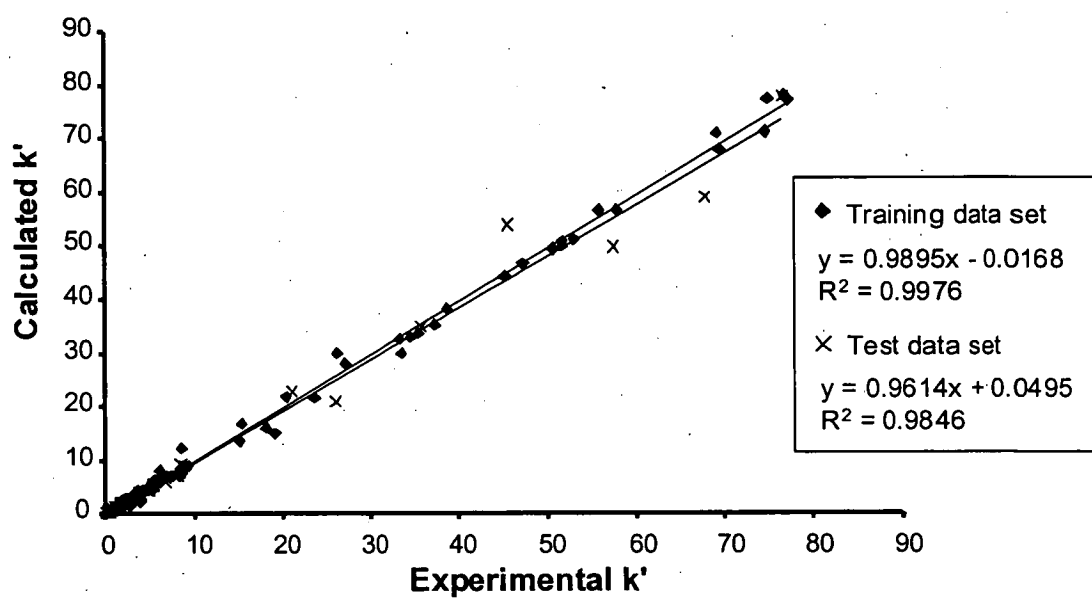also resulted in a poorer correlation ($r^2 < 0.8$).

Figure 6.5 Plot of the calculated k' *versus* experimental k' for the ANN.

6.4 Conclusions

The hard model was able to describe qualitatively the effect of the mobile-phase cation on the zeta potential, as well as the effect of the mobile-phase anion. Reasonable K_{SC} and K_{NA} values were obtained by fitting calculated k' values to experimental k' values, but these same values did not result in accurate calculations of the zeta potential. There was also difficulty in describing the effect of the mobile-phase concentration on k', particularly the large increase in retention for I^- with increasing NaCl concentration, compared with other analytes.

Calculations of the zeta potential depended significantly on the surfactant molecular density on the stationary phase, which provides further complexity to the modelling.

The application of an ANN to the data was successful, with error in the correlation most likely being due to the error in describing nominal variables. Mirroring difficulties in the hard model, the soft model was also poor at handling the significant increase of I^- with increasing Na_2SO_4 and NaCl mobile-phase concentration.

Both models were capable of describing the general trends of this system, however additional studies on the characteristics of the stationary phase stability, as well as determining a more satisfactory description of the nature of the eluent anion species, would be important future work in the development of a useful working model.

6.5 References

(1)   J. Stahlberg, J. Chromatogr. A. 855 (1999) 3-55.

(2)   T. Okada, J.M. Patil, Langmuir 14 (1998) 6241-6248.

(3)   R.J. Hunter. *Foundations of Colloid Science,* Clarendon Press: Oxford, 1987.

(4)   M.G. Cacace, E.M. Landau, J.J. Ramsden, Q. Rev. Biophys. 30 (1997) 241-277.

(5)   W. Hu, Hokkaido University, Sapporo, Japan, personal communication, May 1999.

(6)   Y. Marcus, Chem. Rev. 88 (1988) 1475-1498.

(7)   T. Yokoyama, M. Macka, P.R. Haddad, Anal. Chim. Acta 442 (2001) 221-230.

Conclusions

Investigations into the technique termed "Electrostatic Ion Chromatography (EIC)", detailed in this thesis, revealed a different and broader understanding of this technique than previously reported.

Studies prior to this work generally focussed on determining optimal operating conditions suitable for real ion analysis. As a result, a small range of mobile phases, which were mainly suppressible, and analytes had been explored. These studies provided only a glimpse into the characteristics of EIC, namely, the possibility of using a water mobile phase; the initial abrupt effect of the concentration of electrolyte in the mobile phase on retention, followed by little further effect with an increase in electrolyte concentration; as well as the unique selectivity, following the Hofmeister series of increasing polarisability.

Investigations presented in this thesis began with a comprehensive and systematic investigation into the effect of the mobile-phase anion and cation species, as well as their concentration, on the retention of analyte anions on a sulfobetaine-type stationary phase. The observations were landmark, with a clear trend indicating a displacement between mobile-phase and analyte anions. It became more apparent from further studies into the zeta potential of the stationary phase, which was found to be determined by the nature of the mobile-phase anion and cation, that this displacement

was not due to long-range electrostatic effects, as observed in ion-exchange chromatography.

A major aim of this work was to propose a new separation mechanism that explained all experimental data and was consistent with physically acceptable theories. This was achieved on the basis of these new data. The new mechanism proposed that equilibration of the bound zwitterions with a mobile phase containing electrolyte caused the establishment of a charged layer created by the terminal sulfonate groups of the sulfobetaine-type zwitterion, which acted as a Donnan membrane. The magnitude and polarity of the charge on this membrane depended on the nature of the mobile-phase ions. The Donnan membrane exerted weak electrostatic repulsion or attraction effects on analyte anions. A second component of the retention mechanism was chaotropic interaction of the analyte anion with the quaternary ammonium functional group of the zwitterion. This interaction exerted a major effect on the separation selectivity of EIC, such that analyte anions were eluted in order of increasing chaotropic interactions in accordance with the Hofmeister series. As retention in "Electrostatic Ion Chromatography" was found not to be due predominantly to long-range electrostatic interactions, as the name suggests, the name "Zwitterionic Ion Chromatography (ZIC)" was recommended as an alternative since it does not imply any particular separation mechanism.

A non-stoichiometric, "hard", mathematical model of this system was developed based on the modification of a previous model, to provide consistency with the mechanism

184

proposed in this work. The model was successful in describing the trends observed in the anion retention data set, but accurate prediction of the retention factor and zeta potential proved difficult and elusive. This is an avenue for future work, as a quantitative model is fundamental to an analytically useful technique. A soft model, via an ANN, was successfully applied to the anion retention data, with observed inaccuracies attributed chiefly to the difficulty in describing nominal variables, such as the nature of the anion species.

Previous studies also briefly investigated the analysis of cations in ZIC, utilising a phosphocholine-type stationary phase. A study similar to that carried out for the anion system revealed that cations, despite their lesser chaotropic nature compared to that of anions, were retained by the same interaction as anions on the sulfobetaine-type stationary phase. An analogous retention mechanism was proposed and it was suggested that the proximity of the hydrophobic chain to the inner charge was responsible for cations being more effectively retained on the phosphocholine-type stationary phase and anions more effectively on the sulfobetaine-type stationary phase.

Manipulation of the selectivity in ZIC could be achieved by altering the anion and cation species, but selection of mobile phase components was restricted to species compatible with sensitive detection. The most effective method to vary selectivity was to include a small amount of cationic surfactant (for anion analysis) into the stationary phase coating mixture, allowing modulation between ion-exchange and ZIC mechanisms. SO_4^{2-}, HPO_4^{2-}, and F^- were successfully analysed in tap water by this

method, which was not achievable in pure ZIC using a weak and suppressible mobile phase in a short run time.

Zwitterionic Ion Chromatography is a useful addition to other dynamic or "permanent" stationary phase techniques and should be regarded as a weaker, short-range interacting stationary phase that can complement long-range, electrostatic and stronger-interacting, stationary phases.